UNIVERSITY OF CALIFORNIA

SANTA CRUZ

TRANSCRIPTIONAL REGULATION AT MULIPLE STEPS OF CORTICAL DEVELOPMENT IN *MUS MUSCULUS*

A dissertation submitted in partial satisfaction
of the requirements for the degree of

DOCTOR OF PHILOSOPHY

in

MOLECULAR, CELL AND DEVELOPMENTAL BIOLOGY

by

Jennifer A. Betancourt

June 2013

The dissertation of Jennifer A. Betancourt
is approved:

_____
Professor Bin Chen (Chair)

_____
Professor David Feldheim

_____
Professor Camilla Forsberg

_____
Tyrus Miller
Vice Provost and Dean of Graduate Studies

TABLE OF CONTENTS

LIST OF FIGURES

LIST OF TABLES

ABSTRACT

Transcriptional regulation at multiple steps of cortical development in *Mus musculus*

By

Jennifer A. Betancourt

The highly specialized functions of the mammalian cerebral cortex rely on the temporally precise development and organization of diverse cell types by various cellular processes. However, a complete understanding of the molecular mechanisms that regulate these events is still lacking. Here, I implement *Mus musculus* as a model system for studying neocortical development, given that many processes and genes involved in brain development are conserved from mouse to human. In this thesis, I primarily present results from a detailed characterization of transcription factor, Nuclear Factor One B (*NfiB*), during mouse neocortical development. Additionally I have included a short discussion regarding my contributions toward understanding how another transcription factor, *Fezf2*, functions as a key fate determinant of subcerebral neuron identity. NFIB is expressed in the cortical proliferative zone and in a subpopulation of cortical projection neurons. Given its expression pattern within the cerebral cortex and previously identified functions in CNS development, we hypothesized that *NfiB* was a key regulator of neocortical development. Cell-type specific and temporal expression analysis revealed that NFIB is primarily expressed in the radial glial subclass of neural stem/progenitors and in

corticofugal projection neurons throughout corticogenesis. Using a loss-of-function approach, we compared neocortical development of wildtype (*NfiB*$^{+/+}$) and *NfiB*-deficient (*NfiB*$^{-/-}$) mice to identify the role of *NfiB*. Results revealed that *NfiB* is required for proper generation of outer radial glia and basal progenitors during late corticogenesis. Loss of these neural progenitor populations led to defects in late-stage neurogenesis and cortical lamination. Specifically, there was an increase in corticofugal-like neurons generated after the expected wave of corticofugal neurogenesis. Additionally, there were defects in neuronal migration and an overall reduction in upper layer thickness. We showed that NFIB is also required for axonal outgrowth of corticofugal projection neurons, such that *NfiB*$^{-/-}$ brains displayed a severe loss of axon projections to thalamic and subcerebral targets compared to wildtype controls. Furthermore, genome-wide, RNA-sequencing analysis revealed downstream effectors of NFIB, including genes involved in cell-cycle progression, and neuronal differentiation and migration. Together, these data indicate the broad, yet critical roles for *NfiB* during the development and organization of the mouse cerebral cortex.

ACKNOWLEDGEMENTS

No one deserves a bigger “Thank You” than my mom. Without fail she provided support, love, advice and her “momness”. She would listen to me complain about the stressful times and celebrated when I reached the milestones. She instilled in me the desire to set challenging goals and go after them, but to be selfless along the way. Although she may not have understood the science, she humored me as I doodled the six-layered cerebral cortex on napkins during breakfast. She bragged to her friends about me, her daughter that “studies the wrinkles of the brain”. She is my biggest supporter, my number one fan- I couldn’t have done this with out you, thank you Mom!

I would also like to thank my thesis advisor, Dr. Bin Chen. Without her support, this project would not have been possible. Specifically, I am appreciative of her patience, knowledge and advice throughout my graduate school career. Most importantly, I am now grateful that she allowed me to struggle, to learn from mistakes and to grow as an independent scientist. To my orals committee members, Dr. Lindsay Hinck, Dr. Jeremy Sanford and Dr. Yi Zuo, who overwhelmingly challenged me during my oral qualifying exam but from it, I learned how to present my science with more confidence. Thank you to Dr. David Feldheim and Dr. Camilla Forsberg, who served as members of my thesis committee. Thank you for offering insightful advice on my project, for encouraging me to push forward and for helping me see my project through a different set of lenses. I also thank the members of the Chen Lab, both past and present who have listened to many practice talks, offered discussions at

lab meeting, and with whom I shared many pastries, donuts and coffee. I would like to thank Dr. Will McKenna for the incredible patience, mentorship and guidance along the way. Thank you for answering my millions of questions, for advice on science and for teaching my how to dissect, section, stain, use the microscopes and....you get the point. But most importantly, thanks for being a great friend along the way. I also acknowledge my classmates; I am appreciative of our camaraderie. And to my colleagues: in some way shape or form, they have contributed to making grad school a fun and memorable experience, thank you.

I also thank the rest of my family and friends, old and new, for their endless love, support and humor. Adam: thank you, little brother, for having my back, always. Gabriel: You truly are my brother from another mother. Your mentorship has been imperative to my completion of graduate school. Thank you for building my confidence and having my best intentions in mind. Laura: tu eres como mi hermana. Te quiero mucho, gracias por tus apoyos y por ser amiga simpatica. Tienes una corazon de oro. Kelley: my BFF since the late 90's. Need I say more? Members of Santa Cruz Endurance: I am so grateful to have found a group of crazy people like myself that share the same love of running. Your companionship throughout the years has been memorable. Kona: thanks for listening to my 2am practice talks, for always being happy to see me and for your unconditional love. Lastly, Aaron: Thank you for making me laugh, smile and feel so loved. Your support leaves me speechless. Thank you for sharing you life with me and still loving me even though I am a die-hard Laker fan.

CHAPTER 1

Introduction

1.1 Development and organization of the mammalian cerebral cortex

Development of the mammalian cerebral cortex, a highly specialized region of the brain, constitutes a carefully regulated series of processes that takes place during embryogenesis. However, the exact molecular mechanisms controlling these processes is are only partially understood. The central nervous system (CNS), which includes the brain and spinal cord, originates from the ectoderm layer of the developing embryo. Shortly after gastrulation, neural induction of the ectoderm occurs, resulting in the formation of the neural plate, a subset of ectodermal cells specified for the neural lineage fate (Stern, 2005; Gilbert, 2010). After formation by neural induction and upon receiving signals from the notochord, the neural plate invaginates, thus generating the neural tube. Anterior and posterior regions of the neural tube differentiate into the brain and spinal cord, respectively (Karfunkel, 1974; Copp et al., 2003). As embryogenesis proceeds, the brain undergoes sequential steps of differentiation. The rostral part gives rise to the telencephalon while signals from alternate areas of developing brain, ensure proper specification and patterning of the cerebral cortex (Kudoh et al, 2002).

Organized into layers, the cerebral cortex is composed of neural stem/progenitor cells, excitatory cortical projection neurons, inhibitory interneurons and glia (Peters and Jones, 1984; Ramon y Cajal, 1995; Molyneaux et al., 2007). Together, these cells are responsible for higher order functions including sensory

perception, consciousness and spatial awareness (Finlay and Darlington, 1995), distinguishing humans as an evolutionarily advanced species over other mammals. For this reason, the field of neurobiological research has focused its attention on how these cells are generated, and how they specifically function and interact with one another. In the developing cortex, interneurons are generated in regions ventral to the neocortex, but migrate into and disperse throughout the cortex (Wonders and Anderson, 2006). Multiple subclasses of neural stem and progenitor cells reside in the proliferative zone near the apical surface of the cortex (Heins et al, 2002; Pontious et al., 2008; Lui et al., 2011). The proliferative zone, including the ventricular zone (VZ) immediately adjacent to the apical surface, the subventricular zone (SVZ) and the outer subventricular zone (oSVZ), is where neurogenesis of excitatory projection neurons takes place (Hamilton, 1901; McConnell, 1991; Caviness and Takahashi, 1995; Bentivoglio and Mazzarello, 1999; Lui et al., 2011). In the mature cortex, these cortical neurons are positioned such that distinct neuronal subtypes sharing similarities in molecular expression, morphology and function, are located in the six different layers of the cortical plate (O'Learyand Koester, 1993; McConnell, 1995).

During cortical development, subtypes of cortical projection neurons are sequentially generated in overlapping waves, and layers of the cortical plate form in an inside-out fashion (Angevine and Sidman, 1961; Caviness, 1982; Molyneaux et al., 2007; Leone et al., 2008). The earliest born cortical neurons form the preplate (Allendoerfer and Shatz, 1994). Neural stem/progenitor cells in the proliferative zone then give rise to subsequent subtypes of cortical neurons (Allendoerfer and Shatz,

1994). This results in splitting of the preplate into the subplate and marginal zone, the latter serving as the most superficial layer of the cortex and site of Cajal-Retzius neurons (Meyer et al, 1998; Hevner et al., 2001). Intercalation within the preplate also marks the start of cortical plate development. In mice, this occurs approximately at embryonic day 11.5 (E11.5) (Angevine and Sidman 1961). Using neural progenitor radial fibers as a scaffold, these early born neurons migrate tangentially and form the deepest layer of the cortical plate, layer six. As generation of this subtype comes to an end, generation of a different neuronal subtype begins. This second class of neurons migrates past the earliest born neurons in layer six to occupy a more superficial region of the cortical plate, forming layer five. Similarly, subsequent waves of neurons are generated. Then using neural progenitor radial fibers as a scaffold, these neurons migrate tangentially past earlier born neurons to form layers four, three and two, in that order (Rakic, 1972; O'Leary and Koester, 1993; McConnell, 1995; Britanova et al, 2006). Layer one, however, matures from the marginal zone (Hevner et al, 2001). Clearly, temporal regulation of neurogenesis, by neural stem/progenitors is critical for proper formation of the cortex and all subtypes of cortical projection neurons. However, while much attention has been focused on the laminar composition of the cortex, there is only moderate understanding of the genes responsible for temporally regulating the generation of specific cortical projection subtypes by neural stem/progenitor cells. Here in chapter 2 of this thesis, I investigate potential molecular regulators of neurogenic cell divisions in neural stem/progenitor cells.

1.2 Two major classes of cortical projection neurons

The robust diversity of neurons within the brain was discovered over one hundred years ago by Santiago Ramon y Cajal. By performing Golgi staining on human cortices, he identified many neuronal subtypes. He classified them by cell body morphology, position within the brain and targets of their axons. More importantly, he compared the cortices of mouse and human and found neuronal similarities such that within specific cortical regions, neurons displayed a similar pyramidal shape, suggesting that neuronal subtypes were well conserved across species. Furthermore, tracing of their axons revealed similar axonal targets. (Ramon y Cajal, 1899). This critical finding paved the road for future discoveries in cortical development using the mouse as a model system.

While all cortical projection neurons share some similar features, subtypes are classified by their unique properties, a process made possible by axonal labeling techniques and microarray analyses (Nauta and Bucher, 1954; Valverde, 1962; Arlotta et al., 2005; Sugino et al., 2006). In general, cortical projection neurons are defined as postmitotic neurons generated in the proliferative zone by neural progenitors (Caviness and Takahashi, 1995; Leone et al., 2008; Martynoga et al, 2012). Once generated, they migrate into the cortical plate and begin extending processes, which eventually mature into axons and dendrites. Cell bodies are distinguishably pyramidal in shape and reside within the cortex, dendrites primarily make connections near the superficial, or basal, surface of the cortex and axons transmit information to various regions of the brain, including the cortex itself.

There is a strong correlation between cortical projection neuron subtype and hodology, laminar position, molecular gene expression and birthdate (McConnell, 1995; Molyneaux, 2007; Franco and Muller, 2013). As such, retrograde tracing of axons, allowed broad classification of cortical projection neurons into corticofugal and corticocortical projection neurons (Molyneaux et al., 2007; Leone et al., 2008).

Corticofugal projection neurons are generally located within cortical layers five and six and are defined by extension of axons out of the cortex to other regions of the brain. They are further classified as corticothalamic or subcerebral projection neurons. In mouse embryonic development, generation of corticothalamic neurons begins at E11.5 and peaks approximately at E12.5 (Hevner et al., 2001). Cell bodies primarily reside in layer six and axons project to different nuclei of the thalamus. The transcription factor, T-box brain 1 (*Tbr1*) is specifically expressed by corticothalamic neurons (Hevner et al., 2001; McKenna et al., 2011). Peak generation of subcerebral projection neurons occurs at E13.5. These neurons can be identified by axonal projections terminating in the spinal cord and brainstem and expression of transcription factors, *Fezf2* and *Ctip2*. Their cell bodies are the largest of all projection neurons and are easily distinguished in the deeper region of layer 5 (O'Leary and Koester, 1993; McConnell, 1995; Molyneaux et al., 2007).

Conversely, corticocortical projection neurons are defined by axonal connectivity between two regions of the cortex. For example, callosal projection neurons express the transcription factors *Sabt2* and *Lmo4*, and extend axons contralaterally via the corpus callosum (McConnell, 1995; Britanova et al, 2006) .

Cell bodies are most concentrated in upper layers of the cortical plate (layers 2-4). However, they are also located in deep layers. Generation of this broad class of neurons begins as early as E13.5, and peaks around E15.5 (McConnell, 1995; Frantz and McConnell, 2006; Molyneaux et al, 2007; Franco and Muller, 2013).

Clearly, the specialized functions of the mammalian cerebral cortex are a result of the diverse set of cortical projection neurons. Thus, identifying molecular mechanisms that regulate their production is critical for a complete understanding of cortical development. Results from transplantation assays revealed that newly born neurons maintain the molecular information needed for migration into a laminar position that correlates with its birthdate (McConnell and Kaznowski, 1991; Frantz and McConnell, 1996; Desai and McConnell, 2000). Seemingly, this raises the possibility that the molecular code for neuronal fate specification originates at the level of neural stem and progenitor cells, a possibility that is addressed by use of a loss-of function approach and transgenic mouse model and discussed in Chapter 2.

1.3 Subclasses of neural stem and progenitor cells

Four main subclasses of neural stem and progenitor cells are present during development of the cerebral cortex: neuroepithelial cells, radial glia, basal progenitors and outer radial glia. Similar to classification of cortical projection neurons, neural stem /progenitor cells share similar characteristics, yet are divided into subclasses based on unique features. This includes properties such as position within the proliferative zone, molecular gene expression, morphology and differentiation

potential. Neural stem/progenitor subclasses also differ by when during corticogenesis they are most abundant and by whether they perform symmetric and/or asymmetric cell division (Noctor et al., 2004, 2007b; Pontious et al., 2008; Shitamukai et al., 2011; Wang et al., 2011a.).

Neural stem cells (NSCs) have the ability of self-renewal and potential to differentiate into multiple cell types. Neuroepithelial cells are the first subclass of NSCs present in the developing neocortex. Initially identified in the neural tube as a single sheet of pseudostratisfied cells lining the ventricular lumen, neuroepithelial cells undergo multiple rounds of symmetric division, resulting in expansion of the NSC pool and marking the time at which the neuroepithelial cell population is most abundant. Asymmetric division, occurring in only a small proportion of these cells, generates both multipotent neural progenitors and the earliest born cortical projection neurons. In mice, these initial cell divisions occur approximately at embryonic days 9-11 (E9-11.5) (Noctor et al., 2001). Also at this time, neuroepithelial cells begin expressing molecular markers such as vimentin and nestin (Noctor et al., 2004). Subsequently, once these markers are expressed, neuroepithelial cells begin transforming into a second class of NSC known as radial glia (McKay, 1997).

Radial glia are NSCs that undergo cell division in the cortical VZ and can be identified by a distinct set of molecular markers. First identified in the late 19th century, radial glia are bipolar pseudostratisfied NSCs that divide at the ventricular surface of the cortex (Bentivoglio and Mazzarello, 1999). They have an apical process that attaches to the ventricular surface of the cortex, and a basal process with

end feet that attach at the pial surface. Like neuroepithelial cells, radial glia can perform both symmetric division and asymmetric cell division. Symmetric division results in self-renewal, and consequently, expansion of the radial glial population for additional division. Asymmetric division yields a radial glial daughter cell and either a cortical projection neuron, basal progenitor or outer radial glial daughter cell (Kriegstein and Gotz, 2003; Gotz and Barde, 2005; Noctor et al., 2004, 2007b; Malatesta et al, 2008). Both neuroepithelia and radial glia have the ability for interkinetic nuclear migration (Sauer, 1935). Although radial glial cell bodies are restricted to the VZ, they exhibit movements along the apical-basal axis within the VZ, dependent upon different stages of the cell cycle. For instance, a radial glial cell body contacts the ventricular surface during mitosis (M phase), moves away from the ventricle during G1, reaches the basal VZ as it begins DNA-synthesis (S-phase), then toward the apical surface during G2 (Noctor et al., 2004; Gotz and Huttner, 2005; Taverna and Huttner, 2010). Similar to neuroepithelial cells, radial glia express nestin and vimentin. Additionally, they can be identified by nuclear expression of transcription factors *Pax6* and *Sox2*. During M phase, they are marked by expression of cytoplasmic phosphorylated-vimentin surrounding the cell body and along basal processes and by phophorylated-histone H3 within the nucleus positioned at the ventricular surface. Although most abundant between embryonic day 11.5-15.5, radial glia are present for the duration of cortical neurogenesis. (Gotz et al., 1998; Heins et al., 2002; Noctor, et al., 2007b; Gomez-Lopez et al., 2011). Additionally, whereas neuroepithelial cells only produce the earliest cortical neurons, radial glia,

have the potential to differentiate into all projection neuron subtypes (Gotz anad Barde, 2005).

Radial glia also play a role in neuronal migration and exhibit astroglial characteristics. Newly generated neurons use the basal process of radial glia as a migration scaffold to guide them toward the developing cortical plate (Kriegstein and Gotz, 2003). Upon completion of neurogenesis and neuronal migration, radial glia differentiate into astrocytes that express markers such as brain lipid-binding protein (BLBP), glial fibrillay acidic protein (GFAP) and S100β. These astrocytes exit the VZ, leaving behind a thin layer of ependymal cells in the postnatal cortex (Campbell and Gotz, 2002; Kriegstein and Gotz, 2003). Additionally, a subset of neural progenitors that divide in the VZ were also identified. While they maintain contact at the ventricular surface via an apical process, they differ from radial glia in that they possess only a short basal process that lacks contact with the pial surface of the cortex, hence, they were named short neural precursors. But whether these short neural precursors are just a subset of radial glia, or an independent class of neural progenitor remains to be determined (Gal et al., 2006; Hevner and Haydar, 2012). Taken together, the radial glial subclass of neural stem cells is critical for neocortical development such that they are the original source of almost all cells that comprise the mature cortex and also play a major role in neuronal migration to ensure that neurons properly migrate to laminar positions correlated with their birthdates.

Basal progenitors, also known as intermediate progenitors, were originally identified by Wilhem His (831-1904) in the 19th century as neural progenitors that

undergo cell division away from the ventricle (Bentivoglio and Mazzarello, 1999). However, more recent studies advanced our knowledge of neural progenitor subtypes. Importantly, time-lapse imaging of organotypic slice cultures with fluorescently-labeled neural progenitors, revealed a subset of neural progenitors that appeared to divide in basal regions of the VZ and only produce neurons, therefore depleting that progenitor cell (Miyata et al., 2004; Noctor et al., 2004; Molyneaux et al., 2007). First present at the onset of neurogenesis, basal progenitors are generated by radial glia then migrate away from the ventricular surface to begin forming the SVZ. Unlike radial glia, basal progenitors are multipolar, lacking both apical and basal processes. They do not undergo interkinetic nuclear migration, however, they do express similar molecular markers such as phosphorylated-histone H3 and phophorylated-vimentin. Despite this similarity, basal progenitors are distinguished from radial glia by expression of these M phase markers within the SVZ. Additionally, they uniquely express the transcription factors, T-box brain 2 (*Tbr2*) and subventricular tag-1 (*Svet1*) (Arnold et al., 2008; Sessa et al., 2008; Kowalczyk et al., 2009). Cell division is almost exclusively symmetric and primarily results in the generation of two cortical projection neurons. However, a small fraction of cell divisions yield two additional basal progenitor daughter cells. (Haubensak, et al., 2004; Noctor et al., 2004, 2007b; Basak and Taylor, 2007; Farkas and Huttner 2008). Although most abundant during mid to late corticogenesis (in mouse this is between E13.5-E15.5) they are apparent at the start of corticogenesis. Thus, like radial glia, they have the potential to generate all subtypes of cortical projection neurons that make up the mature cortex.

Additionally, despite that radial glia outnumber basal progenitors during early stages of cortical neurogenesis, a comparative analysis of radial glia versus basal progenitor cell divisions revealed that most neurogenic cell divisions were by basal progenitor cells (Tarabykin et al., 2001; Noctor et al., 2004; Noctor et al., 2007b). Importantly, these results suggested that radial glia mainly function to expand the pool of basal progenitors, in turn, which will function as a critical source of neurogenesis via symmetric divisions.

Outer radial glia, were first identified in the primate cortex as a radial glia-like progenitor. A defining feature of human and primate cortical development is the expansion of an outer subventricular zone (oSVZ. Recent work revealed the presence of neurogenic cell divisions by radial glia-like and intermediate progenitors in the oSVZ (Fietz et al., 2010; Hansen et al., 2010; Lui et al., 2011). Outer radial glia, also known as basal radial glia, are evident across many species including humans, primates and rodents (Reillo et al., 2011; Shitamukai et al., 2011; Wang et al, 2011a, 2011b). However, the number of outer radial glia in gyrencephalic cortices is much greater than those in lissencephalic rodent cortices. This suggested that outer radial glia are critically important for the expansion of human and primate brains but are sufficient for the formation of gyri and sulci (Hevner and Haydar, 2012). The existence of outer radial glia in the lissencephalic brain prompted a thorough investigation of their purpose in mouse cortical development.

Clonal analysis and time-lapse imaging of fluorescently-labeled progenitors revealed both morphological, molecular and behavioral properties of outer radial

glial. Similar to VZ radial glia, outer radial glia have a basal process which may contribute to migration scaffolding for newly generated projection neurons. They however, lack an apical process (Lui et al., 2010; Wang et al., 2011a, 2011b). Upon generation by radial glia, outer radial glia migrate away from the VZ by mitotic somal translocation, whereby cell bodies move quickly up the radial glia basal process to the oSVZ immediately before cytokinesis. Molecular expression profiles are also similar in that radial glia and outer radial glia both express *Pax6* and *Sox2*, yet are distinguishable from one another based on the spatial expression of these markers in the VZ or oSVZ (Bani-Yaghoub et al., 2006; Hutton and Pevny, 2006; Gomez-Lopez et al., 2011) . With regards to cell division, outer radial glia possess the ability for multiple rounds of both symmetric and asymmetric division. Symmetric cell division expands the neural progenitor pool as it yields two outer radial glial daughters while asymmetric cell division produces an outer radial glia daughter cell and a basal progenitor or cortical projection neuron (Farkas and Huttnder, 2008; Hansen et al., 2010; Shitamukai et al., 2011). However, while radial glia and basal progenitors have the differentiative potential to generate all subytpes of cortical projection neurons, outer radial glia are not present until midcorticogenesis, indicating that they do not contribute to production of deep layer neurons (Wang et al., 2011a, 2011b; Franco and Muller 2013). Thus far, lineage-tracing studies have provided insight on their involvement during primate cortical development, however a complete understanding of their role in the developing rodent neocortex is lacking. In Chapter 2, I provide evidence that the outer radial glia population in mice is essential for subsequently

generating late-born basal progenitors, and, does in fact contribute to radial expansion of the mouse cerebral cortex, although to a lesser extent to that of humans.

1.4 Combinatorial genetic codes at different stages of brain development

Much work has been done to identify the specific combination of genes required for embryonic brain development. Patterning by molecular cues coincides with formation of the telencephalon. Transcription factors, Neurogenin 1 and Neurogenin 2 (*Ngn1* and *Ngn2*, respectively) mediate specification of the telencephalon into dorsal and ventral fates by suppression of the ventralizing factor *Mash1* (Fode et al, 2000). The dorsal telencephalon is further specified into the neocortical VZ and other early dorsal structures, by *Lhx2*, a LIM homeobox gene. Bone morphogenetic proteins (BMPs) then mediate expansion of the VZ. Additional transcription factors critical for forebrain regionalization include *Emx1/2, Pax6, Fog1* and *Tlx1*. Together they promote neural progenitor proliferation and suppress neuronal differentiation, while loss of any one results in a combination of ventralization or elimination of neural stem and progenitors (Monuki et al., 2001; Muzio et al., 2002). In addition, morphogenic pathways such as Notch and Sonic Hedgehog (SHH) contribute to early patterning and neocortical functions. For instance, Notch, a cell surface receptor, transduces signals that effect neuronal progenitor maintenance and neuronal migration, while Shh promotes expression of homeobox transcription factors along specific regions of the neural tube and regulates neural progenitor proliferation (Echelard et al., 1993; Dahmane et al.,

2001; Grandbarbe et al., 2003). Most importantly, it is the combination and temporal expression of these morphogens and transcription factors that subsequently control the regulation of downstream targets responsible for fate specification of neural stem/progenitors and cortical projection neurons during neurogenesis.

Gene expression analyses on dissected neocortical regions and creation of transgenic mouse lines have both vastly contributed to identification of neuronal subtype- and laminar-specific transcription factor markers. Beginning with the earliest born neurons, Cajal-Retzius cells are identified by the expression of *Reelin,* and *Tbr1*. The latter is also expressed in layer six corticothalamic projection neurons, along with *Foxp2* (Hevner et al, 2001, 2006; Molyneauz et al., 2007; McKenna e al, 2011). However, when another transcription factor, *Foxg1* is deleted, there is a loss of corticothalamic projection neurons but an increase Cajal-Retzius cell, indicating that generation of corticothalamic projection neurons requires suppression by *Foxg1* (Hanashima et al., 2004). B-cell Leukemia/lymphoma 11B (*Bcl11b* or *Ctip2*) is expressed in a spatial dependent manner in layers 5-6, such that higher levels are evident in subcerebral neurons in layer 5 compared to corticothalamic neurons in layer 6 (Arlotta et al, 2005; Chen et al., 2005; Chen et al., 2008). *Er81* is expressed in a subset of subcerebral projection neurons in layer five but also in neural progenitors, suggesting the potential for *Er81* as a fate determinant of this neuronal subset. Expression of *Cux1/2*, *Lhx2* and *Brn1/2* is apparent in layers 2-4. *Brn1/*2 play a role in neuronal differentiation and migration and *Brn1/2* knockout mice display a loss of upper layer neurons and defects in their migration,

such that they are positioned in the proliferative zone and not in the cortical plate. *Cux1/2* expression, while in a subset of upper layer neurons, are also expressed in a small subset of radial glia, suggesting *Cux1/2* as a fate determinant of *Cux1/2* expressing upper layer neurons (Nieto et al., 2004; Molyneaux et al., 2007; Leone et al, 2008). However, this remains to be confirmed. Additionally, generation of upper layers also requires expression of *Pax6* and *Tlx1* (Nieto et al., 2004; Tarabykin et al., 2001). Although studies have greatly progressed our knowledge of markers identifying cortical projection neuron subtypes, the majority of analysis was performed on postmitotic neurons in the cortical plate and it remains unclear whether these markers are key fate determinants of specific subtypes. However, some molecular mechanisms have, in fact, been established by loss- and gain-of-function approaches.

Two genes first identified as neuron subtype-specific determinants are zinc-finger transcription factors, *Fezf2* (also known as *Fezl* and *Zfp312*) and *Ctip2*. Both are preferentially expressed in subcerebral projection neurons, but FEZF2 is also expressed in cortical neuron progenitors. Results from loss-of-function transgenic mouse studies revealed that CTIP2 is required for the proper formation of the corticospinal tract (CST) such that in CTIP knockout mice, the CST is missing due to loss of CSMNs. Similarly, the CST is also missing in FEZF2-deficient mice. Expression of CTIP2 and many other deep layer-specific markers was lost, yet an increase in callosal projection marker, SATB2, was increased. These mice also display a loss of axonal projection to the tectum and pons, two additional targets of

subcerebral projection neurons. Interestingly, despite the loss of axonal projection to many subcerebral targets, *Fezf2*-mutant neurons in these mice ectopically projected to alternate areas (Arlotta et al., 2005; Chen et al., 2005a; Chen et al., 2005b; Molyneaux et al., 2005; Chen et al; 2008). Additionally, overexpression of *Fezf2* into wildtype animals at the time when callosal projection neurons are typically generated, resulted in a redirection of axons toward subcerebral targets. Together, these results identify Fezf2 as a fate determinant of CSMNs, and Ctip2 as a downstream effector of *Fezf2* (Chen et al., 2008).

The fates of cortical projection neurons are also regulated by the transcription factors, *Satb2* and *Tbr1*. Specifically expressed in callosal projection neurons, SATB2 (Molyneaux et al., 2007; Leone et al., 2008), regulates this neuronal subtype by repression of *Ctip2*. In *Satb2* knockout mice, an increase in CTIP2 expression is evident and *Satb2*-mutant neurons redirect their axons toward subcerebral targets. Conversely, ectopic expression of SATB2 in deep layer neurons, results in a fate switch, such that these neurons redirect axonal projection across the corpus callosum, as evidenced in *Fezf2*-knockout mice (Alcamo et al., 2008; Britanova et al, 2008, Chen et al., 2008). Additionally, it was recently revealed that Tbr1 specifies the identity of corticothalmic projection neurons in layer 6 (McKenna et al., 2011). Results from this study, and my specific contributions to the project are further elaborated on in **Chapter 3: Tbr1 regulates axonal projections of corticofugal neurons to appropriate targets**.

The diversity of daughter cell outcomes from neural stem/progenitor cell divisions has great impact on the developing neocortex yet little is known about genes that control neural stem/progenitor daughter cell fates. Radial glia and basal progenitors have the potential to generate all subtypes of cortical projection neurons, yet their commitment toward specific subtypes narrows throughout neurogenesis (Frantz and McConnell, 1996; Desai and McConnell, 2000). In addition, radial glia are also responsible for generating the basal progenitor and outer radial glia populations, and timing of this is critical to ensure proper availability of neural progenitors (Kriegstein and Gotz, 2003; Malatesta et al., 2008). And while genes that mark individual subclasses of neural progenitors have been discovered, more work is required to identify additional genes that regulate generation of one subclass of neural progenitor over another. In **Chapter 2: NfiB regulates neural stem cell differentiation and axonal projections of corticofugal neurons**, I identify the transcription factor, Nuclear Factor One B, as a potential gene regulator of radial glial differentiation.

1.5 Nuclear Factor One B (NfiB)

Although first identified as critical proteins for adenovirus DNA replication (Nagata et al., 1982), Nuclear Factor One (NFI) proteins have more recently been established as transcriptional regulators, possessing structural features that enable different modes of transcriptional modulation (Gronostajski, 2000; Mason et al., 2009). The NFI family consists of four genes, *Nfia*, *Nfib*, *Nfic* and *Nfix*, each highly

conserved from chicken to human. They are dynamically expressed in various tissue types throughout embryonic development and adulthood, including the brain (Rupp et al., 1990; Kruse et al., 1991). The 200- 220, cysteine-rich amino acid sequence at the N-terminus is highly conserved among all four NFI proteins and mediates dimerization of proteins as homo- or hetero-dimers (Kruse and Sippel, 1994b). This region also mediates DNA-binding (Bandyopadhyay and Gronostajski, 1994; Fletcher et al., 1999). NFI proteins recognize and bind as dimmers to the dyad symmetric consensus sequence, TTGGC(N5)GCCAA or consensus half sites, TTGGC and GCCAA (Gronostajski, et al., 1985; Gronostajski, 1986). These binding sites are present in genes across multiple tissues as well as in genes that are uniquely expressed in the brain. The binding of NFI to consensus sequences is required for transcriptional activation, such that mutations within this region resulted in a decrease of gene expression. Conversely, the proline-rich C-terminal serves as the transcriptional modulation domain of NFI proteins, but is poorly conserved between family members (Chaudhry et al., 1997; Mason et al., 2009). Additionally, alternative splicing is possible for all *Nfi* genes and may result in modifications to the 3' transcriptional modulation sequence (Kruse and Sippel, 1994a; Wang et al., 2007) Finally, NFI proteins can be post-transcriptionally modified via phosphorylation or glycosylation but the functional relevance of these modifications is yet to be determined (Kruse and Sippel, 1994b). Clearly, NFI transcriptional control is very complex, thus characterization of tissue-specific transcriptional modulation is critical for understanding functional roles of NFI proteins during embryonic development.

Nfi genes are dynamically expressed in the many tissues of the developing mouse embryo, and have distinct patterns of expression, however, overlapping expression is also common. For example, analysis *in situ* hybridization revealed exclusive expression of *NfiA* in the developing heart at E9.5, *NfiB* was exclusively expressed in the lung bud at E10.5, but at E11.5, overlapping expression of *NfiA, NfiB* and *NfiX* was apparent in the developing central nervous system. As embryogenesis proceeds, *NfiA, NfiB* and *NfiX* are strongly expressed in the cerebral cortex, suggesting a role for these genes in neocortical development, however, in Chapter 2 of this thesis, I will specifically focus on the involvement of *NfiB* (Nagata et al., 1982; Chaudhry et al., 1997; Mason et al., 2009).

NfiB maps to chromosome 4 of the mouse genome (to chromosome 9 in the human genome), and to date, three splice variants have been identified. Isoform 1 represents the longest mRNA transcript (8.7kb) and encodes the 12 exon, 570 amino acid NFIB protein. Isoform 2 encodes a protein of similar length (560 a.a.) that contains changes within the N-terminal DNA-binding and a shorter C-terminal transcriptional modulation domain. Isoform 3 lacks alternate exons in the 3'end and encodes the shortest of all NFIB proteins (420 a.a.) with a distinguishably shorter C-terminus (Grunder et al., 2003). Despite identification of *Nfib* mRNA and NFIB protein variations, functional differences and expression patterns of individual isoforms remain undetermined.

Preliminary immunohistochemical analyses revealed areal- and temporal-specific patterns of NFIB expression throughout mouse forebrain development. High

levels of NFIB expression were evident in the deep cortical plate and subplate of the early developing cortex (E12.5), while lower levels were apparent in the proliferative zone. Specifically, NFIB was expressed in deep layer neurons and glia but was excluded from interneurons and callosal projection neurons. NFIB was also expressed in other regions of the developing CNS including the hippocampus, ventral thalamus, diencephalon and cortical midline, and subsequent studies indicated that in addition to expression within these structures, Nfib regulated their development (Chaudhry et al., 1997; Steele-Perkins et al., 2005; Plachez, et al., 2008; Piper et al, 2009).

Understanding the role of *NfiB* in the forebrain development was advanced by generation of the *NfiB*-deficient ($NfiB^{-/-}$) mouse line. Taking a replacement vector approach, *Nfib* exon 2, which is essential for DNA-binding and function, was replaced with the *lacZ* reporter gene and nuclear localization sequences, thus allowing identification of *NfiB*-deficient cells by their nuclear expression of βGAL protein (Steele-Perkins et al., 2005). In a comparison of $NfiB^{+/+}$ and $NfiB^{-/-}$ mice, data revealed loss of NFIB function resulted in agenesis of corpus callosum, enlarged lateral ventricles and defects in the hippocampus, thalamus, pons and midline glial populations, thus implicating a role for *NfiB* in the development of these structures (Plachez et al., 2008; Kumbasar et al., 2009; Piper et al., 2009). At the cellular level, studies showed that NFIB regulates migration and axonal projection of cerebellar granule neurons (Wang et al., 2007; Mason et al., 2009; Heng et al., 2012). However, despite NFIB expression in the cortical proliferative zone and in subcerebral and

corticothalamic projection neurons (Plachez et al., 2008; Mason et al., 2009; McKenna et al., 2011), the specific roles of *NfiB* during neocortical development were not investigated.

The work presented in this thesis study addresses two main questions: (1) What is the role of NfiB in expansion and differentiation of neural stem/progenitor subclasses? (2) How does NFIB function in cortical neuron development? Also included, is a short discussion regarding my contribution to the published manuscript: "Tbr1 and Fezf2 regulate alternate corticofugal neuronal identities in neocortical development".

1.6 Contributions to research presented

All the work presented in this thesis dissertation was completed under the direct mentorship and guidance of my thesis advisor, Dr. Bin Chen.

Chapter 2 is a modification of a recently submitted manuscript: **Betancourt, J.**, Katzman, S., and Chen, B (2013). Nuclear Factor One B regulates neural stem cell differentiation and axonal projection of corticofugal neurons. The conceptual framework for this project was a result of scientific discussion between Dr. Bin Chen, Dr. Sol Katzman and myself. I wrote the manuscript, with the exception of the section: "RNA-sequencing (RNA-seq) and data analysis" in 2.3 Material and Methods, which was written by Sol Katzman. This manuscript was edited by Drs. Bin Chen and Sol Katzman. I designed the layouts and created all figures and tables,

which were edited by Dr. Bin Chen. The manuscript is currently under review at the Journal of Comparative Neurology.

Chapter 3 is an abbreviated reproduction from the publication: McKenna, W.L., **Betancourt, J.,** Larkin, K.A., Abrams, B., Guo, C., Rubenstein, J.L., and Chen, B (2011). Tbr1 and Fezf2 regulate alternate corticofugal neuronal identities in neocortical development. J. Neuroscience *31(2)*, 549-564. In this chapter, I present my direct contribution to this publication, earning second authorship. I discuss use of ultrasound guided retrograde tracing to label axons in *Fezf2*-deficient mice, results from the experiment and relevance to the overall findings of the publication. I performed this work during the first part of graduate school under the mentorship of Dr. Will McKenna, who also wrote the manuscript and gave me permission to include a modified version into this thesis.

CHAPTER 2

NfiB regulates neural stem cell differentiation and axonal projections of corticofugal neurons

2.1 Abstract

During development of the cerebral cortex, neural stem cells divide to expand the progenitor pool and generate basal progenitors, outer radial glia and cortical neurons. As these newly born neurons differentiate, they must properly migrate toward their final destination in the cortical plate, project axons to appropriate targets, and develop dendrites. However, a complete identification of genes that regulate each step in temporal and spatial manners is lacking. Here we show that a member of the nuclear factor one (NFI) family of transcription factors, NFIB, is essential for many of these processes in mice throughout development. We performed a detailed analysis of NFIB expression during cortical development, and investigated defects in cortical neurogenesis, neuronal migration and differentiation in *NfiB*$^{-/-}$ brains. We found that NFIB is strongly expressed in radial glia and corticofugal neurons throughout cortical development. However, in *NfiB*$^{-/-}$ cortices, radial glia failed to generate outer radial glia, subsequently resulting in a loss of late basal progenitors. In addition, corticofugal neurons showed a severe loss of axonal projections, while late-born cortical neurons displayed defects in migration and ectopically expressed the early-born neuronal marker, CTIP2. Furthermore, gene expression analysis, by RNA-sequencing, revealed a misexpression of genes that regulate the cell cycle, neuronal differentiation and migration in *NfiB*$^{-/-}$ brains. Together these results demonstrate that

NFIB is critical for processes during late-stage cortical development. Specifically, NFIB regulates generation of outer radial glia and late-born basal progenitors, formation of corticofugal axonal projections and temporally controls neurogenesis all contributing to proper formation of the mouse neocortex.

2.2 Introduction

The mammalian cerebral cortex is a six-layered structure, responsible for higher cognitive function and sensory perception. It is composed of many different neuronal subtypes, each with unique characteristics including laminar position, gene expression profile and axonal targets. The cortex is generated in an inside-out fashion such that cortical projection neurons generated early in development occupy deep layers (layers 5 and 6), while those that reside in upper layers (layers 2-4) are generated later (McConnell et al., 1995; Hevner et al., 2006; Molyneaux et al., 2007).

All cortical projection neurons are generated by neural progenitors in the proliferative region of the cortex, encompassing both the ventricular and subventricular zones (VZ and SVZ) (Haubensak et al., 2004; Farkas and Huttner, 2008). To date, three different types of neural progenitors have been identified: radial glia, outer radial glia and basal progenitors. Each have distinct roles during neurogenesis and can be distinguished by characteristics including morphology, location of cell body and expression of molecular markers (Farkas and Huttner, 2008; Wang et al., 2011a; Shitamukai and Matsuzaki, 2012).

At the onset of neurogenesis, neuroepithelial cells differentiate into radial glia (Shitamukai and Matsuzaki, 2012), which can be genetically defined by their expression of transcription factors, PAX6 and SOX2 (Gotz et al., 1998; Tarabykin et al., 2001; Bani-Yaghoub et al., 2006). Highly polarized, radial glia have apical and basal processes that attach to ventricular and pial surfaces of the cortex, respectively (Shitamukai and Matsuzaki, 2012). Their cell bodies reside in the VZ and they can undergo multiple rounds of cell division, which take place at the ventricular surface (Pontious et al., 2008). Radial glia can self-renew and also divide to generate basal progenitors, outer radial glia and cortical neurons (Shitamukai et al., 2011; Shitamukai and Matsuzaki, 2012). However, the main function of radial glia is likely to expand the progenitor pool (Kowalczyk et al., 2009; Lui et al., 2011; Wang et al., 2011b).

Basal progenitors, the second major class of neural progenitors, uniquely express TBR2, a T-box transcription factor (Arnold et al., 2008; Sessa et al., 2008; Kowalczyk et al., 2009). Unlike radial glia, basal progenitors are multipolar, lack apico-basal processes and their cell bodies reside throughout the SVZ. Although some have reported the potential for few rounds of self-renewing divisions, basal progenitors predominantly undergo neurogenic symmetric division (Farkas and Huttner, 2008; Noctor et al., 2008; Shitamukai and Matsuzaki, 2012). Thus, the main function of basal progenitors is the generation of cortical neurons (Noctor et al., 2004; Pontious et al., 2008; Kowalczyk et al, 2009).

Outer radial glia, the third subclass of neural progenitor, are similar to radial glia in that they have a basal process and express PAX6 and SOX2. However, they lack an apical process and their cell bodies reside in the superficial (outer) region of the SVZ (oSVZ). They are capable of asymmetric self-renewal and also generate neurons or basal progenitors (Reillo et al., 2011; Shitamukai et al., 2011; Wang et al., 2011a, 2011b; Shitamukai and Matsuzaki, 2012). Previous work showed that outer radial glia complete many rounds of self-renewal, exhibit enhanced transit amplification and generate basal progenitors, likely contributing to neocortical expansion in human brains (Hansen et al, 2010; Lui et al., 2011; Reillo et al., 2011). However, there are significantly fewer outer radial glia in the rodent brain and their role in neurogenesis is not fully understood.

Despite well-defined characteristics unique to neural progenitor subtypes, molecular mechanisms regulating their proliferation and differentiation remain undetermined. One genetic candidate in neural progenitor cell maintenance is NFIB, a member of the Nuclear Factor One (NFI) family of transcription factors that is essential for normal brain development. Mice with an *NfiB* gene mutation ($NfiB^{-/-}$), die at birth due to lung defects and suffer from various developmental brains defects (Plachez et al., 2008; Kumbasar et al., 2009; Piper et al., 2009). NFIB regulates the migration and axonal projection of cerebellar granule neurons (Wang et al., 2007; Mason et al., 2009; Heng et al., 2012). It is expressed in proliferative zone cells and in subcerebral and corticothalamic projection neurons (Plachez et al., 2008; Mason et

al., 2009; McKenna et al., 2011). However, its role in regulating neural progenitor maintenance and development of these neurons remains to be elucidated.

In this study, we investigated the function of *NfiB* in differentiation and expansion of distinct neural progenitor subpopulations. Additionally, we characterized its role in cortical neuron development. We asked whether loss of *NfiB* had an effect on neuronal birthdate, migration and/or axon formation and targeting. Similar to previous studies, we found that NFIB was expressed in corticofugal neurons and the proliferative zone throughout development (Plachez et al., 2008; Mason et al., 2009; McKenna et al., 2011). However, we elaborated on prior findings such that within the proliferative zone, we specifically identified high expression of NFIB in radial glia, however, little to no expression was observed within basal progenitors and outer radial glia. We also observed defects in both neurogenesis and cortical neuron differentiation in $NfiB^{-/-}$ mice. Radial glia failed to generate outer radial glia and basal progenitors during late corticogenesis, corticothalamic and subcerebral axons were severely diminished, and late-born neurons ectopically expressed early-born neuronal marker, CTIP2, and displayed migration defects. Additionally, genes that regulate cell cycle progression, neuronal differentiation and axon projection were mis-regulated in $NfiB^{-/-}$ cortices, as revealed by gene expression analysis. Our study clearly demonstrates that NFIB is essential in regulating differentiation of radial glia, migration of cortical projection neurons and development of corticofugal axons.

2.3 Material and Methods

Abbreviations used are listed in Table 2.1.

Generation of *NfiB*$^{-/-}$, *NfiB*$^{-/-}$;*Fezf2*$^{+/PLAP}$ and *NfiB*$^{-/-}$;*Golli-τ-GFP*$^{+}$ mice

The generation of the following mouse strains were described previously: *NfiB*$^{+/-}$ (Steele-Perkins et al., 2005), *Golli-τ-GFP*$^{+}$ (Jacobs et al., 2007), and *Fezf2*$^{+/PLAP}$ (Chen et al., 2005a). *NfiB*$^{+/-}$ mice were time-mated to generate *NfiB*$^{+/+}$ and *NfiB*$^{-/-}$ embryos. *NfiB*$^{+/-}$ and *Fezf2*$^{+/PLAP}$ mice were mated to generate *NfiB*$^{+/-}$; *Fezf2*$^{+/PLAP}$ mice. These mice were then time-mated with *NfiB*$^{+/-}$ mice to generate *NfiB*$^{+/+}$;*Fezf2*$^{+/PLAP}$, *NfiB*$^{+/-}$;*Fezf2*$^{+/PLAP}$ and *NfiB*$^{-/-}$;*Fezf2*$^{+/PLAP}$ embryos for PLAP staining studies of axonal projections. *NfiB*$^{+/-}$ and *Golli-τ-GFP*$^{+}$ mice were mated to generate *NfiB*$^{+/-}$;*Golli-τ-GFP*$^{+}$ mice. These mice were then time-mated to *NfiB*$^{+/-}$ to generate *NfiB*$^{+/+}$;*Golli-τ-GFP*$^{+}$ and *NfiB*$^{-/-}$;*Golli-τ-GFP*$^{+}$ embryos for GFP immunostaining of axonal projections. To acquire timed-pregnant mice, male and female mice were put together overnight. The following morning, females were inspected for a vaginal plug; observation of a plug day was defined as embryonic day (E)0.5. Postnatal day (P)0 was designated as the day of birth. Genders of embryonic mice were not determined.

All embryos were genotyped by PCR. Genotyping of *NfiB* alleles was accomplished using two sets of primers. The wild type allele was genotyped by using p1 (GCTGAGTTGGGAGATTGTGTC) and p2 (TTCTGCTTGATTTTCGGGCTTC) with an expected PCR product of about 300bp. The PCR conditions were 94°C for 2 min, followed by 30 cycles of 94°C for 30 sec, 64°C for 1 min and 72°C for 1 min.

The mutant allele was genotyped using primers, p3 (TTTCCATGTTGCCACTCGC) and p4 (AACGGCTTGCCGTTCAGCA). This set of primers detects the LacZ gene, yielding a product of about 400bp. The PCR conditions were 94°C for 2 min, followed by 30 cycles of 94°C for 30 sec, 55°C for 1 min and 72°C for 1 min. Genotyping of *Fezf2* alleles was previously reported (Chen et al., 2005a). To determine whether embryos contained a copy of a *Golli-τ-GFP* allele, we used one set of primers, p5 (CCTACGGCGTGCCAGTGCTTCAGC) and p6 (CGGCGAGCTGCACGCTGCGTCCTC), yielding an expected product of about 300bp. PCR conditions were 94°C for 5 min, followed by 30 cycles of 94°C for 20 sec, 55°C for 30 sec and 72°C for 1 min. All experiments and animal husbandry were executed in accordance with protocols approved by the Institutional Animal Care and Use Committee at University of California, Santa Cruz and institutional and federal guidelines.

Antibody characterization

Antibodies, sources and dilutions that they were used at are listed in Table 2.2.

β-Gal. The anti-βGal antibody detects the full length native β Galactosidase, a protein encoded by the *lacZ* gene in the lac operon of *E. coli*. In the *NfiB* mutant allele, the *lacZ* gene and a nuclear localization sequence were inserted into the *NfiB* locus resulting in the expression of β-Galactosidase within cells expressing the *NfiB* mutant allele (Plachez et al. 2008). Using an $NfiB^{+/-}$ brain, we use the anti-βGal

antibody to show that β-Galactosidase expression recapitulates that of NFIB protein (**Figure 1**).

BETA3 (officially BHLHE22; also known as BHLHB5). The anti-BETA3 antibody specifically detects a single band at 55 kDa on western blots of rat lung and brain extracts (manufacturer's information). We used the anti-BETA3 antibody to label cortical projection neurons of layers 2-5 of the cortex. BETA3 expression in *NfiB*$^{+/+}$ mice is consistent with that of previously published results (Joshi et al., 2008).

BrdU. The anti-BrdU antibody specifically detects bromodeoxyuridine (BrdU), a haplopyrimidine that labels proliferating cells in S phase (Struikmans et al., 1997). This was confirmed by testing the antibody's precipitation against 5-Methyl Cysteine (5-MeC), BrdU or no antigen (as a control). There was an 8-fold increase of reactivity with BrdU over 5-MeC (manufacturer's information). We, and others, have shown that use of this anti-BrdU antibody allows for analysis of neurogenesis (Taupin 2007; McKenna et al., 2011). In this study, we inject BrdU into mice and then use the anti-BrdU antibody to identify neural progenitors in S-phase and, based on signal intensity, neurons born on the day of BrdU injection (see Material and Methods for BrdU incorporation analysis). Note: antigen retrieval is needed for this antibody (10mM Citrate Buffer in PBS; 10 min at 95°C).

Cleaved Caspase-3 (officially CASP3; also known as CC3, CPP32 and SCA-1). The anti-Cleaved Caspase-3 (Asp175), or anti-CC3, antibody specifically detects bands at 17 or 19 kDa on western blots of HeLa, NIH/3T3 and C6 cell extracts representing the large fragment of activated caspase-3 resulting from cleavage of this

protein adjacent to Asp175 (manufacturer's information). Immunostaining with this antibody detects apoptotic cell death *in vitro* and on brain tissue. Staining was evident in HT-29 cells treated with cell-death-inducing Staurosporine (Cell Signaling #9953), but not in untreated cells (manufacturer's results). In newborn rat brain tissue, the antibody detected apoptotic cells in transient cerebral ischemic tissue versus control (Dr. Bingren Hu, University of Miami School of Medicine, Florida) and in the vomeronasal organ of *Fezf2*$^{-/-}$ mice (Eckler et al., 2011). In this study we used the anti-CC3 antibody to detect and quantify apoptotic cells within the proliferative zones in *NfiB*$^{+/+}$ and *NfiB*$^{-/-}$ mice.

CTIP2 (officially BCL11B; also known as Rit1)**; clone 25B6.** The rat monoclonal anti-CTIP2 antibody (clone 25B6) specifically detects two bands at about 95-100 kDa on a western blot of Jurkat cells immunoprecipitated with anti-Sir2 antibody and mouse brain tissue lysate. Immunohistochemical specificity was confirmed by staining on mouse cortical, spinal cord and hippocampal tissue (manufacturer's information). CTIP2 is expressed in postmitotic neurons residing in layers 5 and 6 of the mouse cortex and is critical for development of corticospinal motor neurons (Chen et al., 2005a; McKenna et al., 2011). In this study we use the anti-CTIP2 antibody to detect layer 5 and 6 neurons throughout cortical development.

DARPP32 (officially known as PPP1R1B)**; clone EP27Y.** The mouse monoclonal anti-DARPP32 (clone EP27Y) antibody specifically detects a band of approximately 32 kDa on western blots of rat brain lysate (manufacturer's information). DARPP32 expression is cytoplasmic and was reported in layer 6

neurons (Molyneaux et al., 2005); we also observed the same staining pattern (McKenna et al., 2011). In our study, we use the anti-DARPP32 antibody to identify layer 6 postmitotic neuronal cell bodies and processes in *NfiB*$^{+/-}$ and NfiB$^{-/-}$ brains at E18.5. We use DP32 as nomenclature for this antibody (see Table 2.1).

GFP. The anti-GFP antibody specificity was confirmed by both western blot and immunohistochemical analyses (manufacturer's information) using transgenic mice expressing the green fluorescent protein (GFP) gene product. In this study, we use the anti-GFP antibody to detect the expression of GFP protein in *NfiB*$^{+/+}$*;Golli-τ-GFP*$^{+}$, *NfiB*$^{+/-}$*;Golli-τ-GFP*$^{+}$ and *NfiB*$^{-/-}$*;Golli-τ-GFP*$^{+}$ brains. In these mice, the *Golli-τ-GFP* allele directs expression of GFP in cell bodies and axons of deep layer cortical neurons (Jacobs et al., 2007).

Ki67; clone B56. The mouse monoclonal Ki67 antibody (clone B56) specifically detects a double band at 345 and 395 kDa on western blots of proliferating cells. Ki67 is a nuclear cell-proliferation associated antigen expressed in all active stages of the cell cycle (manufacturer's information). Antibody specificity is validated in various ways: In flow cytometric analysis, reactivity to the Ki67 immunogen by the Ki67-B56 antibody is blocked by a second Ki67 antibody (clone MIB). Immunostaining with the antibody (clone B56) on human tonsil, successfully labels proliferating cells (manufacturer's results). In this study, we used the Ki67 antibody to label neural progenitors and perform quit fraction analyses at different stages throughout development, as we have done previously (McKenna et al., 2011). This antibody requires antigen retrieval.

NFIA. The anti-NFIA antibody specifically detects a single band at about 50 kDa on western blots of MCF-7, HeLa (manufacturer's information) and JEG-3 cells (Plachez et al., 2008). In an electromobility shift assay, addition of the NFIA probe and antibody results in a supershift. However, in the presence of a neutralizing peptide, there is no shift, indicating antibody specificity (manufacturer's information). Additionally, the antibody did not cross-react against other NFI proteins nor did it detect any signal in *NfiA*$^{-/-}$ mice (Plachez et al., 2008). Here, we use the anti-NFIA antibody, as others have, to label postmitotic neurons of layers 5/6 and neural progenitors in E18.5 *NfiB*$^{+/-}$ and *NfiB*$^{-/-}$ brains (Plachez et al., 2008).

NFIB. The anti-NFIB antibody specifically detects a band at about 50 kDa on western blots of rat liver nuclear extract. Addition of the immunizing peptide eliminates the band, thereby confirming specificity of the antibody (manufacturer's information). Immunostaining showed specificity, such that the antibody did not cross-react with other NFI proteins nor was any staining detected in *NfiB*$^{-/-}$ mice (Plachez et al., 2008). Similar to previous protocols (Palchez et al., 2008; McKenna et al., 2011), we use the anti-NFIB antibody to label layer 5/6 postmitotic neurons and neural progenitors and analyze its co-expression with other factors critical for cortical development.

PAX6 (also known as SEY or AN2). The anti-PAX6 antibody specifically detects PAX6 protein expression by immunohistochemical analysis of mouse retina, brain tissue and human epididymis tissue (manufacturer's information). PAX6 expression has been reported in both radial glia and outer radial glia in the developing

cortex (Davis and Reed, 1996; Gomez-Lopez et al., 2011). Here, we use the anti-PAX6 antibody to identify radial glia and outer radial glia in *NfiB*$^{+/+}$ and *NfiB*$^{-/-}$ brains throughout cortical development.

PHH3; clone 6G3. The mouse monoclonal anti-phosphorylated histone H3 (Ser10) antibody (clone 6G3), or anti-PHH3 antibody, recognizes endogenous histone H3 only when it is phosphorylated at serine 10, a hallmark of cells in M phase (manufacturer's information). It specifically detects a band at 16.5 kDa on western blots of NIH/3T3 whole cell lysate treated with serum plus calyculin A (which induces phosphorylation) but not on untreated lysate. Flow cytometric analysis of pacilitaxel-treated THP1 cells using this antibody revealed higher DNA content in cells stained by the antibody, corresponding to cells that progressed through S phase and into M phase of the cell cycle. Specificity was also confirmed by co-immunostaining NIH-3T3 cells with anti-PHH3 and anti-tubulin antibodies, and by staining in mouse subventricular zone and third instar *Drosophila* larval neuroblasts. PHH3 staining is evident in prophase, metaphase and anaphase of mitosis but is absent in non-mitotic cells and in cells pre-treated with phosphatase or phosphohistone H3 (Ser10) blocking peptide (Cell Signaling, #1000) (manufacturer's results). We use the anti-PHH3 antibody to detect and quantify mitotic cells in *NfiB*$^{+/+}$ and *NfiB*$^{-/-}$ brains throughout cortical development.

SATB2. The anti-SATB2 antibody detects a band at approximately 85 kDa on western blots of mouse brain tissue lysate and immunofluorescent staining revealed expression in human osteosarcoma 2 cell nuclei (manufacturer's

information). SATB2 is an established marker of callosal projecting neurons (Alcamo et. al, 2008; Britanova et. al, 2008; Chen et al., 2008; McKenna et al., 2011). In this study, we use the anti-SATB2 antibody in combination with deep layer markers to identify layer 2-4 neurons and define upper cortical layers in *NfiB*$^{+/+}$ and *NfiB*$^{-/-}$ mice.

SOX2 (also referred to as ANOP3); clone Y-17. The anti-SOX2 antibody specifically detects a band at 34 kDa on western blots of human and mouse embryonic stem cell lysates. Immunofluorescence staining is evident in the mouse embryonic stem cell nuclei (Dr. Nobuaki Kikyo, Stem Cell Institute, University of Minnesota). It was reported that SOX2 is expressed in radial glia and outer radial glia in developing mouse cortex (Wang et al., 2011a). In this study, we use the anti-SOX2 antibody to label and quantify these two cell types in *NfiB*$^{+/+}$ and *NfiB*$^{-/-}$ mice, throughout cortical development.

TBR1 (also referred to as TES-56). The anti-TBR1 antibody specifically detects a band at 74 kDa on western blots of mouse and rat hippocampal whole cell lysates (manufacturer's results). Immunostaining with this antibody revealed nuclear staining in human cortical tissue (manufacturer's results), pyramidal neurons of rat brains (Ruma Raha-Chowdhury), rat cortical neurons in culture (Dr. Ioana Carcea), and layer 6 neurons of embryonic and adult mouse cortical tissue (manufacturer's results and Dr. Carlos Perez-Garcia), all which confirmed its specificity. McKenna et al., additionally showed specificity in layer 6 neurons of the developing mouse cortex. In this study, we use the anti-TBR1 antibody to identify layer 6 neurons in *NfiB*$^{+/+}$ and *NfiB*$^{-/-}$ brains at E18.5.

TBR2 (officially EOMES). The anti-TBR2 antibody detects a 72 kDa band on western blots of human mesoderm lysate, mouse brain tissue lysate and EL4 cells expressing a V5 tagged Eomesodermin. However, no band was detected when using the TBR2 antibody on human mesoderm whole cell lysate incubated with TBR2 blocking peptide (Abcam, #ab25698), or on EL4 cells expressing an empty vector or V5 tagged vector, thus validating antibody specificity (manufacturer's results). Immunostaining results showed specificity to developing mouse cerebral cortical tissue (Guillermo Estivill-Torrus), human embryonic stem cells that differentiated into mesoderm (Ludovic Vallier, University of Cambridge), and in adult mouse hippocampal tissue (Hongjun Song Lab). As others have done (Arnold et al., 2008), we use the anti-TBR2 antibody to detect and analyze basal progenitors in $NfiB^{+/+}$ and $NfiB^{-/-}$ brains throughout cortical development.

Tuj1. The mouse Tuj1 monoclonal antibody has been used to detect the neuronal class III β-tubulin protein (officially known as TUBB3) in axons and dendrites of postmitotic neurons (Casanovas et al., 2008). It was produced from the Tuj1 hybridoma mouse clone developed from immunizing mice with rat brain microtubules. The Tuj1 antibody does not react with β-tubulin in glial cells and staining on rat hippocampal tissue revealed immunohistochemical specificity (manufacturer's results). In this study we use laminar position of Tuj1 positive cells to determine location of postmitotic neurons within the cortex on $NfiB^{+/+}$ and $NfiB^{-/-}$ mice.

Immunohistochemistry

To obtain embryonic tissue, pregnant mice were sacrificed by cervical dislocation and embryos were removed. E12.5 heads were drop-fixed in 4% paraformaldehyde in 1x phosphate buffered saline (PBS; pH 7.4) at 4°C. E13.5-E16.5 brains were dissected from skull then drop-fixed in 4% paraformaldehyde (PFA) in 1x PBS at 4°C. Older embryos were transcardially perfused with PBS followed by 4% PFA in 1x PBS before drop-fixation as above. All embryonic brains were cryoprotected in 30% sucrose, frozen in Optimal Cutting Temperature Compound (Tissue-Tek) and cut using a cryostat or sliding microtome. Coronal or sagittal sections were cut at 20μm via cryostat (**Figures 2.1-2.4, 2.6-2.11**) or 50μm (**Figure 2.5**) on sliding microtome.

For immunofluorescence, sections were blocked in 5% horse serum and 0.1%Triton X-100 in 1x PBS for 1 hour at room temperature. Sections were incubated with primary antibodies at appropriate dilutions (**Table 2.2**) overnight at 4°C. The following day, slides were washed with 0.1%Triton X-100 in 1x PBS three times for five minutes, incubated with Alexa Fluor-conjugated secondary antibodies for one hour at room temperature, then washed with 1x PBS for three times at 5 minutes before mounting with Fluoromount (Southern Biotech). Secondary antibodies used in this study were Donkey Anti-Mouse IgG Alexa Fluor 547 or 647, Donkey Anti-Rabbit IgG Alexa Fluor Cy3, Cy5 or 488, Donkey Anti-Sheep IgG Alexa Fluor 488 or 647, Donkey Anti-Chicken IgG Alexa Fluor Cy3 or 488, Donkey

Anti-Rat IgG Alexa Fluor 488 or 647 and Donkey Anti-Goat IgG Alexa Fluor Cy3, 488 or 647 (all at 1:1000; Jackson ImmunoResearch Laboratories, West Grove, PA).

Nuclei were visualized using DAPI (4',6-Diamidino-2 Phenylindole; at 1:10,000; Molecular Probes) (**Figure 2.9**) or DRAQ5 (1,5-bis((2-(dimethylamino) ethyl)amino)-4, 8- dihydroxyanthracene-9, 10-dione; at 1:5000; Cell Signaling Technology) (**Figure** 2.**6**). At least 3 brains/genotype were analyzed for all experiments; all tissue sections were collected onto Superfrost slides (Fisher Scientific)

Detection of PLAP activity

Human placental alkaline phosphotase (PLAP) staining (**Figure 2.5A-H**) was performed as previously described (Chen et al., 2005a). Brain tissue was collected and sectioned at 50μm using a sliding microtome, washed in 1x PBS and post-fixed in 4% PFA in 1x PBS at 4°C for 1 hour. Sections were again washed with 1x PBS, then incubated at 70°C for 1 hour in 1x PBS. Sections were incubated with NBT/BCIP (1 mg/ml nitroblue tetrazolium/0.1 mg/ml 5-bromo-4-chloro-3-indolyl phosphate in 100 mM Tris·Hcl, pH 9.5/100 mM NaCl) at 37°C for 3 hours, then washed with 0.3% Triton X-100 in 1x PBS and mounted in Fluoromount.

***In situ* hybridization**

Non-radioactive *in situ* hybridization was essentially performed as previously described (Schaeren-Wiemers and Gerfin-Moser, 1993). Slides with fixed brain

sections were post-fixed in 4% PFA for 10 minutes, treated with proteinase K for 10 minutes, fixed again in 4%PFA for 10 minutes and acetylated for 10 minutes, all at room temperature, with DEPC PBS washes in between each step. Slides were prehybridized for 2 hours at 65°C, hybridized with Digoxigenin (DIG) labeled cRNA and sealed with coverslips (HybriSlip, Grace Bio-Labs). The cDNA templates for cRNA probes for *Notch1*, *Hes1* and *Hes5* genes were generous gifts from Drs. Toshiyuki Ohtsuka and Ryoichiro Kageyama from Kyoto University, Kyoto, Japan. Nucleotides 4270-5611 of mouse *Notch1* cDNA was used to prepare the *Notch1* probe. Full-length cDNA sequences for *Hes1* and *Hes5* were used to prepare *Hes1* and *Hes5* probes, respectively. Slides were then placed in a humidity chamber overnight at 65°C. The following day, slides were washed with SSC, incubated with RNase A at 37°C for 30 minutes and washed with the following: SSC, 0.1MTris (pH 7.4)/0.15M NaCl (Buffer 1) for 5 minutes, Buffer 1 containing 1% heat inactivated goat serum for one hour at room temperature. Slides were incubated with an anti-DIG antibody in a humidity chamber overnight at 4°C. On the third day, slides were washed with Buffer 1 and equilibrated with 0.1M Tris (pH9.5)/0.1M NaCl/50mM $MgCl_2$ (Buffer 2) for 5 minutes at room temperature. To visualize probe-tissue interaction, slides were incubated for 6 hours with NBT/BCIP substrate in Buffer 2. Slides were washed with PBS, then with PBS containing 0.3% Triton X-100. Lastly, slides were fixed with 4% PFA and mounted with Fluormount-G.

Image acquisition and digital retouching.

Images for quantitative analyses were captured on a Leica SP5 confocal microscope. The detector gain was set such that <1% of pixels were saturated. Additional fluorescent and bright field images were captured on an Olympus BX51 microscope and Q-imaging Retiga camera. Adjustments of contrast and brightness and image cropping for presentation were done using Adobe Photoshop to the same degree on entire images of *NfiB*$^{+/+}$ and *NfiB*$^{-/-}$ matched cortical sections.

Quantitative analyses

For all measurements and cell-counting, statistical analyses were performed by an unpaired t-test; significance was defined as *$p \leq 0.05$, **$p \leq 0.005$, ***$p \leq 0.0005$; error bars represent standard error of means (SEM). Specific numbers of mice used in each quantitative experiment can be found in figure legends. Briefly, at least nine matched sections/age from anterior, middle and posterior regions from at least three mice/genotype were used in each quantitative comparison. Matched sections were defined as brain sections from approximately the same anterior-posterior axial position in *NfiB*$^{+/+}$ and *NfiB*$^{-/-}$ littermates. Unless otherwise noted, data presented in figures are from sections midway along the anterior-posterior axis of the brain.

Measurements of cortical area thickness. To measure independent thicknesses of upper layers (UL-S) or deep layers (DL-C), coronal sections of *NfiB*$^{+/+}$ and *NfiB*$^{-/-}$ mice were immunostained as described above with antibodies against

SATB2 and CTIP2. DL-C was defined as the region along the dorsal-ventral (D-V) axis containing CTIP2-expressing cells; UL-S was defined as the region containing SATB2-expressing cells dorsal to DL-C, along the D-V axis (schematic **Figure 2.4Q**). For each cortical image, three measurements were taken along 300μm of the mediolateral axis and averaged. To measure the proliferative zone, the region containing the VZ, SVZ and oSVZ (VZ + o/SVZ), *NfiB*$^{+/+}$ and *NfiB*$^{-/-}$ mice were immunostained as described above with antibodies against Ki67 and TBR2. The VZ + o/SVZ was defined as the region along the D-V axis of cells expressing Ki67 and/or TBR2 (schematic **Figure 2.6C**).

Cell-counting analysis. Cell counting was performed on individual Z-slices from confocal microscopic images. For each brain analyzed, the cortex was divided into anterior, middle and posterior regions. Cells on 300μm wide sections of the mediolateral axis of cortical sections expressing indicated markers were counted.

BrdU incorporation analysis. For analysis of cells in S-phase, BrdU (Bromodeoxyuridine at 100μg/g body weight; US biologicals, Swampscott, MA) was intraperitoneally (i.p.) injected into timed pregnant mice at E18.5; embryos were collected 2 hours post-injection and processed for BrdU immunostaining and quantification. To analyze the distribution of BrdU-labeled cells, cortices were divided into ten bins of equal thickness and BrdU-labeled cells in each bin were quantified (schematic **Figure 2.6N**). For birthdating analysis, BrdU (100 μg/g body weight) was i.p. injected into timed pregnant mice at E15.5; embryos were collected at E18.5 and processed for BrdU immunostaining and quantification. Only strong

BrdU-labeled cells, cells with ≥75% BrdU nuclei saturation, were counted. The distribution of strong BrdU-labeled cells was analyzed by binning, as described above.

Quit fraction analysis. BrdU (100 μg/g body weight) was i.p. injected into timed pregnant mice at E11.5, E12.5, E13.5, E14.5 or E15.5. Embryos were collected 24 hours later and processed for BrdU and Ki67 immunostaining, as described above. The numbers of all cells stained for BrdU (all $BrdU^+$) and cells stained for BrdU but not for Ki67 ($BrdU^+Ki67^-$) were counted. The quit fraction (QF%) was calculated as the percentage of $BrdU^+Ki67^-$ among all $BrdU^+$ cells.

RNA sequencing (RNA-seq) and data analysis

E15.5 *NfiB*$^{+/+}$ and *NfiB*$^{-/-}$ cortices were dissected (n=3/genotype), total RNAs were isolated from each cortex (Qiagen RNAeasy kit) and used to prepare RNA-seq libraries (Illumina RNA Truseq Library Prep protocol). Libraries were paired-end (50 nucleotides per end) sequenced on Illumina Hiseq2000 platform. Between 77 and 88 million read pairs were obtained for each sample. After filtering out read pairs that matched elements in the mouse RepeatMasker library (Smit et al, 1996-2010) (less than 2% per sample), reads were mapped to the UCSC (mm9) mouse assembly with TopHat (Trapnell et al., 2009), using Bowtie (Langmead et al., 2009) as the underlying aligner. Only uniquely-mapping, fully-paired reads were kept and potential PCR duplicates were removed using SamTools (Li et al., 2009). Between 49 and 57 million mapped read pairs remained per sample. From these mappings, the

count of reads was determined for the canonical transcript of each gene in the set of UCSC Known Genes (Hsu et al., 2006) for the UCSC mm9 mouse assembly. These counts were analyzed for differential expression of genes between *NfiB*$^{+/+}$ and *NfiB*$^{-/-}$ samples using DESeq (Anders and Hubers, 2010), which models the expression variation within replicates as a function of total gene expression, to determine the significance of expression differences between conditions. A threshold for significance was set at the DESeq adjusted p-value of 0.1.

To understand the biological meaning of the output gene list, we used the Database for Annotation, Visualization and Integrated Discovery (DAVID) (Huang et al., 2009a, 2009b). The list of differentially expressed genes was uploaded into DAVID then analyzed by functional annotation clusters. A summary of gene clusters exhibiting the highest enrichment scores are in Table 3 and 4.

2.4 Results

NFIB is expressed in radial glia and corticofugal neurons throughout corticogenesis

NFIB is expressed in both deep layer neurons and neural progenitor cells (Mason et al., 2009; McKenna et al., 2011), but its expression profile in individual subtypes of neural progenitors is not known. To determine which progenitor cells expressed NFIB during cortical development, we used specific antibodies on E12.5-E18.5 brain sections to co-label cells expressing NFIB against known neural progenitor and layer-specific neuronal markers. Taking advantage of the *LacZ* insertion into the *NfiB* locus of *NfiB*$^{+/-}$ mice (Steele-Perkins et al., 2005), in addition

to *NfiB*$^{+/+}$ mice, we used *NfiB*$^{+/-}$ mice to maximize detection of NFIB and cell-type specific marker co-expression. To ensure βGAL was an appropriate marker of NFIB-expressing cells, we performed immunohistochemistry with antibodies against βGAL and NFIB and found that βGAL expression recapitulates that of NFIB in *NfiB*$^{+/-}$ brains (Figure 1).

Immunohistochemical analysis of E12.5 and E13.5 brains revealed coexpression of NFIB and Ki67, confirming NFIB expression in neural progenitors (Figure 2A, E, P and T) (Plachez et al., 2008; Mason et al., 2009). Starting at E12.5, two major progenitor cell types were present: radial glia and basal progenitors. Radial glia in the ventricular zone (VZ) were SOX2^{+}PAX6^{+} (Figure 2F-H and J). Basal progenitors in the SVZ were TBR2^{+}SOX2^{low} (Figure 2K-M and O) (Arnold et al., 2008). βGAL was expressed at high levels in all SOX2^{+}PAX6^{+} radial glia (Figure 2F-J), but expression was generally low or completely absent in TBR2^{+} basal progenitors, despite the presence of a few TBR2^{+}βGAL^{+} cells (Figure 2K-O). It is likely that these TBR2^{+}βGAL^{+} cells were in transition from radial glia to basal progenitors, or from basal progenitors to neurons. Similarly, very few TBR2^{+} basal progenitors expressed βGAL at E15.5 or E18.5 (Figure 2EE, 2II and 3E).

Beginning at E15.5, the presence of outer radial glia, identified by SOX2 expression in the outer subventricular zone (oSVZ), became apparent (Figure 2W, and FF). Both SOX2^{+} and PAX6^{+} radial glia expressed NFIB (or βGAL) at E15.5 and E18.5, however, only low-level expression was apparent in outer radial glia (Figure 2U, Y, Z, DD, EE, FF, II and 3A, C). Together, these data demonstrate that during

corticogenesis, radial glia express NFIB, but expression is almost entirely excluded from basal progenitors and outer radial glia.

We next characterized NFIB expression in the developing cortical plate. Immunostaining analyses revealed co-expression of NFIB and known markers of corticofugal projection neurons. Subcerebral marker, CTIP2, and NFIB were co-expressed in deep layers of the cortical plate at E12.5 and E13.5 (Figure 2A, E, P and T), the time when these neurons are generated (Leone et al., 2008; McKenna et al., 2011). $CTIP2^{+}$ neurons also expressed NFIB (or βGAL) at E15.5 (Figure 2U, Y, Z, DD).

To further characterize the molecular identity of NFIB-expressing cells, we analyzed co-expression with NFIA, DARPP32 and SATB2 (Figure 3G, I, K). NFIA, another transcription factor in the *Nfi* gene family, is expressed in proliferative zones and deep layer cortical neurons (Plachez et al., 2008; Mason et al., 2009), but whether NFIA and NFIB are expressed in the same cells is unknown. We observed βGAL and NFIA co-expression in the VZ and layer 6 (Figure 3G). βGAL was also co-expressed with layer 6 corticothalamic marker, DARPP32 (Molyneaux et al., 2005) (Figure 3I). Conversely, there was little co-expression with SATB2, a known marker of callosal projection neurons (Alcamo et. al, 2008; Britanova et. al, 2008; Chen et al., 2008) (Figure 3K). However, of the few $SATB2^{+}\beta GAL^{+}$ neurons, most were located in layer 6 (Figure 3K). Additionally, NFIB and βGAL expression was noticeably stronger in postmitotic neurons compared to that in neural progenitors (Figure 2). Collectively, analysis of neuronal marker expression indicates that NFIB is expressed

in corticofugal neurons throughout corticogenesis and may also be expressed in a small subset of deep layer callosal projection neurons. Overall, the expression profile of NFIB throughout cortical development suggests it may regulate neurogenesis and differentiation of radial glia and corticofugal neurons.

NfiB$^{-/-}$ mice display a reduction in upper cortical layer thickness during late neurogenesis

To determine the function of NFIB in cortical development, we investigated what effects the loss of NFIB had on overall cortical organization in *NfiB*$^{-/-}$ mice. We first determined the molecular identity of βGAL^{+} cells in E18.5 *NfiB*$^{-/-}$ mice by immunostaining with antibodies against βGAL and markers of neural progenitors or postmitotic neurons. Similar to *NfIB*$^{+/+}$ and *NFiB*$^{+/-}$ brains, we found that in *NfiB*$^{-/-}$ mice, βGAL was expressed in SOX2^{+} and PAX6^{+} radial glia, but expression was weak or absent in SOX2^{+} outer radial glia and TBR2^{+} basal progenitors (Figure 3A-F). We observed βGAL and NFIA co-expression in layer 6 and the proliferative zone (Figure 3H), and βGAL expression in DARPP32^{+} corticothalamic projection neurons (Figure 3J). The majority of SATB2^{+} callosal projection neurons did not express βGAL (Figure 3L) and those that did were predominantly in layer 6, similar to *NfiB*$^{+/-}$ cortices (Figure 3K-L). Together, these results indicated that the molecular identity of βGAL^{+} NFIB-mutant cells was similar to NFB-expressing cells in *NfiB*$^{+/+}$ and *NfiB*$^{+/-}$ cortices.

While the overall expression of cell-type specific markers was comparable in control (*NfiB*$^{+/+}$ or *NfiB*$^{+/-}$) and *NfiB*$^{-/-}$ cortices, thickness of upper layers 2-4 appeared smaller in *NfiB*$^{-/-}$ cortices (Figure 3). To further investigate this, we compared laminar organization of control (*NfiB*$^{+/+}$) and *NfiB*$^{-/-}$ cortices. CTIP2 expression was higher in layer 5 than in layer 6 in both control (Figure 4A, C, D) and mutant (Figure 4E, G, H) littermates. Co-immunostaining with CTIP2 and SATB2 clearly revealed a reduction in upper layer (2-4) thickness as well as a modest expansion of deep layers 5-6 (Figures 4A-H). Immunostaining with additional antibodies against layer specific markers, BETA3 and TBR1, revealed a similar outcome. In control mice, BETA3 is strongly expressed in layer 5 and to a lesser extent in upper layers (Figure 4I, K, L). However, in *NfiB*$^{-/-}$ cortices, we observed an increase in BETA3^{+} cell density within layer 5 (Figure 4M, O, P), ectopic BETA3^{+} neurons in layer 6 (arrows, Figure 4P) and a reduction in upper layer thickness (Figures 4I, K, L, M, O, and P). In *NfiB*$^{+/+}$ mice, TBR1 was predominantly expressed in layer 6 corticothalamic neurons, while some TBR1^{+} neurons were also observed in upper layers (Figure 4J-L). However, *NfiB*$^{-/-}$ mice displayed an absence of TBR1^{+} cells in upper layers (Figure 4N-P).

To quantitatively assess the loss of *NfiB* on cortical lamination, we measured and compared thicknesses of regions containing upper layer SATB2^{+} neurons (UL-S) or deep layer CTIP2^{+} neurons (DL-C) in *NfiB*$^{+/+}$ and *NfiB*$^{-/-}$ brains. Subsequently, this enabled comparison of overall cortical plate thickness. For measurements, we performed immunostaining with antibodies against CTIP2 and SATB2 at E16.5 and E18.5. We defined (UL-S), layers 2-4, as the cortical region containing SATB2^{+} but

not CTIP2^{+} neurons. DL-C, layers 5 and 6, were defined as the region containing CTIP2^{+} cells, regardless of SATB2 expression. Cortical plate thickness was defined as the sum of upper and deep layer thicknesses (schematic in Figure 4Q). At E16.5, the overall thickness of the cortical plate was significantly reduced in *NfiB*$^{-/-}$ mice (171.8 ± 10.9μm) compared to *NfiB*$^{+/+}$ (215.5 ± 15.1μm, $p=0.0313$), predominantly due to a reduction in UL-S thickness. In *NfiB*$^{+/+}$ mice, UL-S (41.8 ± 3.1μm) comprised approximately 19.5% of the cortical plate but in *NfiB*$^{-/-}$ littermates, UL-S (13.5 ± 2.7μm, $p<0.0001$) was only 7.7% of the cortical plate.

Likewise, at E18.5, UL-S was significantly thinner in *NfiB*$^{-/-}$ brains compared to *NfiB*$^{+/+}$ mice (*NfiB*$^{+/+}$ 90.6 ± 4.1μm vs. *NfiB*$^{-/-}$ 57.2 ± 1.6μm, $p=<0.0001$). Regardless of an overall reduction in cortex thickness (from apical to basal surfaces) (Figure 3, 4), the thickness of the cortical plate was comparable between mutant and control littermates, a result explained by an expansion of the DL-C (Figure R). Collectively, immunostaining and quantitative analysis reveal that in *NfiB*$^{-/-}$ mice, the ratio of deep to upper layers in the cortical plate shifted more toward a deep layer profile. Observed changes in cortical layer thickness in *NfiB*$^{-/-}$ mice and NFIB expression in radial glia and corticofugal neurons, together suggest that NFIB is required for proper neurogenesis and neuronal differentiation.

NfiB$^{-/-}$ mice display a significant loss of corticothalamic and corticospinal axonal projections

Considering that NFIB is robustly expressed in corticofugal neurons, we asked whether NFIB is required for proper differentiation of corticofugal neurons, specifically, for axon development. To answer this, we used transgenic methods to label and analyze axonal projections. *Fezf2* (also known as *Fezl*, *Zfp312* and *Znf312*) is expressed in both subcerebral and corticothalamic projection neurons (Chen et al., 2005a; Chen et al., 2008; Leone et al., 2008; McKenna et al., 2011). In the *Fezf2* mouse, an *ires-PLAP* (internal ribosomal entry site-Placental Alkaline Phosphatase) was inserted into the *Fezf2* open reading frame (Chen et al., 2005a), thus cell bodies and axons of subcerebral and corticothalamic projection neurons are made visible by PLAP staining. Similarly, the *Golli-τ-GFP*$^{+}$ allele directs expression of GFP in corticofugal projection neurons (Jacobs et al., 2007), allowing direct observation of GFP-labeled axons.

We analyzed corticofugal axons in *NfiB*$^{+/+}$*;Fezf2*$^{PLAP/+}$, *NfiB*$^{+/-}$*;Fezf2*$^{PLAP/+}$ and *NfiB*$^{-/-}$*;Fezf2*$^{PLAP/+}$ mice at E18.5 by PLAP staining. As expected, in *NfiB*$^{+/+}$*; Fezf2*$^{PLAP/+}$ mice, bundles of PLAP^{+} axons were observed projecting through the internal capsule (Figure 5B, asterisk), toward the thalamus (Figure 5B, arrowhead) and projecting through the cerebral peduncle toward the spinal cord (Figure 5A, C, D, arrows,). There was a modest reduction of PLAP^{+} corticofugal axons in *NfiB*$^{+/-}$*;Fezf2*$^{PLAP/+}$ mice (data not shown). Strikingly, in *NfiB*$^{-/-}$*; Fezf2*$^{PLAP/+}$ mice, very few PLAP^{+} axons projected through the internal capsule (Figure 5F, asterisk), and axons projecting toward the thalamus (Figure 5F, arrowhead) or through the cerebral peduncle (Figure 5E, G, H, arrows) were not detected. In addition, no ectopic axons

were observed. These results suggest that in the absence of *NfiB*, corticofugal neurons failed to project axons out of the cerebral cortex.

We also analyzed GFP-labeled corticofugal axons in *NfiB*$^{+/+}$*; Golli-τ-GFP*$^{+}$, *NfiB*$^{+/-}$*; Golli-τ-GFP*$^{+}$ and *NfiB Golli-τ-GFP*$^{+}$ mice at E18.5. In *NfiB*$^{+/+}$*; Golli-τ-GFP*$^{+}$ animals, GFP^{+} axons projected through the internal capsule (Figure 5K, L, asterisks) toward the thalamus (Figure 5K-M, open arrows), pons (Figure 5I and J, white arrows) and cerebral peduncle (Figure 5N, white arrowheads). There was an intermediate loss of GFP^{+} corticofugal axons in *NfiB*$^{+/-}$*; Golli-τ-GFP*$^{+}$ mice (data not shown). However, in *NfiB*$^{-/-}$*; Golli-τ-GFP*$^{+}$ mice, very few GFP^{+} axons were detected in the internal capsule (Figure 5Q, R, asterisks) and thalamus (Figure 5Q-S, open arrows). A drastic reduction of GFP^{+} axons projecting through the pons (Figure 5O and P, white arrows) and cerebral peduncle (Figure 5T, white arrowheads) was also observed. Collectively, these results showed that in *NfiB*$^{-/-}$ mice, corticofugal neurons failed to project axons to expected targets, indicating that NFIB is required for proper differentiation of corticofugal neurons.

Loss of M phase and S phase neural progenitors within the SVZ and oSVZ during late corticogenesis

To determine the function of NFIB in neural progenitors, we first compared proliferative zone organization of *NfiB*$^{+/+}$ and *NfiB*$^{-/-}$ mice from E12.5 to E18.5 by analyzing the expression of TBR2 and Ki67. Together, these markers labeled the VZ, SVZ and oSVZ, thus defining the boundaries of the proliferative zone (VZ + o/SVZ) (Figure 6A-C). At E12.5 and E14.5, the thickness of the proliferative zone, as both

an absolute measurement and as a percentage of overall cortical thickness, was similar in control and mutant mice (Figure 6D). At E16.5, *NfiB*$^{-/-}$ brains displayed a significant decrease in proliferative zone thickness compared to *NfiB*$^{+/+}$ brains (Figure 6D). As a percentage of overall cortical thickness, the proliferative zone in *NfiB*$^{+/+}$ animals made up 47.6% ± 2.2% of the cortex, while in *NfiB*$^{-/-}$, it was only 39.0% ± 5.1%, *p=0.0004.* Most notable was the striking absence of TBR2^{+} cells in the oSVZ and compaction of these cells near the ventricular surface in *NfiB*$^{-/-}$ cortices (Figure 6A-B). A significant decrease was also observed at E18.5 (*NfiB*$^{+/+}$ 41.6% ± 3.4% versus *NfiB*$^{-/-}$ 32.0% ± 3.6%, *p<0.0001*) (Figure 6D), indicating that proliferative zone thickness was specifically affected at later stages of cortical development.

To further examine defects in the proliferative zone, we analyzed neural progenitors during different phases of the cell cycle. First, we compared the number and cortical location of cells in E12.5-E18.5 *NfiB*$^{+/+}$ and *NfiB*$^{-/-}$ mice that expressed phosphorylated histone H3 (PHH3), a marker for cells in M phase (Figure 6E-I). At E12.5 and E14.5, the number of PHH3^{+} cells and their cortical position were similar in *NfiB*$^{+/+}$ and *NfiB*$^{-/-}$ brains (Figure 6I). However, a significant loss of total number of PHH3^{+} cells (*NfiB*$^{+/+}$ 77.1 ± 6.6 cells/mm vs. *NfiB*$^{-/-}$ 41.1 ± 3.0 cells/mm, *p=<0.0001*) was observed in E16.5 mutant brains (Figure 6E-I). The loss was due to significantly fewer PHH3^{+} cells in both the o/SVZ (*NfiB*$^{+/+}$ 37.1 ± 4.0 cells/mm vs. *NfiB*$^{-/-}$ 16.1 ± 2.8 cells/mm, *p=0.0006*) and VZ (*NfiB*$^{+/+}$ 40.2 ± 3.9 cells/mm vs. *NfiB*$^{-/-}$ 25.1 ± 2.3 cells/mm, *p=0.0044*) (Figure 6E-I). Interestingly, despite a significant

loss of total number of PHH3^{+} cells in E18.5 *NfiB*$^{-/-}$ brains (*NfiB*$^{+/+}$ 24.1 ± 2.5 cells/mm versus *NfiB*$^{-/-}$ 16.4 ± 1.9 cells/mm, *p=0.0263*), a comparable number of PHH3^{+} cells were observed in the VZ, indicating that the loss was specifically due to significantly fewer PHH3^{+} cells within the o/SVZ (Figure 6I). These results suggest a loss of actively dividing neural progenitors in *NfiB*$^{-/-}$ mice during late corticogenesis, an effect more striking in the SVZ and oSVZ.

Next, we compared number and cortical distribution of neural progenitors in S phase (Figure 6J-O). BrdU was administered to pregnant mice carrying E18.5 embryos; brains were collected 2 hours later and processed for BrdU immunohistochemistry. BrdU^{+} cells were quantified by cortical binning (10 bins). When individual cortices were divided into bins, there was a trend such that the marginal zone was in bin 1, the cortical plate was in bins 2-6, the SVZ and oSVZ (o/SVZ) was in bins 7-9 and the VZ was predominantly in bin 10 (Figure 6N, schematic). We determined the distribution of S phase progenitors by quantification of BrdU^{+} cells in each of the following regions: the cortical plate (including the marginal zone), o/SVZ, and VZ. There was a significant loss of total number of BrdU^{+} cells in *NfiB*$^{-/-}$ mice (54.6 ± 2.2 cells/100 μm, *p=0.0316*) compared to littermate controls (70.5 ± 6.5 cells/100 μm) (Figure 6J-O). While the number of BrdU^{+} cells in bin 10 was similar in *NfiB*$^{+/+}$ and *NfiB*$^{-/-}$ animals, loss of total number was due to significantly fewer BrdU^{+} cells in bins 7-9 (*NfiB*$^{+/+}$ 33.3 ± 2.8 cells/100 μm vs. *NfiB*$^{-/-}$ 18.5 ± 1.7 cells/100 μm, *p<0.0001*) and 1-6 (*NfiB*$^{+/+}$ 8.9 ± 1.2 cells/100 μm vs. *NfiB*$^{-/-}$ 2.0 ± 0.4 cells/100 μm, *p<0.0001*) (Figure 6O), clearly indicating a

severe loss of S phase progenitors within the SVZ and oSVZ in *NfiB*$^{-/-}$ mice. Taken together with the observed reduction in proliferative zone thickness in *NfiB*$^{-/-}$ mice, these results suggest that NFIB is required for the generation or survival of neural progenitors located specifically within the SVZ and oSVZ, but not VZ.

Outer radial glia and basal progenitors are absent in *NfiB*$^{-/-}$ mice during late corticogenesis

To determine which subclasses of neural progenitors were affected by loss of *NfiB*, we immunostained E12.5-E18.5 *NfiB*$^{+/+}$ and *NfiB*$^{-/-}$ brains with PAX6, SOX2 and TBR2 antibodies. Tuj1 (Figure 7A-L) or CTIP2 (Figure 7M-V) antibodies were used to label cortical neurons. PAX6 and Tuj1 expression was similar in *NfiB*$^{+/+}$ and *NfiB*$^{-/-}$ mice at E12.5 (Figure 7A-F). At E14.5, expression of PAX6 was unaffected in *NfiB*$^{-/-}$ mice compared to controls, as was the expression of SOX2 and TBR2 (Figure 7G, I, J, L and 8A, B, D, E, F, H). However, Tuj1 staining revealed fewer axons at E14.5, a time when most cortical neurons are of corticofugal identity (Figure 7H, I, K, L and Figure 8C, D, G, H). These results indicate that axon defects in corticofugal neurons due to a loss of NFIB begin around mid-corticogenesis (E14.5), yet all subclasses of neural progenitors were unaffected up to this timepoint.

Defects in the expression of markers for neural progenitor subtypes in *NfiB*$^{-/-}$ mice were observed during late (E16.5-E18.5) corticogenesis. In E16.5 *NfiB*$^{-/-}$ cortices, despite a similar total number, there was significantly more PAX6^{+} cells in the VZ (*NfiB*$^{-/-}$ 153.9 ± 9.1 cells/100μm vs. *NfiB*$^{+/+}$ 128.9 ± 7.6 cells/100μm, *p=0.0095*), yet markedly fewer in the o/SVZ (*NfiB*$^{-/-}$ 12.9 ± 1.0 cells/100μm vs.

NfiB$^{+/+}$ 40.4 ± 3.1 cells/100μm, *p<0.0001*) (Figure 7M, O, Q, R, T, V and EE), indicating more radial glia but a loss of outer radial glia. TBR2^{+} cells were present in both the SVZ and oSVZ in *NfiB*$^{+/+}$ mice (Figure 8I and J). However, the total number of TBR2^{+} basal progenitors was significantly reduced in *NfiB*$^{-/-}$ littermates (*NfiB*$^{+/+}$ 156.2 ± 10.0 cells/100μm vs. *NfiB*$^{-/-}$ 99.9 ± 3.6 cells/100μm, *p<0.*0001), and although there were significantly fewer TBR2^{+} basal progenitors in the deeper SVZ, more dramatic was the loss in the oSVZ (*NfiB*$^{+/+}$ 47.2 ± 4.0 cells/100 μm vs. *NfiB*$^{-/-}$ 13.0 ± 1.2 cells/100 μm, *p<0.0001*) (Figure 8I-L and Q).

At E18.5, *NfiB*$^{-/-}$ mice displayed a loss of PAX6^{+}/SOX2^{+} outer radial glia and TBR2+ basal progenitors (Figure 7W-EE and 8M-Q). Although there was approximately the same total number of PAX6^{+} cells in *NfiB*$^{+/+}$ and *NfiB*$^{-/-}$ cortices, there were significantly fewer PAX6^{+} cells in the *NfiB*$^{-/-}$ o/SVZ (Figure 7W, Y, Z, AA, CC, DD and EE). Similar to analysis at E16.5, we observed a significant decrease in the number of TBR2^{+} basal progenitors in both the SVZ and oSVZ (Figure 8M-Q), Taken together, these results reveal that *NfiB*$^{-/-}$ mice have more radial glia but display a striking loss of outer radial glia and basal progenitors at E16.5 and E18.5. This suggests that NFIB may regulate the differentiation of radial glia into outer radial glia and basal progenitors during late corticogenesis.

To explain the loss of these two neural progenitor subtypes, we asked whether the absence of NFIB resulted in an increase in apoptosis or a decrease of their generation. We assayed the number of apoptotic cells in *NfiB*$^{+/+}$ and *NfiB*$^{-/-}$ cortices by immunostaining with an antibody against activated caspase 3 (CC3) at E15.5, one

day prior to the observed loss of neural progenitors (Figure 9). No statistical difference in $CC3^+$ cell number was observed (Figure 9J), indicating that loss of outer radial glia and basal progenitors in *NfiB*$^{-/-}$ cortices was not due to cell death, but instead, due to the lack of their generation. Furthermore, compared to the SVZ, the more severe loss of $TBR2^+$, $SOX2^+$ and $PAX6^+$ cells in the oSVZ strongly suggests that the fewer number of outer radial glia contributes to the reduction of basal progenitor generation in *NfiB*$^{-/-}$ mice.

Late-born neurons express deep-layer neuronal marker, CTIP2, and migration is delayed

To further investigate the function of NFIB in regulating neural progenitor proliferation and differentiation, we compared the quit fractions in *NfiB*$^{+/+}$ and *NfiB*$^{-/-}$ cortices at several timepoints throughout neurogenesis. BrdU was administered to pregnant mice at E11.5, E12.5, E13.5, E14.5 and E15.5; embryonic brains were collected 24 hours later and immunostained with Ki67 and BrdU antibodies. The quit fraction was calculated as the percentage of $BrdU^+Ki67^-$ cells among all $BrdU^+$ cells, representing the fraction of cells that exited the cell cycle on a given day. Compared to *NfiB*$^{+/+}$ littermates, the quit fraction was unaffected in *NfiB*$^{-/-}$ cortices at E11.5, E12.5, E13.5 and E14.5. However, a significant increase was observed at E15.5 (*NfiB*$^{+/+}$ 64.5% ± 1.7% versus *NfiB*$^{-/-}$ 76.8% ± 1.8%, $p=0.0045$) (Figure 10A).

The increased quit fraction in E15.5 *NfiB*$^{-/-}$ brains suggested more neurons were generated at this time. To test this, we performed birthdating analysis by injecting BrdU into pregnant mice carrying E15.5 embryos, collecting brains at E18.5

and immunostaining with antibodies against BrdU, CTIP2, and SATB2 (Figure 10B-I). The number of E15.5 $BrdU^+$ cells (see Material and Methods) was compared between $NfiB^{+/+}$ and $NfiB^{-/-}$ cortices. Consistent with results from quit fraction analyses (Figure 10A), the number of E15.5 $BrdU^+$ cells was significantly higher in $NfiB^{-/-}$ brains (70.0 ± 3.1 cells/100 μm, *p=0.0001)* than controls (49.4 ± 2.8 cells/100 μm) (Figure 10B, E, F, I, J).

To address whether NFIB plays a role in migration of neurons generated at E15.5, we compared the cortical distribution of E15.5 $BrdU^+$ cells by binning (refer to schematic, Figure 6N). E15.5 $BrdU^+$ cells per bin were quantified as a percentage of total E15.5 $BrdU^+$ cells. In $NfiB^{+/+}$ cortices, almost all E15.5 $BrdU^+$ cells were located in the cortical plate, with many of them in upper layers (Figure 10B, E, K). Conversely, in $NfiB^{-/-}$ mice, a significantly higher percentage of E15.5 $BrdU^+$ cells were positioned below the cortical plate while a significantly lower percentage were in upper cortical layers (Figure 10F, I, K). This indicates a delay or improper termination of neuronal migration, which may lead to the observed thinning of upper cortical layers (Figure 3, 4 and 10E, I).

Additionally, we investigated the identity of E15.5 $BrdU^+$ cells by their expression of CTIP2 and SATB2. There was no significant difference between the percentage of E15.5 $BrdU^+$ cells expressing SATB2 in $NfiB^{+/+}$ and $NfiB^{-/-}$ cortices. However, the percentage of those expressing CTIP2 was significantly higher in $NfiB^{-/-}$ brains ($NfiB^{+/+}$ 7.9% ± 1.4% versus $NfiB^{-/-}$ 21.1% ± 1.9%, $p<0.0001$) (Figure 10E, I, L). Similar to BrdU staining, many more $SATB2^+$ and $CTIP2^+$ cells were located

below the cortical plate in *NfiB*$^{-/-}$ cortices (Figure 10B-I), suggesting a migration defect. This possibly explains our observations of ectopic CTIP2^{+} cells located below the cortical plate and morphological abnormalities of CTIP2^{+} cells within the cortical plate of E16.5 *NfiB*$^{-/-}$ cortices (Figure 7N-P and S-V). In *NfiB*$^{+/+}$ mice, CTIP2^{+} neurons in the cortical plate were round in shape, a morphology typical of neurons that have completed migration (Figure 7N-P). In *NfiB*$^{-/-}$ mice, however, CTIP2^{+} neurons displayed an elongated morphology that is associated with neurons that are currently migrating (Figure 7S-U). Collectively, these results suggest that at E15.5, more cells exited the cell cycle and differentiated into neurons in *NfiB*$^{-/-}$ mice. They ectopically expressed early-born neuron marker, CTIP2, and their migration was defective. Thus, NFIB is required for proper neurogenesis and migration of late-born neurons.

Genome-wide transcriptome analysis revealed that NFIB regulates axonal projection and cell cycle progression

To investigate the function of NFIB in regulating cortical neurogenesis and neuronal differentiation, we performed gene expression analysis of E15.5 *NfiB*$^{+/+}$ and *NfiB*$^{-/-}$ cortices by RNA-seq (see Material and Methods). We used the DESeq program to compare gene expression of *NfiB*$^{-/-}$ samples against controls (Anders et al., 2010) and found that expression levels of 1844 genes in E15.5 *NfiB*$^{-/-}$ mice were significantly changed. Among them, 929 were increased by at least 1.17-fold and 915 were decreased by at least 0.85-fold.

We performed gene annotation analysis using the online bioinformatics tool, DAVID (Database for Annotation, Visualization and Integrated Discovery). Misregulated genes in *NfiB*$^{-/-}$ cortices were clustered with regards to their function; clusters were organized by enrichment score (Huang et al., 2009a; Huang et al., 2009b). Cluster 1 had the highest enrichment score and included 168 genes known to regulate cell cycle properties, such as M phase progression and cell division. There were 123 genes in Cluster 2, including transcription factors correlated with neuron differentiation and axon guidance molecules. Gene members of the Notch, Fgf, Shh and Wnt signaling pathways, all of which are important for cortical development (Gaiano et al., 2000; Cornell and Eisen, 2005; Louvi and Artavanis-Tsakonas, 2006; Dong et al., 2012; Tiberi et al., 2012), were also listed in Cluster 2. Cluster 3 included 100 genes, those of which regulate cell motion, neuron migration and cell localization (Table 3 and 4). Mis-regulation of these specific gene clusters in E15.5 *NfiB*$^{-/-}$ cortices provides further evidence that NFIB is essential for both proliferation and differentiation of cortical progenitor cells, and axonal projection of cortical neurons. Notch signaling is essential for regulating radial glia and outer radial glia maintenance and differentiation (Cornell and Eisen, 2005; Yoon and Gaiano, 2005; Louvi and Artavanis-Tsakonas, 2006; Guillemot, 2007; Shitamukai et al., 2011; Saito, 2012). In E15.5 *NfiB*$^{-/-}$ cortices, many members of the Notch signaling pathway were mis-regulated, including Dll1, Notch3, Hes1, Hes5, Hey1, and Hey2 (Table 4 and data not shown). We performed *in situ* hybridization on E18.5 *NfiB*$^{+/+}$ and *NfiB*$^{-/-}$ brains for several of these genes (Figure 11) and found that mis-regulation of Notch1,

Hes1 and Hes5 persisted throughout the remainder of cortical development. Compared to controls, expression of Notch1, Hes1 and Hes5 mRNA was significantly upregulated in the VZ (Figure 11), suggesting an increase in Notch signaling, specifically in radial glia, resulting in observed defects in radial glia differentiation in *NfiB*$^{-/-}$ mice.

2.5 Discussion

By carefully analyzing NFIB expression at embryonic stages and investigating the defects in *NfiB*$^{-/-}$ brains, our study revealed both novel and broad functions of NFIB in regulating the generation of cortical projection neurons, including radial glial differentiation, neuronal migration and axon projection. Multiple steps are involved in generating cortical projection neurons. First, radial glia expand the progenitor pool and generate outer radial glia, basal progenitors and neurons. Newly generated neurons migrate to their final laminar destinations, project axons and dendrites to appropriate targets to form functional neural circuits, and differentiate into mature neurons. Each of these processes is regulated by specific genetic pathways and embryonic environmental factors. A detailed comparison of *NfiB*$^{+/+}$ and *NfiB*$^{-/-}$ mice throughout cortical development revealed defects in both cortical neurogenesis and neuronal differentiation in *NfiB*$^{-/-}$ brains. During corticogenesis, NFIB is highly expressed in radial glia and in deep layer corticofugal neurons, suggesting important functions in regulating cortical development. Indeed, in *NfiB*$^{-/-}$ mice, outer radial glia and basal progenitors were absent, corticofugal neurons failed to project axons to the

thalamus and spinal cord, and migration of upper layer cortical neurons was defective. Additionally, RNA-sequencing revealed a misexpression of genes regulating cell cycle, neuronal differentiation, axonal projection, and cell migration in *NfiB*$^{-/-}$ cortices. Together, these results demonstrated the necessity of NFIB in neural stem and progenitor cell differentiation, corticofugal axon projection, and migration of late-born cortical projection neurons. Thus NFIB regulates the development of cortical projection neurons across many levels.

Compared to radial glia and basal progenitors, despite having been discovered over three decades earlier, outer radial glia have only recently been more thoroughly investigated in mice, ferrets and humans (Hevner and Haydar, 2012). In humans, outer radial glia and basal progenitors greatly amplify the neural progenitor pool for neuronal production, which in turn, is likely responsible for the expansion of upper layer cortical neurons (Fietz et al., 2010; Hansen et al., 2010; Reillo et al., 2011; Shitamukai et al., 2011; Wang et al., 2011a, 2011b; Hevner and Haydar, 2012). Other research indicates that the basal process of outer radial glia serve as migrating scaffolds for newly born neurons in the human cerebral cortex (Reillo et al., 2011). However, in rodents, there are significantly fewer outer radial glia; their roles in cortical neurogenesis and as migration guides are not fully understood.

Our results strongly indicate the importance of outer radial glia in both generation and migration of late born cortical projection neurons in mice. Outer radial glia were absent, cortical upper layers were thinner, and late born cortical neurons exhibited a delay in migration toward the cortical plate in *NfiB*$^{-/-}$ mice. Among these

defects, delayed migration of late-born cortical neurons may have contributed to the reduction in upper cortical layer thickness. NFIB expression in late-born neurons before birth is weak or absent (Figure 1), indicating that migration defects of these neurons in *NfiB*$^{-/-}$ mice may not be a direct consequence of lacking NFIB in the upper-layer neurons. The lack of a migration-scaffold provided by basal processes of outer radial glia is one likely cause of delayed migration. Additionally, ectopic expression of CTIP2 in late-born neurons in *NfiB*$^{-/-}$ mice suggests that lack of NFIB expression in neural progenitors can effect gene expression and differentiation of cortical neurons, which may indirectly leads to the neuronal migration defect. Collectively, these results suggest that NFIB is critical for generation of outer radial glia, and in turn, is essential for proper differentiation and migration of upper layer neurons.

To date, several genes and molecular pathways that regulate neural progenitor proliferation and differentiation have been identified. For example, increase in activation of the Notch signaling pathway in radial glia has been associated with maintaining ”stemness”, while low Notch signaling is correlated with neuronal differentiation (Gaiano et al., 2000; Yoon and Gaiano, 2005; Basak and Taylor, 2007; Imayoshi et al., 2011). Here we show that several genes in the Notch signaling pathway are upregulated in *NfiB*$^{-/-}$ cortices (Table 4 and Figure 11), supporting previous results indicating that NFI family members regulate Notch signaling (Deneen et al., 2006; Mason et al., 2009; Piper et al., 2010). However, molecular mechanisms that determine the outcome of radial glial progeny are not fully

understood, accordingly, further analysis of differentially expressed genes in *NfiB*$^{-/-}$ mice will provide insight into this process.

In addition to its role in generation of outer radial glia, NFIB is also essential for differentiation of corticofugal neurons as evidenced by the severe reduction of corticofugal axons in *NfiB*$^{-/-}$ mice (Figure 5). Moreover, NFIB is highly expressed in corticofugal neurons (Figures 2-4) and RNA-sequencing revealed a misexpression of genes that regulate axonal projections and axonogenesis in *NfiB*$^{-/-}$ mice (Table 3 and 4). Together, these results strongly indicate an extensive role for NFIB in differentiation of corticofugal projection neurons. Generation of a neuron-specific *NfiB* mutant mouse or selective interference of NFIB function in corticofugal neurons may further facilitate our understanding of its role in regulating corticofugal neuron differentiation and axon projection.

2.6 Acknowledgements

We thank Drs. Richard Gronostajski at State University of New York at Buffalo for generously providing the *NfiB*$^{+/-}$ mice and Dr. Anthony T. Campagnoni from University of California, Los Angeles for providing the *Golli-τ-GFP*$^{+}$ mice. We thank Matthew Eckler, William McKenna, Chao Guo and other members of the Chen lab for technical help and scientific discussions. This work was funded by R01MH082965 from National Institute of Health (to BC), a New Faculty Award RN1-00530-1 from California Institute of Regenerative Medicine (to BC), and a training grant R25GM058903 from National Institute of Health (to JB).

Figure 2.1. βGAL expression recapitulates NFIB expression in the cerebral cortex.

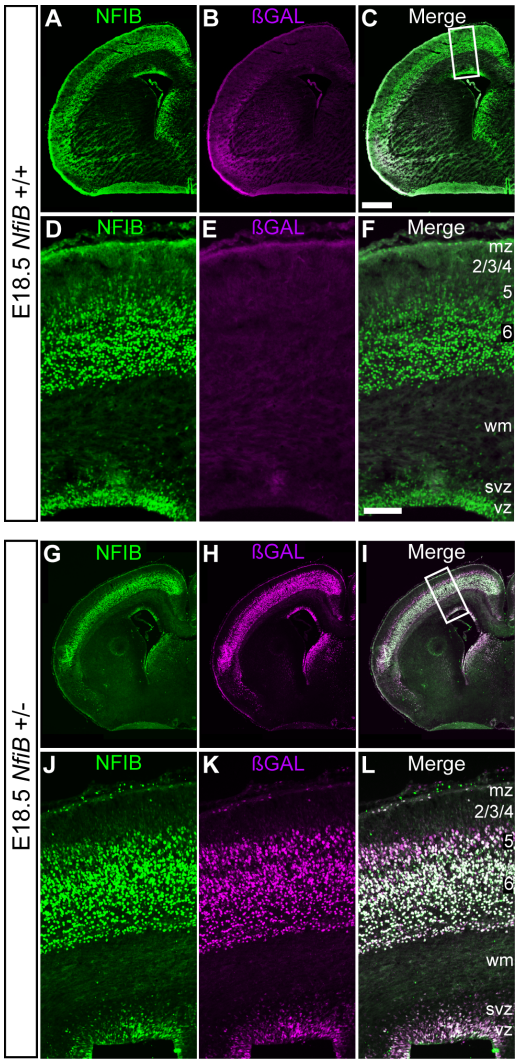

Immunohistochemistry and confocal microscopy were used to determine expression of βGAL and NFIB expression in coronal sections of E18.5 *NfiB*$^{+/+}$ (**A-F**) and *NfiB*$^{+/-}$ (**G-L**) brains. NFIB was expressed in deep cortical layers, 5 and 6, and proliferative zone of *NfiB*$^{+/+}$ (**A, D)** and *NfiB*$^{+/-}$ (**G, J**) cortices. βGAL was not expressed in *NfiB*$^{+/+}$ **(B, E)** cortices, and therefore did not coincide with NFIB expression (**C, F**). In *NfiB*$^{+/-}$ cortices, βGAL expression was restricted to nearly all NFIB-expressing cells in deep cortical layers and proliferative zones (**H, K**; Merge **I, L**), thus validating the use of βGAL immunostaining in identifying NFIB-expressing cells in *NfiB*$^{+/-}$ cortices. **A-C**, **G-I** Low magnification; scale bar, 500μm. **D-F**, **J-L** show boxed regions in **C** and **I**, respectively; scale bar, 100μm.

Figure 2.2. NFIB is expressed in neural progenitors and deep layer neurons throughout cortical development.

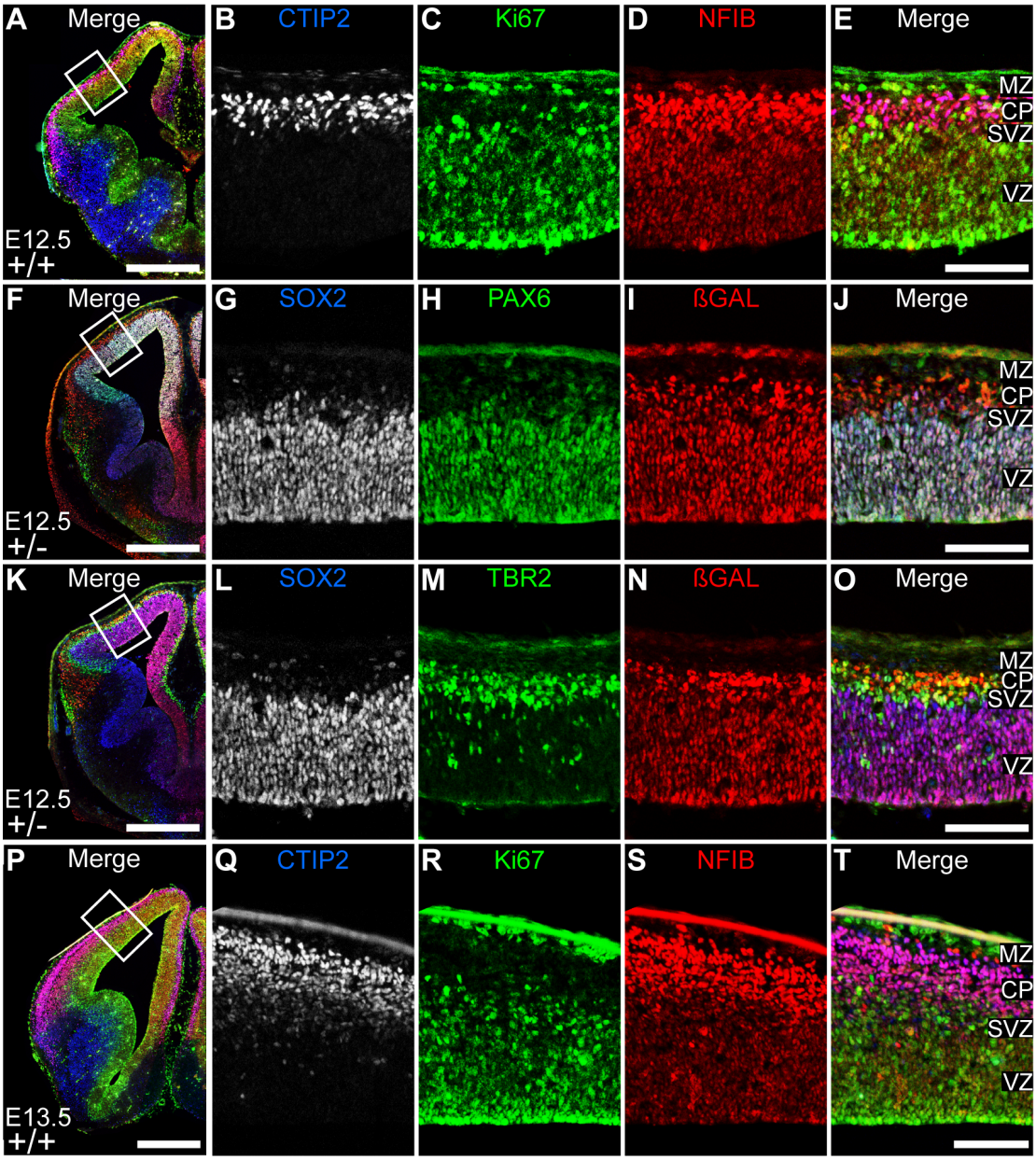

Figure 2.2 (*continued*) and caption on following page.

Figure 2.2 (*continued*). NFIB is expressed in neural progenitors and deep layer neurons throughout cortical development.

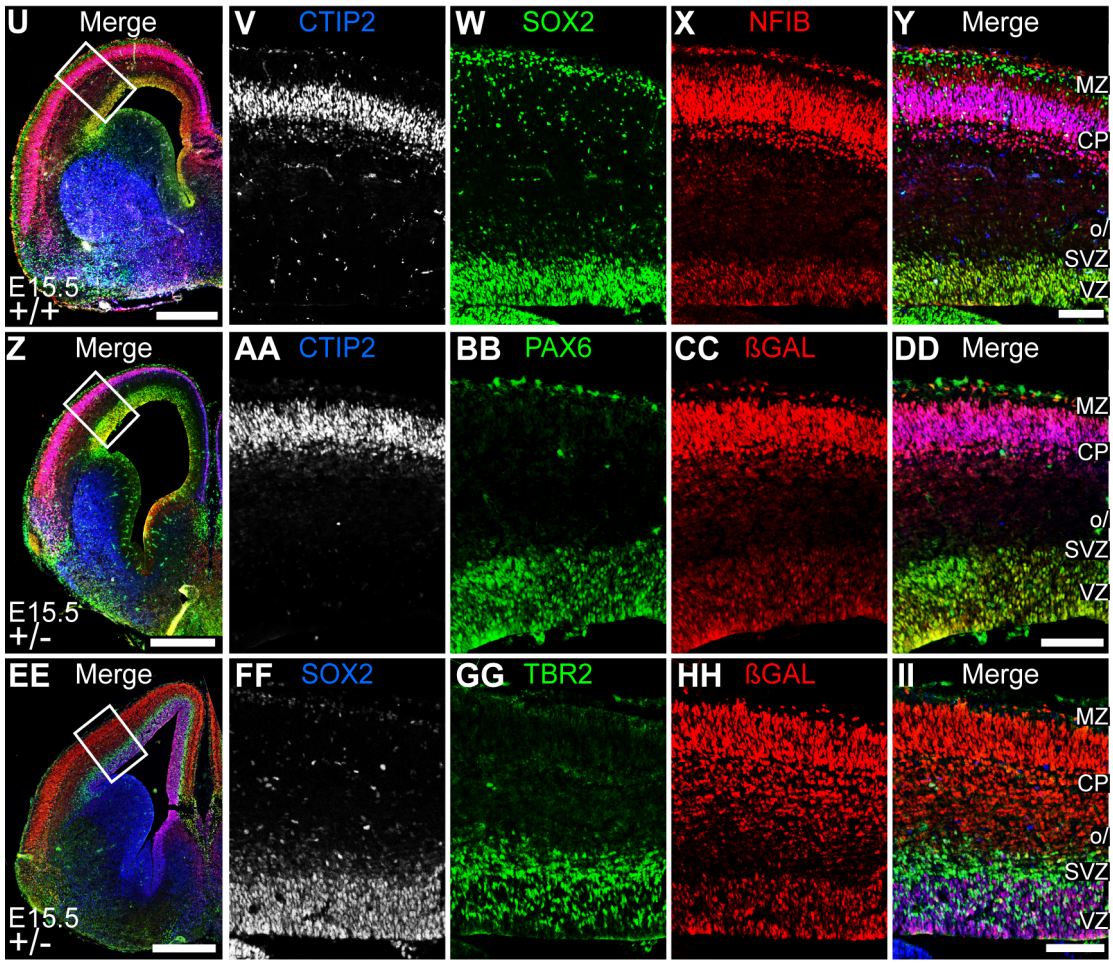

NFIB is expressed in neural progenitors and deep layer neurons throughout cortical development. Immunohistochemistry and confocal microscopy were used to determine cell-type specific expression of NFIB and βGAL in coronal sections of *NfiB*$^{+/+}$ (**A-E, P-T, U-Y**) and *NfiB*$^{+/-}$ (**F-O, Z-II**) brains, respectively. A-O, E12.5; P-T, E13.5; U-II, E15.5. **A, F, K, P, U, Z, EE** Low magnification; scale bars, 500μm. **B-E, G-J, L-O, Q-T, V-Y, AA-DD, EE-II** show boxed regions (**A, F, K, P, U**, **Z, EE**, respectively); scale bars, 100μm.

Figure 2.3. The molecular identity of *NfiB* mutant cells is similar to NFIB-expressing cells.

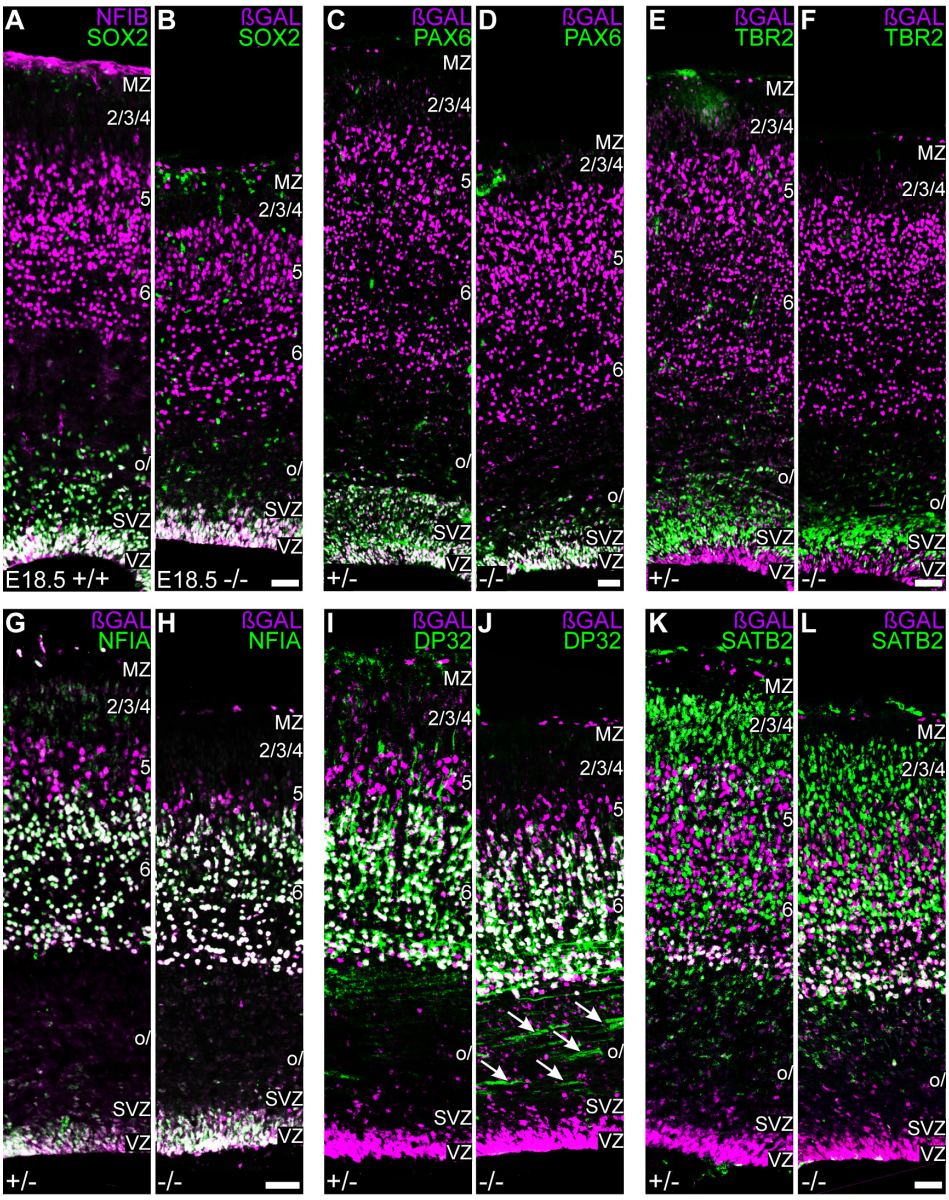

Immunohistochemistry and fluorescent microscopy were used to compare the molecular marker identities of NFIB or βGAL expressing cells in coronal sections of *NfiB*$^{-/-}$ and *NfiB*$^{+/+}$ or *NfiB*$^{+/-}$ cortices at E18.5. **A-B** Expression of NFIB (magenta, **A**) or βGAL (magenta, **B**) and SOX2 (green) in *NfiB*$^{+/+}$ (**A**) and *NfiB*$^{-/-}$ (**B**) cortices, respectively. **C-L** Expression of βGAL (magenta) and PAX6 (**B-C**), TBR2 (**D-E**), NFIA (**G-H**), DARPP32 (denoted as DP32, **I-J**) or SATB2 (**K-L**) (all in green) in *NfiB*$^{+/-}$ (**C, E, G, I** and **K**) and *NfiB*$^{-/-}$ (**D, F, H, J, L**) cortices. Scale bars, 25μm.

Figure 2.4. Severe thinning of upper cortical layers in *NfiB*$^{-/-}$ mice.

Immunohistochemistry and confocal microscopy were used to compare overall cortical lamination and expression of specific neuronal makers in *NfiB*$^{+/+}$ (**A-D, I-L, Q-R**) versus *NfiB*$^{-/-}$ (**E-H, M-R**) brains at E18.5. **A-H** Expression of CTIP2 and SATB2 in *NfiB*$^{+/+}$ and *NfiB*$^{-/-}$ cortices. **I-P** Expression of BETA3 and TBR1 in *NfiB*$^{+/+}$ and *NfiB*$^{-/-}$ cortices. Arrows (in **P**) point to BETA3-expressing cells in layer 6. **A-C, E-G**, **I-K, M-O** scale bar, 100μm. **D, H, L** and **P** show boxed region in **C, G, K** and **O**, respectively; dashed lines indicate estimated boundaries between cortical layers; scale bar, 50μm. **Q** Schematic shows definitions of regions containing upper layer SATB2^{+} neurons (UL-S) and deep layer CTIP2^{+} neurons (DL-C); see materials and methods for details. **R** Graph showing comparison of UL-S and DL-C thickness (μm) between *NfiB*$^{+/+}$ and *NfiB*$^{-/-}$ mice at E16.5 and E18.5. *p = 0.0077, ***p ≤ 0.0001 by t-test; n = 12 matched sections/age, 4 mice/genotype; error bars indicate SEM. Figure on following page.

Figure 2.4. Severe thinning of upper cortical layers in *NfiB*$^{-/-}$ mice.

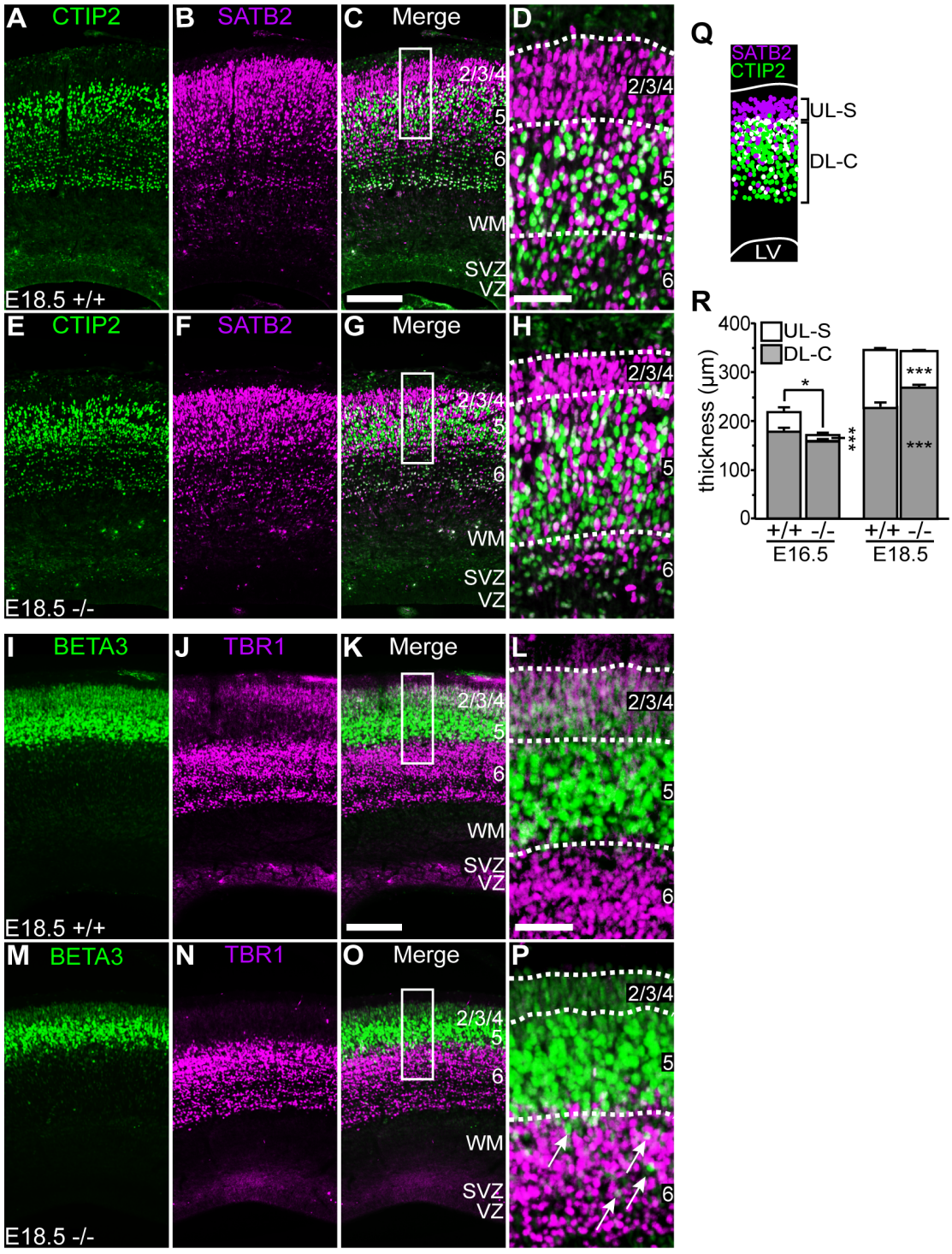

Figure 2.5. *NfiB*$^{-/-}$ mice display a significant loss of corticofugal axonal projections.

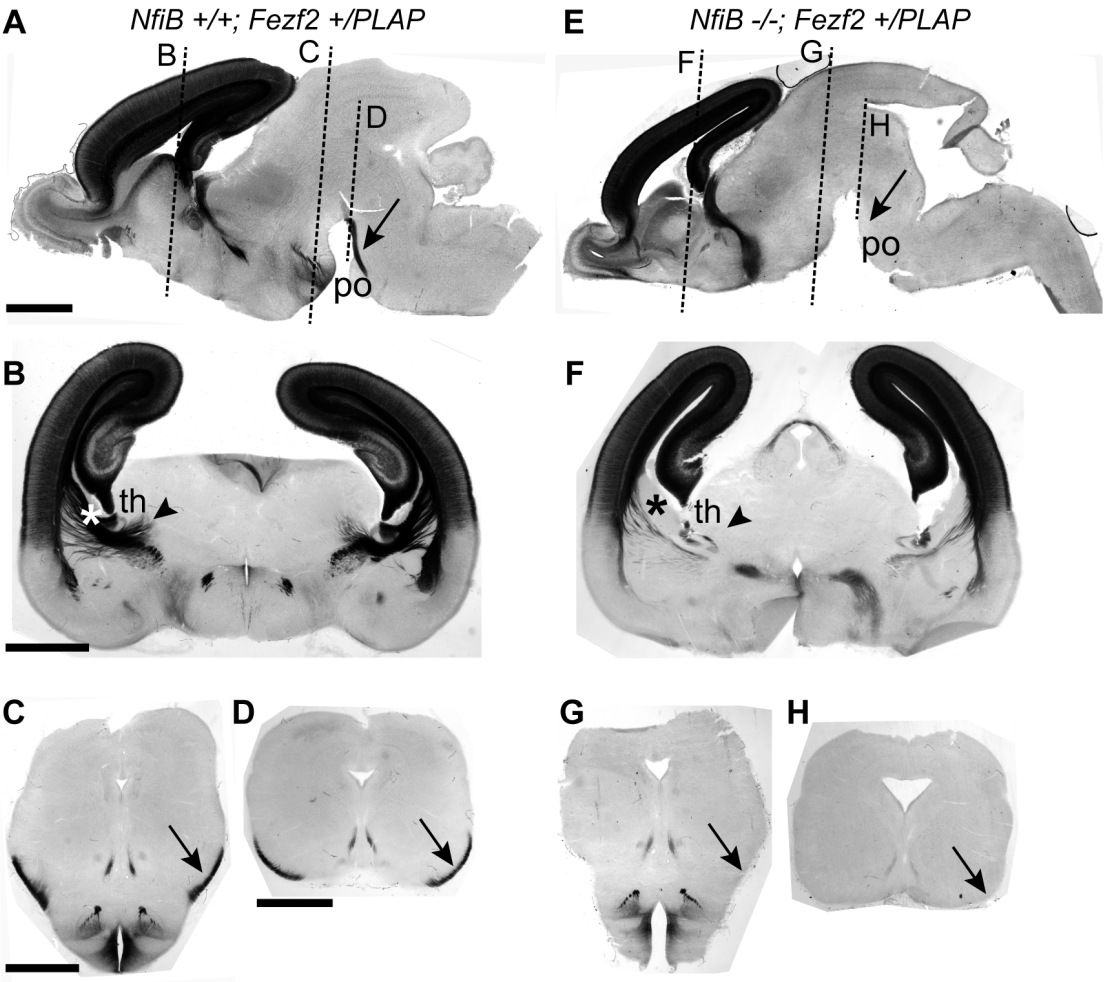

A-H PLAP-staining and bright field microscopy were used to identify PLAP-labeled (black) corticofugal axon tracts in *NfiB*$^{+/+}$; *Fezf2*$^{+/PLAP}$ (**A-D)** and *NfiB*$^{-/-}$; *Fezf2*$^{+/PLAP}$ (**E-H**) brains at E18.5. Sagittal sections (**A, E**) with dashed lines indicating approximate anterior-posterior location of coronal images displayed below (**B-D, F-H**, respectively).

Figure 2.5 and caption (*continued*) on following page.

Figure 2.5 (*continued*). *NfiB*$^{-/-}$ mice display a significant loss of corticofugal axonal projections.

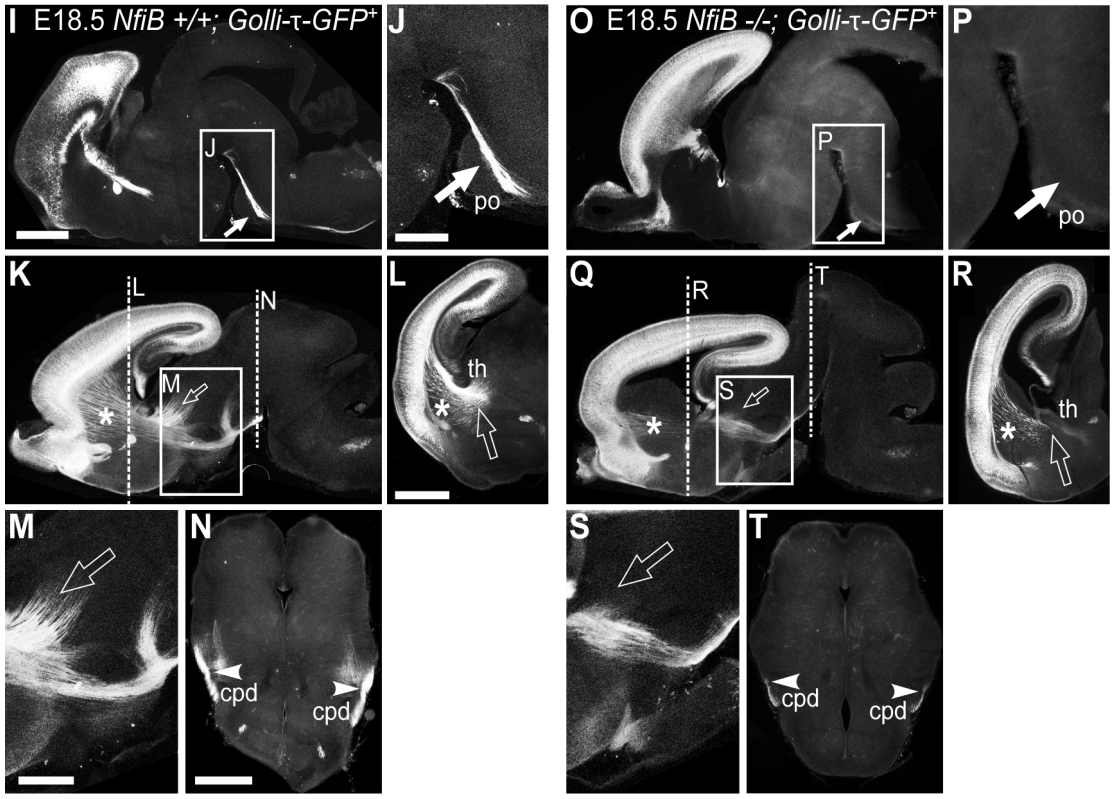

(*continued)* I-T Immunohistochemistry and fluorescent microscopy were used to identify GFP-labeled (white) corticofugal axon tracts in *NfiB*$^{+/+}$*; Golli-τ-GFP*$^{+}$ (**I-N**) and *NfiB*$^{-/-}$*; Golli-τ-GFP*$^{+}$ (**O-T**) brains at E18.5. **I-N** Sagittal (**I, J, K, M**) and coronal (**L, N)** views of subcerebral (**I** and **J**, **N**) and corticothalamic (**K** and **M, L**) tracts. Dashed lines in **K** and **Q** indicate approximate anterior-posterior location of coronal images (**L** and **N**, **R** and **T**, respectively). Black arrows (**A, C, D, E, G, H**) point to cerebral peduncle, black arrowheads (**B, F**) point to the thalamus. White arrows point to corticospinal tract through pons (**I, J**) or reduction thereof (**O, P**); open arrows point to corticothalamic tract (**K-M**) or reduction thereof (**Q-S**); asterisks (**B, F, K, L, Q** and **R**) indicate internal capsule; white arrowheads point to corticospinal tract through cerebral peduncle (**N**) or reduction thereof (**T**). **A-H, I, K, L, N, O, Q, R, T** Low magnification; scale bars, 1000μm. **J, M, P, S** show boxed region (**I, K, O, Q,** respectively); scale bars, 500μm. po, Pons; th, thalamus; cpd, cerebral peduncle Scale bars, 1000μm.

Figure 2.6. Loss of actively dividing neural progenitors during late corticogenesis.

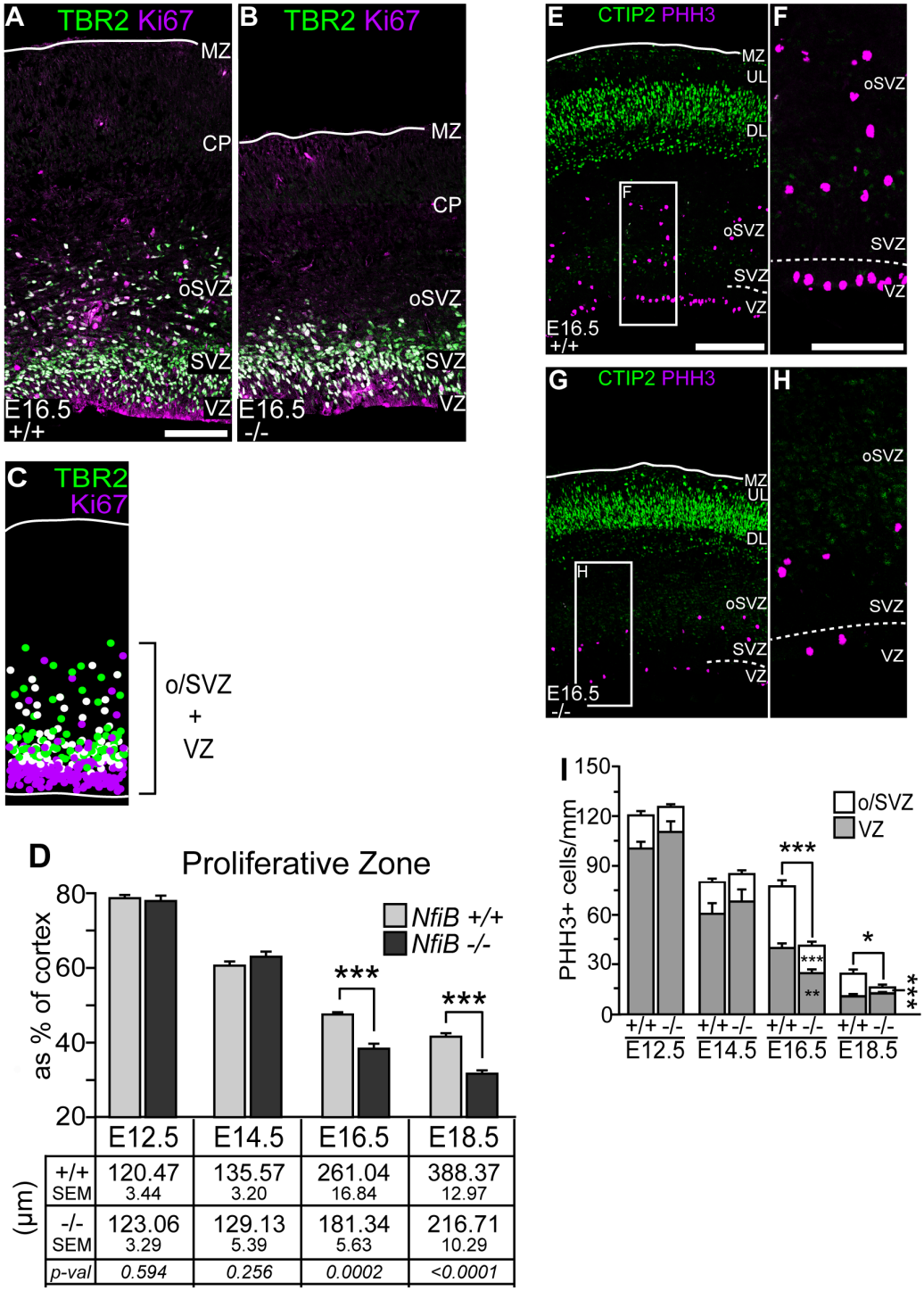

Figure 2.6 (*continued*) and caption on following page.

Figure 2.6 (*continued*). Loss of actively dividing neural progenitors during late corticogenesis.

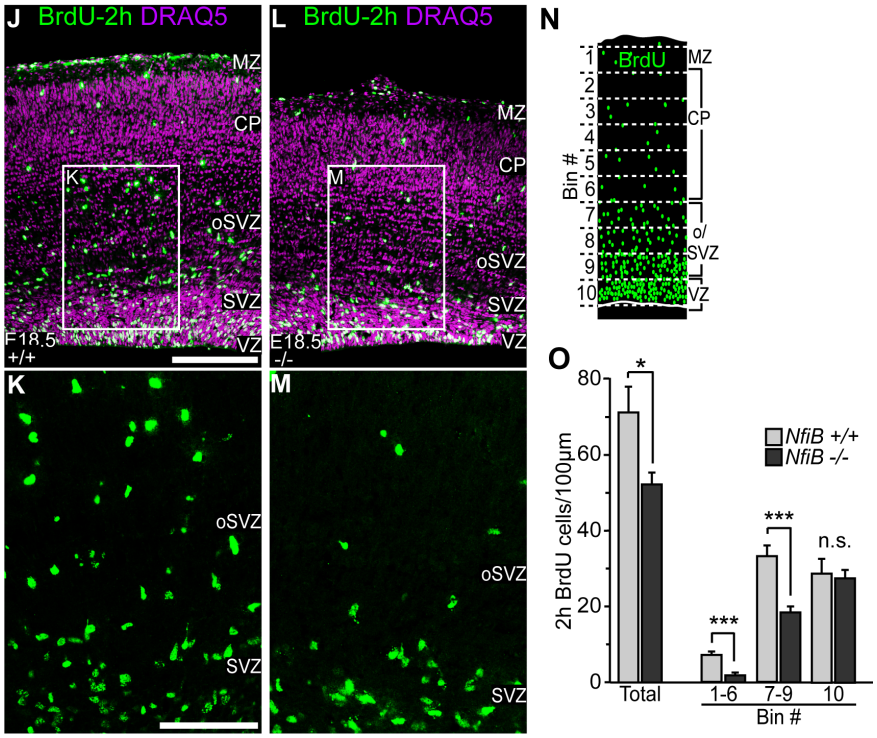

Immunohistochemistry and confocal microscopy were used to quantify and analyze the distribution of proliferating cells in coronal sections of *NfiB*$^{+/+}$ and *NfiB*$^{-/-}$ brains throughout cortical development. **A-D,** Expression of TBR2 (green) and Ki67 (magenta) in *NfiB*$^{+/+}$ (**A**) and *NfiB*$^{-/-}$ (**B**) cortices at E16.5. **C** Schematic showing definition of the proliferative zone (V + o/SVZ); see materials and methods for details. **D** Graph and table representing V + o/SVZ thickness as both a percentage of total cortical thickness and as absolute value (µm) in *NfiB*$^{+/+}$ and *NfiB*$^{-/-}$ mice at E12.5, E14.5, E16.5 and E18.5. ***p = 0.0004 (E16.5), ***p < 0.0001 (E18.5). **E-I** Expression of CTIP2 (green) and PHH3 (magenta) in *NfiB*$^{+/+}$ (**E, F**) and *NfiB*$^{-/-}$ (**G, H**) cortices at E16.5. **I,** Graph showing comparison of the number of PHH3-expressing cells/mm in VZ and o/SVZ (and total number) between *NfiB*$^{+/+}$ and *NfiB*$^{-/-}$ mice. *p = 0.0263, **p = 0.0044, ***p = 0.0001. **J-O** BrdU-labeled cells (green) and DRAQ5 nuclear stain (magenta) in E18.5 *NfiB*$^{+/+}$ (**J, K**) and *NfiB*$^{-/-}$ (**L, M**) cortices, 2 hours post BrdU-labeling. **N,** Schematic showing analysis of cortical distribution of BrdU-labeled cells by binning; see Materials and Methods for details. **O** Number of total BrdU-labeled cells/100µm and in bins 1-6, 7-9 and 10 was compared between E18.5 *NfiB*$^{+/+}$ and *NfiB*$^{-/-}$ cortices. *p = 0.0267, ***p < 0.0001. Statistical analyses by t-test, error bars represent SEM; n = 12 matched sections/age, 4 mice/genotype (graphs **D, I, O**). **A, B, E, G, J, L** scale bars, 100µm. **F, H, K, M** show boxed regions in **E, G, J, L**, respectively; scale bar 50µm.

Figure 2.7. *NfiB*$^{-/-}$ brains display a major loss of outer radial glia during late corticogenesis.

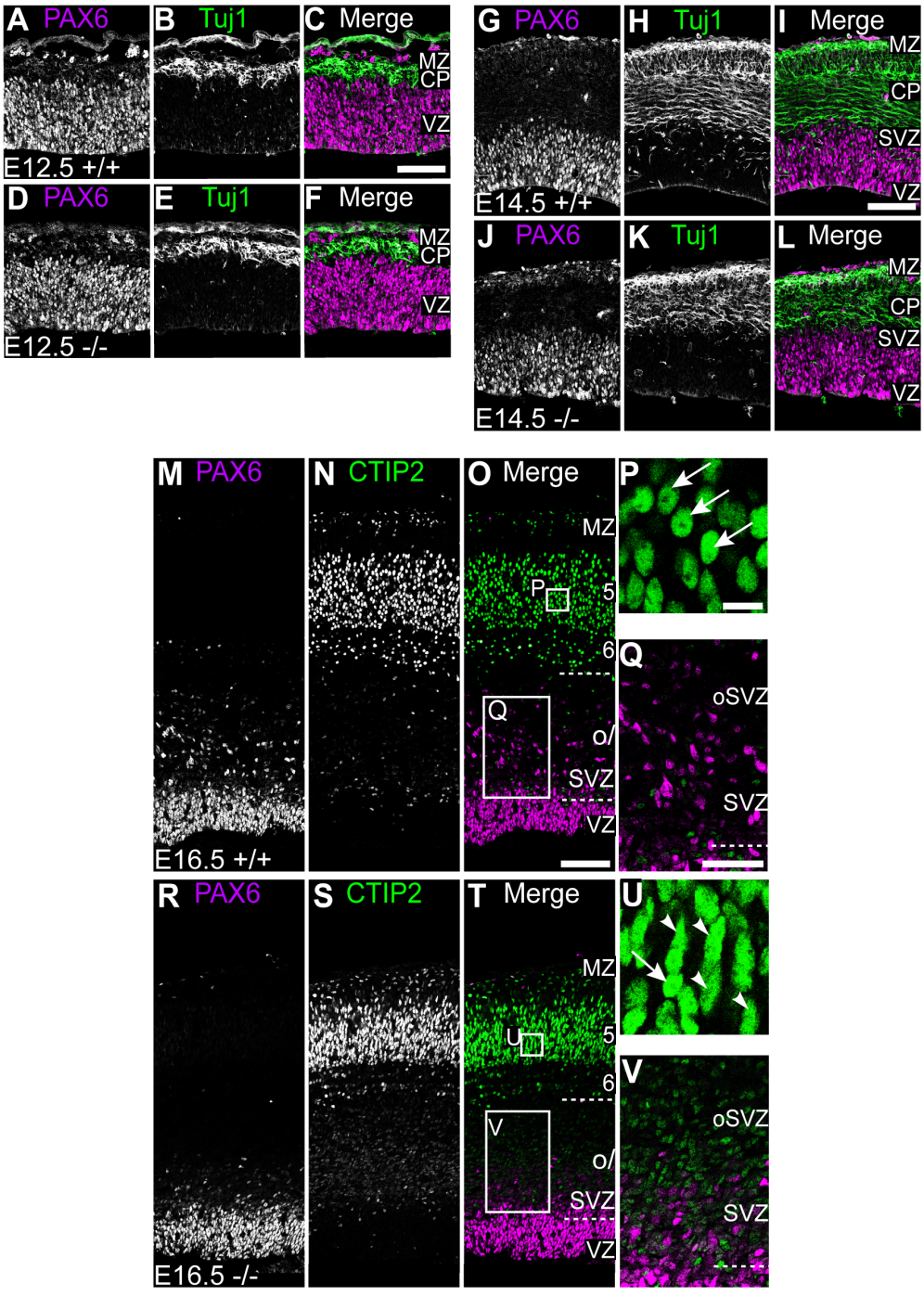

Figure 2.7 (*continued*) and caption on following page.

Figure 2.7 (*continued*). *NfiB*$^{-/-}$ brains display a major loss of outer radial glia during late corticogenesis.

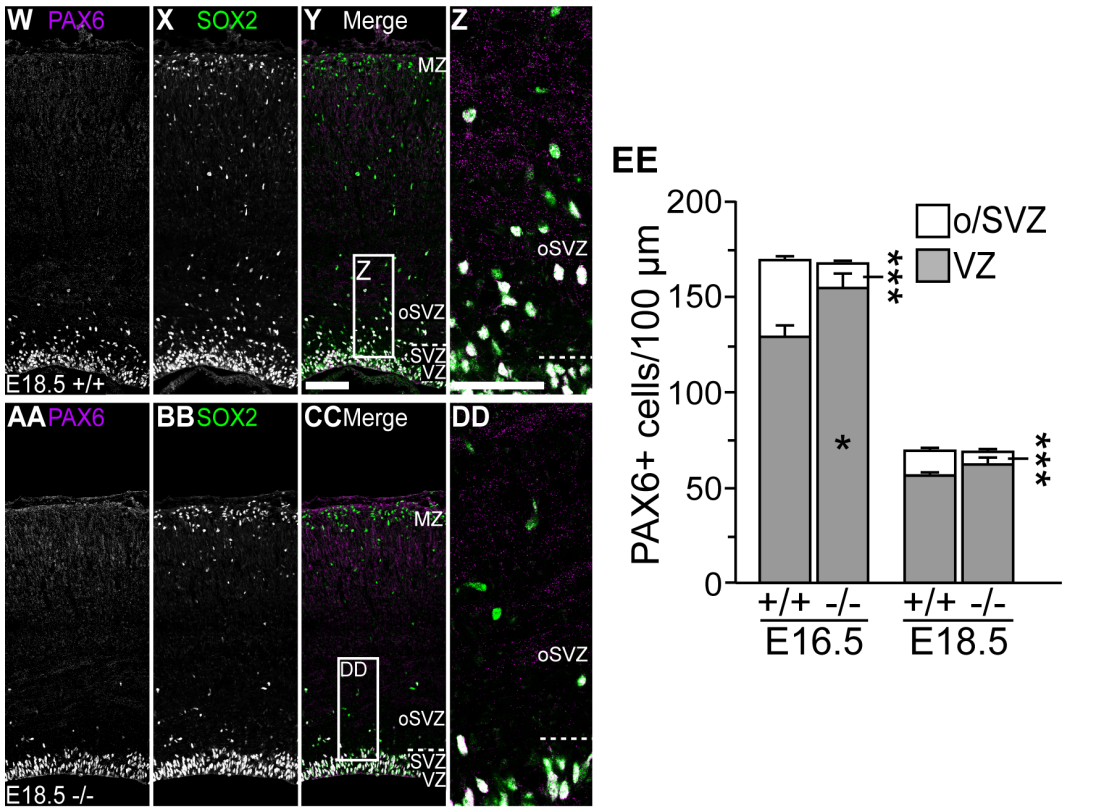

Immunohistochemistry and confocal microscopy of coronal brain sections were used to compare the quantity and distribution of PAX6-expressing cells in *NfiB*$^{+/+}$ and *NfiB*$^{-/-}$ mice throughout cortical development. **A-F** PAX6 (magenta) and Tuj1 (green) expression in E12.5 *NfiB*$^{+/+}$ (**A-C**) and *NfiB*$^{-/-}$ (**D-F**) cortices. **G-L** PAX6 (magenta) and Tuj1 (green) expression in E14.5 *NfiB*$^{+/+}$ (**G-I**) and *NfiB*$^{-/-}$ (**J-L**) cortices. **M-V** PAX6 (magenta) and CTIP2 (green) expression in E16.5 *NfiB*$^{+/+}$ (**M-Q**) and *NfiB*$^{-/-}$ (**R-V**) cortices. Arrows (**P, U**) point to CTIP2^{+} cells with rounded morphology; arrowheads (**U**) point to CTIP2^{+} cells with elongated morphology; dashed lines (**O, Q, T, V**) indicate D-V boundaries of o/SVZ. **W-DD** PAX6 (magenta) and SOX2 (green) expression in E18.5 *NfiB*$^{+/+}$ (**W-Z**) and *NfiB*$^{-/-}$ (**AA-DD**). Dashed lines (**Y, Z, CC, DD**) indicate approximate border between SVZ and oSVZ. **A-O, R-T, W-Y, AA-CC** scale bars, 100µm. **P** and **U** show boxed regions in layer 5 of **O** and **T**, respectively; scale bars, 10µm. **Q** and **V** show boxed regions in o/SVZ in **O** and **T** respectively; scale bars, 50µm. **Z** and **DD** show boxed regions in **Y** and **CC,** respectively; scale bars 25µm. **EE,** Total number of PAX6^{+} cells/100µm and in VZ, o/SVZ were compared between *NfiB*$^{+/+}$ and *NfiB*$^{-/-}$ mice at E16.5, and E18.5. *p = 0.0461, ***p < 0.0001 by t-test, error bars represent SEM; n = 10 matched sections/age, 4 mice/genotype.

Figure 2.8. Loss of basal progenitors in *NfiB*$^{-/-}$ brains during late corticogenesis.

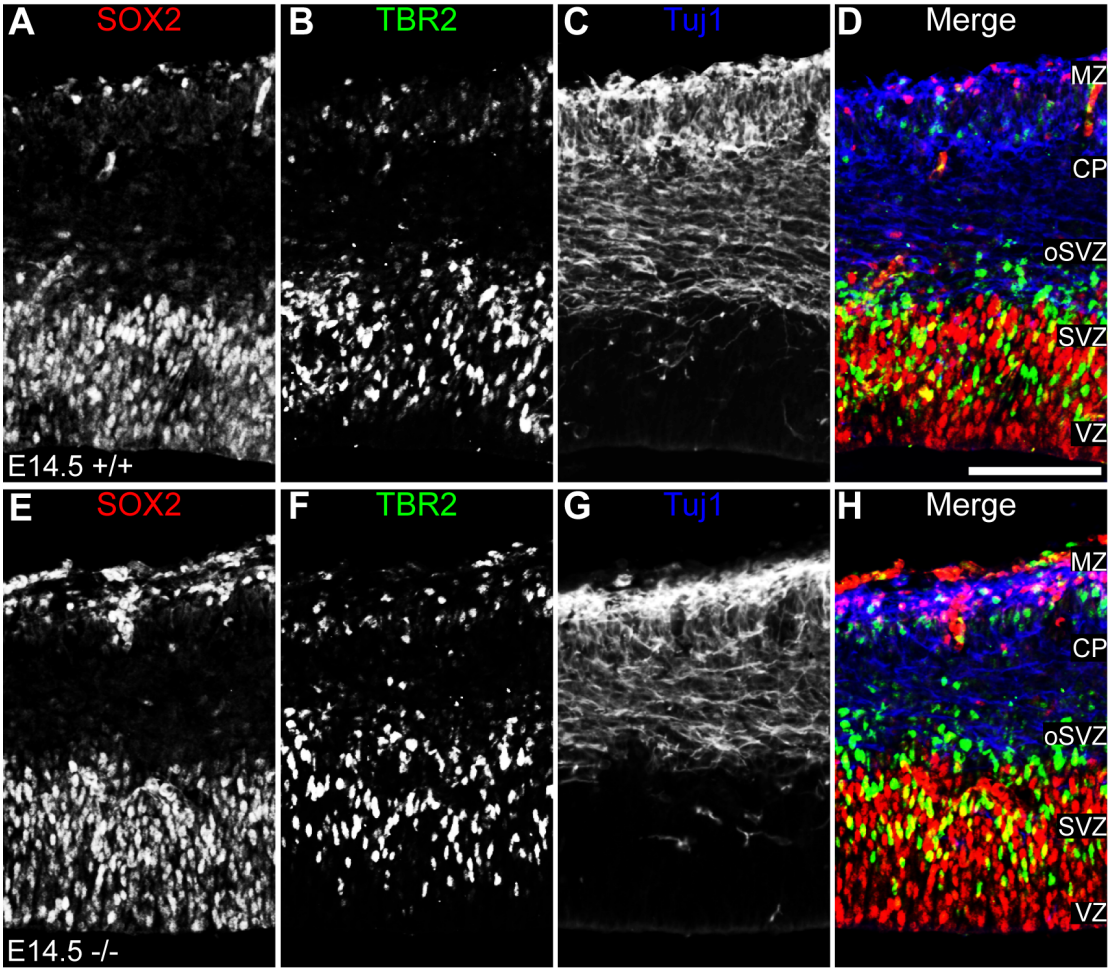

Immunohistochemistry and confocal microscopy of coronal brain sections were used to compare the number and distribution of TBR2-expressing cells in *NfiB*$^{+/+}$ and *NfiB*$^{-/-}$ mice throughout cortical development. **A-H** SOX2 (red, **A, E**), TBR2 (green, **B, F**) and Tuj1 (blue, **C, G**) expression (Merge **D, H**) in *NfiB*$^{+/+}$ (**A-D**) and *NfiB*$^{-/-}$ (**E-H**) cortices at E14.5. **I-L** TBR2 expression in *NfiB*$^{+/+}$ (**I, J, M, N**) and *NfiB*$^{-/-}$ (**K, L, O, P**) at E16.5 (**I-L**) and E18.5 (**M-P**). White outlines (**I, K, M, O**) indicate apical and basal surfaces of the cortex, yellow dashed lines (J, L, N, P) indicate approximate boundary between SVZ and oSVZ. **J, L, N,** and **P** show boxed regions in **I, K, M** and **O,** respectively. Scale bars, 100μm. **Q** Total numbers of TBR2^{+} cells/100μm and in VZ and o/SVZ were compared between *NfiB*$^{+/+}$ and *NfiB*$^{-/-}$ mice at E16.5, and E18.5. *p = 0.0095 (E16.5), *p = 0.0429 (E18.5), **p = 0.0011 (E18.5 oSVZ), **p = 0.0028 (E18.5 total number), ***p < 0.0001 by t-test, error bars indicate SEM; n = 9 matched sections/age, 4 mice/genotype.

Figure 2.8 (*continued*) on following page.

Figure 2.8 (*continued*). Loss of basal progenitors in *NfiB*$^{-/-}$ brains during late corticogenesis.

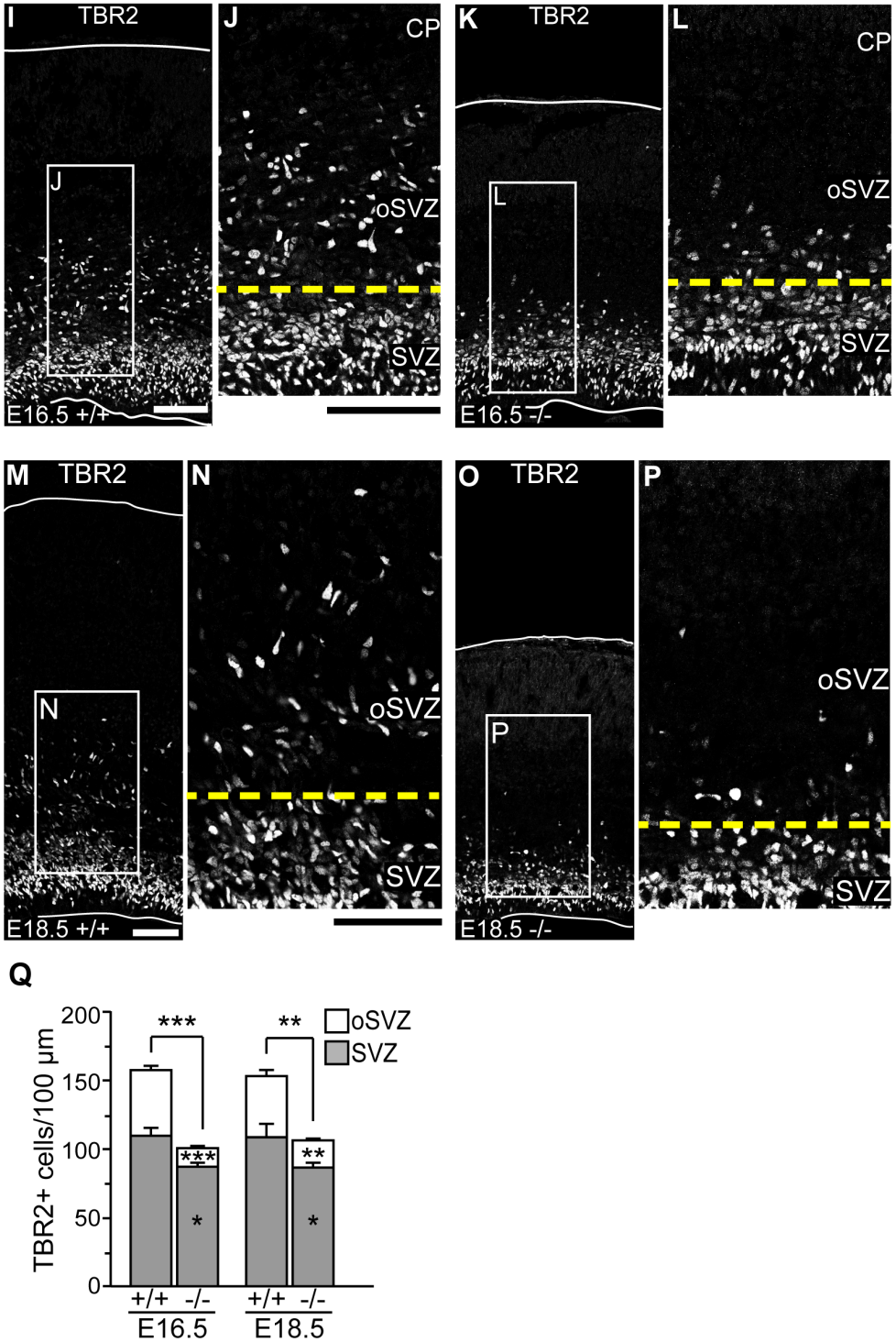

Figure 2.9. Number of apoptotic cells is similar in *NfiB*$^{+/+}$ and *NfiB*$^{-/-}$ cortices at E15.5.

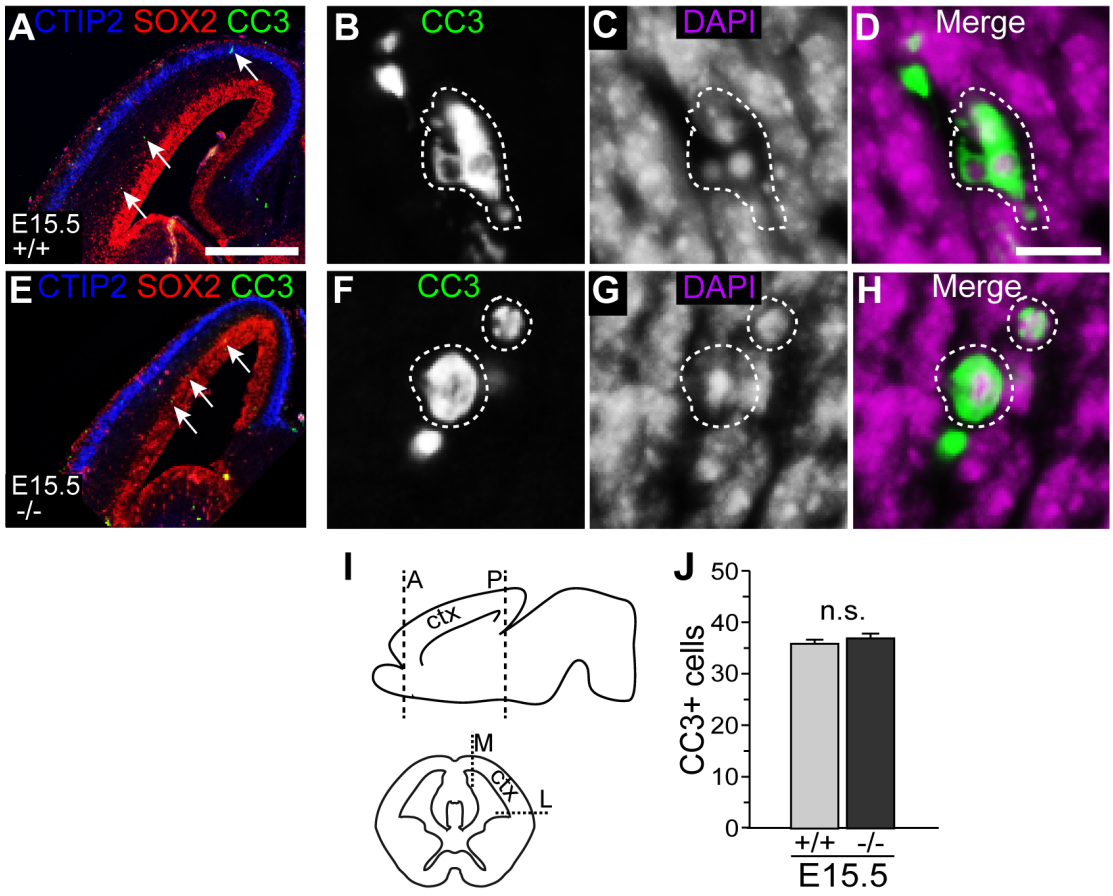

Immunohistochemistry and confocal microscopy of coronal brain sections were used to quantify CC3^{+} cells in *NfiB*$^{+/+}$ and *NfiB*$^{-/-}$ mice at E15.5. **A, E** Low magnification view of CTIP2 (blue), SOX2 (red) and CC3 (green) expression in *NfiB*$^{+/+}$ (**A**) and *NfiB*$^{-/-}$ (**E**) cortices; arrows point to CC3-expressing cells. **B-D, F-H** Higher magnification view of CC3 (green) and DAPI nuclear stain (magenta) expression (**B, F** and **C, G**, respectively, Merge **D, F**) in *NfiB*$^{+/+}$ (**B-D**) and *NfiB*$^{-/-}$ (**F-H**) cortices; CC3^{+} cells are indicated by dashed outlines. **A, E** scale bars, 500μm; **B-D, F-H** scale bars, 10μm. **I** Schematics showing regions of CC3^{+} cell quantification. Coronal sections within anterior (A) to posterior (P) region indicated by dashed lines (top panel) were used; CC3^{+} cells were quantified on the medial (M) to lateral (L) axis within region indicated by dashed lines (bottom panel); ctx, cortex. **J** Number of CC3^{+} cells was compared between *NfiB*$^{+/+}$ and *NfiB*$^{-/-}$ cortices at E15.5. p = 0.379 by t-test, error bars indicate SEM; n=10 matched sections, 4 mice/genotype.

Figure 2.10. Increase in neurogenesis at E15.5 and defects in neuronal migration.

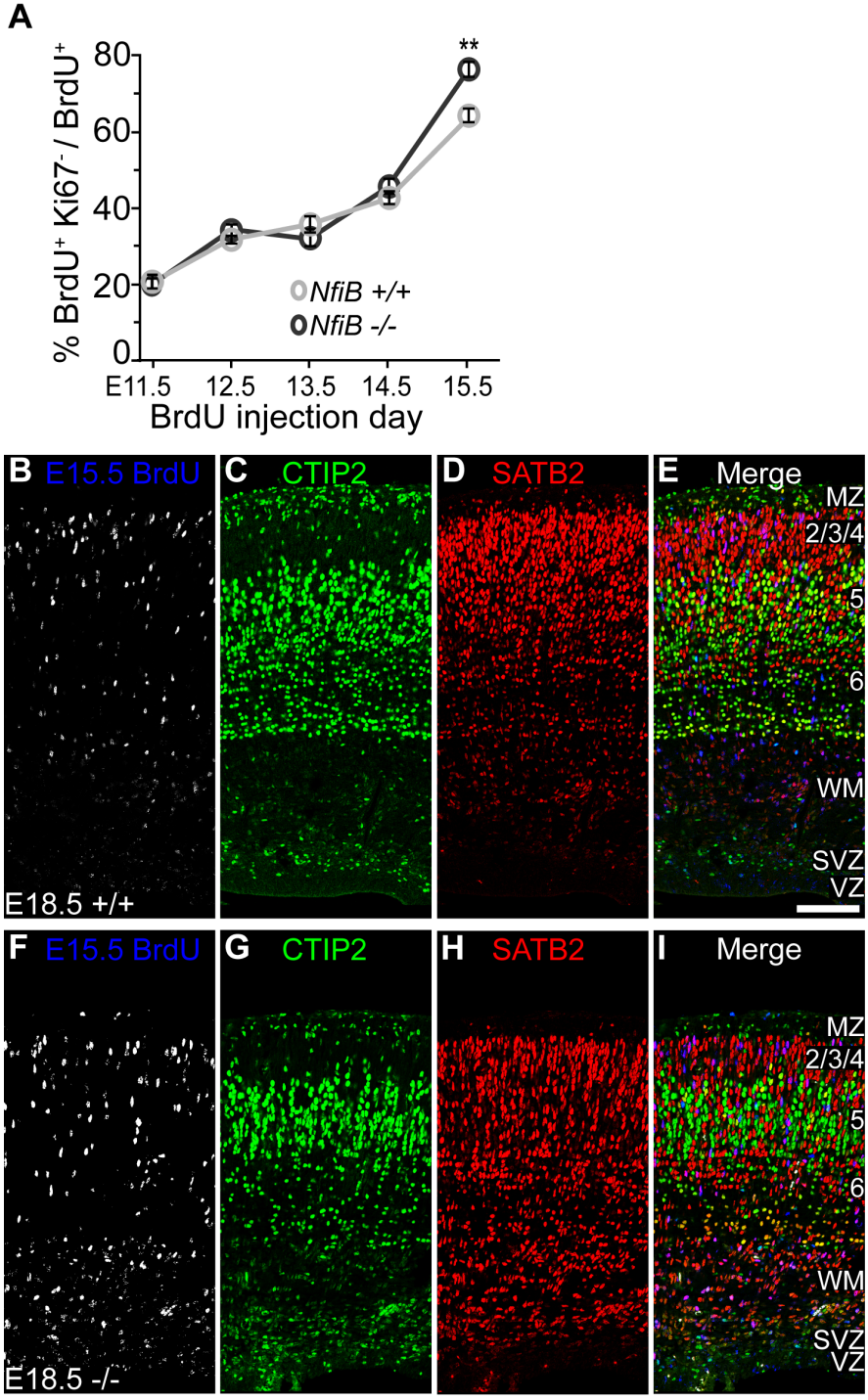

Figure 2.10 (*continued*) and caption on following page.

Figure 2.10 (*continued*). Increase in neurogenesis at E15.5 and defects in neuronal migration.

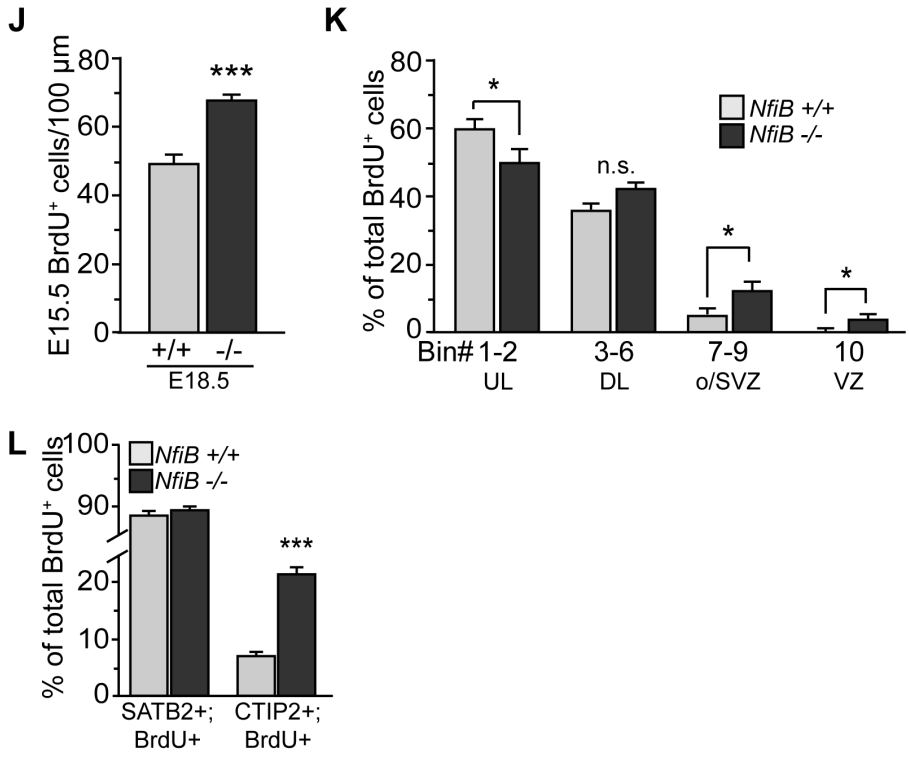

Immunohistochemistry and confocal microscopy of coronal brain sections were used to compare the quit fractions throughout neurogenesis and molecular identities of neurons born at E15.5 in *NfiB*$^{+/+}$ and *NfiB*$^{-/-}$ cortices. **A** Quit fractions in *NfiB*$^{+/+}$ and *NfiB*$^{-/-}$ mice at E11.5-E15.5. **p = 0.0045 by t-test, error bars indicate SEM; n = 9 matched sections/age, 3 mice/genotype. **B-L** BrdU labeling was used to quantify and analyze the distribution of neurons generated at E15.5 in *NfiB*$^{+/+}$ and *NfiB*$^{-/-}$ cortices; combining with SATB2 and CTIP2 immunostaining (**B-I** and **L**) allowed for analysis of neuronal marker expression. **B-I** E15.5 BrdU^{+} cells (**B, F**) and expression of CTIP2 and SATB2 (**C, G** and **D, H**, respectively, Merge **E, I**) in E18.5 *NfiB*$^{+/+}$ (**B-E**) and *NfiB*$^{-/-}$ (**F-I**) cortices; scale bar, 100µm. **J** Total number of E15.5 BrdU^{+} cells/100µm was compared between *NfiB*$^{+/+}$ and *NfiB*$^{-/-}$ cortices; ***p = 0.0001. **K** The cortical distribution of E15.5 BrdU^{+} cells was analyzed by binning; see Materials and Methods for details. E15.5 BrdU^{+} cells in bins 1-2, 3-6, 7-9 and 10 as a percentage of total number were compared between *NfiB*$^{+/+}$ and *NfiB*$^{-/-}$ cortices. *p = 0.038, *p = 0.0287, *p = 0.0066 (bins 1-2, 7-9 and 10, respectively). **L** Percentages of total E15.5 BrdU^{+} cells that expressed either SATB2 or CTIP2 were compared between *NfiB*$^{+/+}$ and *NfiB*$^{-/-}$ cortices. ***p <0.0001. **J-L** p-values calculated by t-test, error bars indicate SEM; n = 12 matched sections, 4 brains/genotype.

Figure 2.11. mRNA expression of *Notch* signaling pathway members is upregulated in *NfiB*$^{-/-}$ mice.

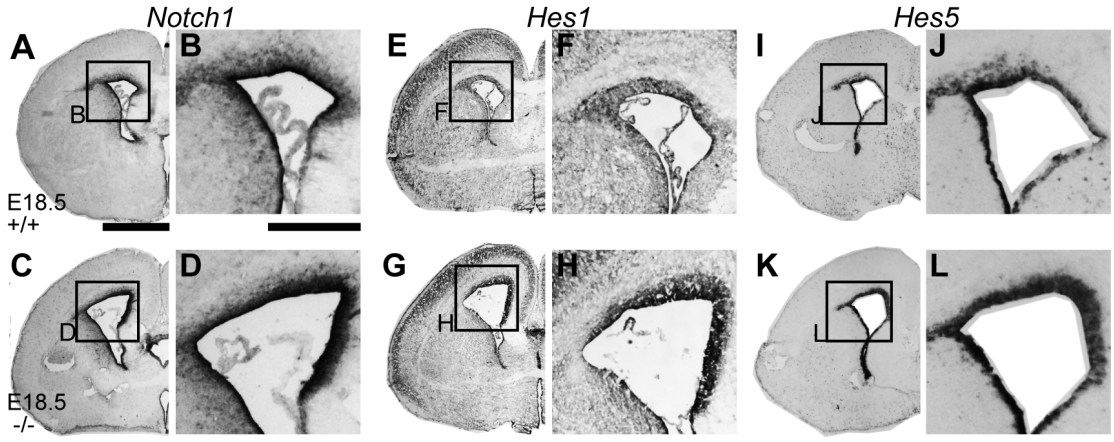

In situ hybridization and bright field microscopy were used to compare mRNA expression levels (black) of *Notch1* (**A-D**), *Hes1* (**E-H**) and *Hes5* (**I-L**) in E18.5 *NfiB*$^{+/+}$ (**A, B, E, F, I, J**) and *NfiB*$^{-/-}$ (**C, D, G, H, K, L**) brains. **A, C, E, G, I, K** Low magnification views; scale bar, 1000μm. **B, D, F, H, J** and **L** show boxed regions in **A, C, E, G, I** and **K**, respectively. Scale bar 500μm.

Table 2.1 List of abbreviations used in Chapter 2.

A	Anterior
BrdU	5-Bromo-2-deoxyuridine
CC3	Cleaved Caspase 3
CP	Cortical plate
cpd	Cerebral peduncle
ctx	Cerebral cortex
DAPI	4',6-diamidino-2-phenylindole
DL-C	Region of deep layer (5-6) CTIP2+ neurons
DRAQ5	1,5-bis {[2-(Di-methylamino) ethyl]amino}-4, 8-dihydroxyanthracene-9, 10-dione
DP32	DARPP32 antibody
E	Embryonic Day
GFP	Green Fluorescent Protein
L	Lateral
M	Medial
NFIB	Nuclear Factor One B
n.s.	not significant
oSVZ	Outer subventricular zone
o/SVZ	Region containing oSVZ and SVZ
P	Posterior
PLAP	Human placental alkaline phosphatase
po	pons
SEM	Standard error of means
SVZ	Subventricular zone
th	Thalamus
UL-S	Region of upper layer (2-4) SATB2+ neurons
VZ	Ventricular zone
WM	White Matter

Table 2.2 Summary of primary antibodies used for immunofluorescence (IF) in Chapters 2 and 3.

Antibody (clone)	Immunogen	Source (Catalog No.)	Host	Dilution
β-GAL	Purified full length native protein of *E. coli* β-Galactosidase	Abcam (ab9361)	Chicken (P)	1:1000
*BETA 3 (E-17)	Synthetic peptide to N-terminal amino acid residues ERGLHLGAAAASEDDLFLC of hamster BETA 3 (a.a. 4-22)	Santa Cruz Biotechnology (sc-6045)	Goat (P)	1:100
#BrdU	Bromodeoxyuridine coupled to keyhole limpet hemocyanin (KLH)	Abcam (ab1893)	Sheep (P)	1:250
*Cleaved Caspase-3	Synthetic peptide (KLH coupled) to N-terminal amino acid residues CRGTELDCGIETD of human Caspase-3 (a.a. 163-175)	Cell Signaling Technology (9661)	Rabbit (P)	1:100
*CTIP2 (25B6)	Fusion protein of amino acid residues MSRRKQG-NPQHLSQRELITPEADHVEAAILEEDEGLEIE-EPSGLGLMVGG of human CTIP2 (a.a.1-50)	Abcam (ab18465)	Rat (M)	1:750
*DARPP32 (EP27Y)	N-terminal amino acid residues MLFRLSEHSSP-EEEASPHQRASGEGHHLKSKRPNPCAYTPPSL-KAVGRIA of human DARPP32 (a.a.1-50)	Abcam (ab40801)	Rabbit (M)	1:200
GFP	Recombinant GFP protein emulsified in Freund's adjuvent	Aves Labs (GFP-1020)	Chicken (P)	1:1000
Ki67 (B56)	Immunodominant amino acid residues APKEKAQPLED-LASFQELSQ of human Ki67 (a.a. 2547-2566)	BD Pharmingen (550609)	Mouse (M)	1:100
NFIA	Amino acid residues PSTSPANRFVSVGPR of human NFIA (a.a. 478-492)	Active Motif (39397)	Rabbit (P)	1:500
NFIB	Amino acid residues PAPSSYFSHPTIRY of human NFIB (a.a. 402-415)	Active Motif (39091)	Rabbit (P)	1:500
*PAX6	C-terminal amino acid residues QVPGSEPD-MSQYWPRLQ of mouse PAX6 (a.a. 420-436)	Covance (PRB-278P)	Rabbit (P)	1:200
PHH3 (6G3)	Synthetic phospho-peptide (KLH coupled) to amino acid residues ATKQTARKSTGGKA of human histone H3 (a.a. 2-15)	Cell Signaling Technology (9706)	Mouse (M)	1:200
SATB2	Synthetic peptide (KLH coupled) to C-terminal amino acid residues ENDSEEGSEEMYKVEAEEENAD-KSKAAPAETDQR of mouse SATB2 (a.a. 700-733)	Abcam (ab34735)	Rabbit (P)	1:1000
*SOX2 (Y-17)	Synthetic peptide to C-terminal amino acid residues YLPGAEVPEPAAPSRLH of human SOX2 (a.a. 277-293)	Santa Cruz Biotechnology (sc-17320)	Goat (P)	1:200
*#TBR1	Synthetic peptide (KLH coupled) to amino acid residues SPLKKITRGMTNQSDTDNFPDSKDSPGDVQRSKLSPVLDG-VSELRHSFDGS of mouse TBR1 (a.a. 50-100)	Abcam (ab31940)	Rabbit (P)	1:500
*TBR2	Synthetic peptide (KLH coupled) to acid residues STPSNGNSPPIKCEDINTEEYSKDTSKGMG-AYYAFYTSP of mouse TBR2 (a.a. 650-688)	Abcam (ab23345)	Rabbit (P)	1:200
Tuj1	Raised against microtubules from rat brains	Covance (PRB-278P)	Mouse (M)	1:1000

(P), polyclonal; (M), monoclonal
* Official and/or alternate gene names included in Antibody characterization of Material and Methods section.
# Antibody used in Chapter 2 and 3

Table 2.3 Functional annotational clustering of genes affected in E15.5 *NfiB*$^{-/-}$ mice

Annotation Cluster	No. of genes	Enrichment score	GO_TERMS	p-value
1	168	19.89	cell cycle	1.4E-26
			M phase	1.9E-22
			cell division	3.8E-20
2	123	15.61	neuron differentiation	3.7E-24
			axonogenesis	1.2E-16
			axon guidance	3.5E-13
3	100	16.64	cell motion	1.5E-15
			neuron migration	4.0E-10
			localization of cell	4.1E-09

Table 2.4 Significantly changed expression of genes from Clusters 1-3.

Cluster	Gene Symbol	Gene Name	Fold change	p-value
1	Sycp3	synaptonemal complex protein 3	6.080	1.01E-02
	Id4	inhibitor of DNA binding 4	2.257	2.08E-43
	Gas1	growth arrest specific 1	1.893	2.25E-28
	Cenpe	centromere protein E	1.488	1.62E-06
	Cdca3	cell division cycle associated 3	1.475	3.13E-09
	Cdc14a	cell division cycle 14a	1.452	8.42E-05
	G0s2	G0/G1 switch gene 2	0.402	6.16E-07
	Trnp1	TMF-regulated nuclear protein 1	0.553	2.26E-13
	Rec8	rec8 homolog	0.616	5.55E-04
2	Robo3	roundabout homolog 3	5.898	5.54E-25
	Neurog1	neurogenin1	2.476	7.01E-36
	Gli3	glioma 3	1.804	1.91E-21
	Hes5	hairy and enhancer of split 5	1.729	2.33E-18
	Hes1	hairy and enhancer of split 1	1.721	4.81E-13
	Dll1	delta like-1	1.646	4.69E-16
	Notch3	notch gene homolog 3	1.599	2.09E-12
	Neurog2	neurogenin2	1.480	4.93E-12
	Notch1	notch gene homolog 1	1.205	1.16E-03
	Lhx8	LIM homeobox protein 8	0.147	1.34E-07
	Nkx2-2	NK2 transcription factor related, locus 2	0.174	7.40E-07
	Isl1	islet 1 transcription factor	0.227	1.74E-35
3	Mnx1	motor neuron and pancreas homeobox 1	9.075	3.87E-16
	Emx1	empty spiracles homolog 2	1.653	2.08E-43
	Smo	smoothened homolog	1.415	8.31E-37
	Nkx2-1	NK2 homeobox 1	0.295	2.62E-09
	Nkx2-3	NK2 transcription factor related, locus 3	0.507	3.31E-06
	Pou3f2	POU domain, class 3, factor 2	0.547	1.03E-14
	Cttnbp2	cortactin binding protein 2	0.550	4.47E-20
	Ntn1	netrin 1	0.588	1.03E-08
	Nrp1	neuropilin 1	0.611	5.08E-04
	Reln	reelin	0.774	1.62E-04

CHAPTER 3

Contributions to "Tbr1 and Fezf2 regulate alternate corticofugal neuronal identities during neocortical development"

The following work presented is a reproduction of Figure 7 from the article: McKenna, W.L., **Betancourt, J.,** Larkin, K.A., Abrams, B., Guo, C., Rubenstein, J.L., and Chen, B (2011). Tbr1 and Fezf2 regulate alternate corticofugal neuronal identities in neocortical development. J. Neuroscience *31(2)*, 549-564. The **3.2 Introduction** section summarizes the rationale and major findings of the article. Both **3.3 Material and Methods** and **3.4 Results** sections pertain exclusively to Figure 7. Note: In this thesis dissertation, Figure 7 from the article has been re-named **Figure 3.1**.

3.1 Abstract

Gene regulators for subcerebral and corticothalamic fate specification in the developing neocortex have been identified. Through a comparative analysis of wildtype (*Tbr1*$^{+/+}$) and *Tbr1*-deficient (*Tbr1-/-*) mice, authors show that TBR1 is expressed in layer 6 corticothalmic neurons and regulates their identity through repression of the subcerebral fate determinant, *Fezf2*. *Tbr1-/-* mice display a loss in layer 6-specific marker expression and axonal projections terminating at the thalamus. Conversely, these mice display an increase in layer-5 subcerebral specific markers and ectopic axonal projections to subcerebral targets. In addition, authors reveal that *Fezf2* specifies subcerebral identity by suppression of TBR1 expression

in this neuronal population. In this chapter, I present my use of retrograde tracing by ultrasound injection in wildtype (*Fezf2*$^{+/+}$) and *Fezf2*-deficient (*Fezf2*$^{-/-}$) mice to label corticothalamic projection neurons. By combining this technique with neuronal birthdating analysis and immunohistochemistry, I observed neurons born at E13.5, ectopically expressed TBR1 and projected axons to the thalamus in *Fezf2*$^{-/-}$ mice. Whereas in *Fezf2*$^{+/+}$mice, E13.5 born neurons project axons to subcerebral targets, and generally do not express TBR1. Hence, my work contributed to the finding that Tbr1 and Fezf2 regulate alternate corticofugal fates by repression of each other in temporal- and laminar-specific manners.

3.2 Introduction

Two broad classes of cortical projection neurons are present in the mammalian cerebral cortex: corticofugal and corticocortical projection neurons. Within each class there are distinct subtypes that differ by a combination of properties including neuronal birthdate, laminar position and/or axonal targets. In addition, recent studies have advanced our knowledge regarding gene expression profiles of specific subtypes (O'Leary and Koester, 1993; McConnell; 1995 and Molyneaux et al., 2007). However, much work remains in identifying which of these genes function as neuronal fate determinants and the molecular mechanisms by which it occurs. Recently, work in our lab revealed at least two determinants of corticofugal identity, *Tbr1* and *Fezf2*, and revealed their modes of transcriptional regulation of fate specification.

Corticothalamic and subcerebral projections are both deep-layer corticofugal projection neuron subtypes. Corticothalamic projection neurons are one of the earliest born cortical neuron subtypes, generation starting as E11.5 and peaking approximately one day later during mouse embryogenesis. Cell bodies are primarily positioned in layer 6 of the mature cortical plate and axons project through the internal capsule to various thalamic nuclei. Some genes that expressed in layer 6, but are not necessarily restricted to this region. For example: *NfiA, NfiB, Sox5, Tle4, Lmo4* and low levels of *Ctip2* and *Fezf2*. *Foxp2, Darpp32* and *Tbr1* are primarily expressed at high-levels in layer 6, however, a few neurons in layer 5 also strongly express *Tbr1* (Hevner et al., 2001; Molyneaux, et al., 2007; McKenna et al., 2011). Conversely, subcerebral projection neurons direct axons to the spinal cord, pons and hindbrain. Peak generation approximately occurs at E13.5, at which time, neurons migrate toward their final cortical position in layer 5. Similar to layer 6, high levels of *NfiA, NfiB, Sox5* and *Tle4* are expressed in layer 5, yet *Lmo4* was expressed at low levels. *Ctip2* and *Fezf2* are weakly expressed in layer 6, but expressed at high levels in layer 5 (O'leary and Koester, 1993; Chen et al., 2005; Molyneaux, et al., 2007; Chen et al., 2008; McKenna et al., 2011). While expression of many genes overlap within subcerebral and corticothalamic neuron subtypes, the inverse patterns of *Tbr1* expression versus *Fezf2* and *Ctip2* expression, in layers 5 and 6, suggested that, together, these genes play a role in regulating corticofugal subtype identity.

Previous studies comparing $Fezf2^{+/+}$ and $Fezf2^{-/-}$ mice revealed that *Fezf2* regulates subcerebral fate identity of corticospinal motor neurons (CSMNs), a

distinct subcerebral subtype, such that axons were misdirected to abnormal targets in *Fezf2*$^{-/-}$ mice. These mice also displayed an increase in expression of layer 6 markers, including expansion of TBR1 expression into layer 5. Research also showed that *Fezf2* indirectly regulates *Ctip2*. CSMN's in wildtype mice express high levels of CTIP2 but in *Fezf2*$^{-/-}$ mice, expression was severely reduced (Chen et al., 2005a, 2005b; Chen et al., 2008; McKenna et al., 2011). In another study, comparing *Tbr1*$^{+/+}$ and *Tbr1*$^{-/-}$ mice revealed that TBR1 expression was critical for the proper generation and differentiation of layer 6 neurons (Hevner et al., 2001). However, it did not address whether *Tbr1*, in fact, directly specified corticothalamic neuron identity.

In the scientific article, Tbr1 and Fezf2 regulate alternating corticofugal identities during neocortical development (2011). J. Neurosci. *31(2)*, 549-564, authors first investigated whether TBR1 regulates corticothalamic neuron identity, and secondly, they explored the potential for a transcriptional relationship between Tbr1, Fezf2 and Ctip2 in specifying the identities of layer 5 versus layer 6 corticofugal neurons. Results from this study demonstrated that corticothalamic neurons expressed high-level TBR1 and low-level CTIP2. In a detailed comparison of *Tbr1*$^{+/+}$ and *Tbr1*$^{-/-}$ mice, authors observed a reduction in neurons that express layer 6 markers, FOXP2, DARPP32 and TLE4. Conversely, there were more neurons that displayed layer 5 subcerebral markers, and an increase in high-level CTIP2 and *Fezf2* expression. Results also showed a redirection in axons projecting from layer 6 neurons in *Tbr1*$^{-/-}$ mice, such that instead of thalamic projections, layer

6 neurons extended axons to subcerebral targets. Interestingly, these additional layer 5-like neurons are generated at E11.5-E12.5, the time during neurogenesis when layer 6 corticothalamic neurons are typically generated. Additionally, chromatin immunoprecipitation analysis indicated direct binding of TBR1 to *Fezf2*. Taken together, this data suggests that TBR1 is necessary for specification of corticothalamic fate and repression of subcerebral fate (McKenna et al., 2011). Finally, given that TBR1 expression is expanded into layer 5 of *Fezf2-/-* brains and that TBR1 specifies the corticothalamic identity, we questioned whether these TBR1-expressing cells possessed layer 5 neuronal properties in additional to laminar position. Here, I discuss how I addressed this question as a contribution to the publication.

3.3 Material and Methods

Generation of *Fezf2*$^{-/-}$ mice

Generation of the *Fezf2*$^{+/-}$ mouse strain was described previously (Chen et al., 2005). Male and female *Fezf2*$^{+/-}$ mice were time-mated overnight to generate *Fezf2*$^{+/-}$ and *Fezf2*$^{-/-}$ offspring. Females were inspected for a vaginal plug the next day; observation of a plug day was defined as embryonic day (E)0.5. Postnatal day (P)0 was designated as the day of birth. Genders of embryonic mice were not determined. All embryos were genotyped by PCR as previously described (Chen et al., 2005). All experiments and animal husbandry were executed in accordance with

protocols approved by the Institutional Animal Care and Use Committee at University of California, Santa Cruz and institutional and federal guidelines.

BrdU birthdating analysis, ultrasound-guided retrograde tracing and immunohistochemistry

BrdU (Bromodeoxyuridine at 100µg/g body weight; US biologicals) was intraperitoneally injected into timed pregnant mice at E13.5; dams carried pregnancy to term. Retrograde tracing was performed at P1 using ultrasound guided (VisualSonics Vevo 770) injection of AlexaFluor^{TM} 488-conjugated Choleral Toxin β subunit (CTβ) into the thalamus of *Fezf2*$^{+/-}$ and *Fezf2*$^{-/-}$ pups. Pups were collected at P4 and processed for BrdU and TBR1 immunostaining (antibody information in **Table 2.2**). Cells with ≥75% BrdU nuclei saturation, were identified as E13.5-born neurons.

Image acquisition

Images were captured on a Zeiss LSM5 confocal microscope. The detector gain was set such that <1% of pixels were saturated.

3.4 Results

To characterize the ectopic TBR1-expressing cells observed in layer 5 *Fezf2*$^{-/-}$ brains, I performed a combination of BrdU-birthdating, retrograde axonal tracing and immunohistochemistry. Peak generation of layer 5 neurons typically occurs at E13.5

and due to their position in layer 5, we asked whether ectopic TBR1-expressing cells were born at this time. To identify E13.5-born neurons, we injected BrdU into timed-pregnant *Fezf2*$^{+/-}$ dams at E13.5. Once pups from this litter were born, we performed retrograde axonal tracing at P1 by injecting pups with CTβ in the thalamus. This enabled us to determine the laminar position of neuronal cell bodies from which these axons were projected. At P4, we collected the brains and immunostained with antibodies against BrdU and TBR1.

As expected, when analyzing TBR1 expression in control cbrains, we observed almost all layer 6 neurons but very few layer 5 neurons expressed high-level TBR1 (Figure 3.1 A, D, D'). Retrograde tracing by injection of CTβ into the thalamus (Figure 3.1 I-L) revealed that corticothalamic projections originated from TBR1-expressing neurons in layer 6 (Figure 3.1 A, B, D, D'). Additionally, BrdU-birthdating indicated that the majority of E13.5-born neurons were positioned in layer 5 of *Fezf2*$^{+/-}$ brains and did not express TBR1 nor project axons to thalamic targets (Figure 3.1 A-D'). Conversely, in *Fezf2*$^{-/-}$ brains, many more layer 5 neurons expressed high-level TBR1 yet the expression in layer 6 was comparable to control littermates (Figure 3.1 E, H, H') (Hevner et al., 2001). E13.5 BrdU-labeled neurons were concentrated in layer 5, although there some E13.5-born neurons were observed in other cortical layers (Figure 3.1 G-H'). Retrograde axonal tracing labeled neuronal cell bodies in both layer 5 and 6 in *Fezf2*$^{-/-}$ brains (Figure 3.1 F, H, H'). Of those in layer 5, many if not all, expressed TBR1 and were labeled with BrdU. Collectively, these results indicated that some layer 5 neurons, despite proper neuronal birthdate

and laminar positioning, expressed TBR1 and subsequently projected their axons to the thalamus. Furthermore, it demonstrated a fate switch from a subcerebral to a corticothalamic neuronal identity, and suggested that Fezf2 specifies the subcerebral fate by blocking corticothalamic fate in layer 5 neurons. Hence *Tbr1* and *Fezf2* specify opposing corticofugal fates by repression of one other in a laminar-dependent manner.

3.5 Discussion

A summary of major findings from our publication (McKenna et al., 2011) was presented here; importantly, I discuss my contributions as an author. While results from a previous study revealed a subcerebral to callosal fate switch in *Fezf2*$^{-/-}$ brains (Chen et al, 2008), the presented data provides evidence for an alternate fate switch from that of a subcerebral to corticothalamic fate. Together, these findings have begun to elucidate the transcriptional network responsible for fate specification of cortical projection neurons. At initial stages of neurogenesis, neural progenitors express FEZF2. When neuronal progenitors produce the first-born neurons of the cortex (E11.5-E12.5), TBR1 expression is turned on, which represses *Fezf2*, resulting in the corticothalamic identity of these neurons. During the next wave of neurogenesis (E12.5-E13.5), FEZF2 represses TBR1 expression to low-levels but promotes high-level expression of CTIP2 in newly-generated postmitotic neurons. Concurrently, FEZF2 blocks callosal identity by repression of the callosal fate determinant, *Satb2* (Chen et al., 2008). Together, these transcriptional activities specify a subcerebral identity. Subsequently, during final waves of neurogenesis

(E13.5-E16.5), SATB2 represses *Ctip2* in postmitotic neurons, thus blocking the subcerebral fate and resulting in specification of a callosal identity. Together, *Fezf2, Ctip2, Tbr1* and *Satb2* form an intricate network of neuronal fate determinants, but interactions with additional laminar markers remains unknown (Chen et al., 2005a, 2008; McKenna et al., 2011).

Interestingly, TBR1 is expressed at low-levels in upper layers 2-4, yet the role of TBR1 in these layers is not understood (McKenna et al., 2011). TBR1-expressing neurons in upper layers do not project to the thalamus, but it would be of interest to investigate whether corticocortical projection neurons express TBR1. In this study, expression of upper layer-specific markers were not analyzed, yet based on its expression pattern, it is possible that loss of TBR1 function could lead to disruption in upper-layers. Thus, the transcriptional relationship between Tbr1 and Satb2, if any, remains to be investigated.

Birthdating analysis revealed additional defects in the *Fezf2*$^{-/-}$ brain. Compared to littermate controls, the distribution of E13.5-born neurons, while primarily restricted to layer 5, was very sporadic throughout the cortical plate. Because neuronal subtypes are generated in sequential waves, BrdU-labeled neurons located in regions superficial to layer 5, are likely true representations of layer 3 and/or layer 4 neurons born at E13.5. However, we observed multiple E13.5 BrdU-labeled neurons below layer 5, suggesting a potential defect in neuronal migration. It is possible that *Fezf2* has additional roles in neuronal migration, such that a loss of FEZF2 function results in premature termination. Performing a genome wide

analysis to identify direct downstream effectors of *Fezf2*, would provide increasingly useful information in regards to the potential roles of *Fezf2* in both neural progenitors and postmitotic neurons.

Lastly, it is evident that ultrasound guided injection proves extremely useful for retrograde tracing of axons. Given that we are beginning to understand the genetic code for fate specification of cortical projection neurons, it is possible to apply our findings in combination with available technologies, to therapeutic developments. The human cerebral cortex is the most highly specialized structure in the animal kingdom and controls cognitive function and sensory perception. The intricate networks of neurons responsible for these processes are also the networks that degenerate and become defective in diseases such as Alzheimer's and Parkinson's. Upon a complete understanding of the transcriptional code regulating neocortical development, it will then be possible to synthetically generate specific subtypes of neurons *in vitro* and transplant them *in vivo* by ultrasound guided injection and analyze their potential as a disease treatment.

Figure 3.1 Ectopic TBR1-expressing cells in layer 5 of *Feaxf2-/-* brains were born on E13.5 and extended axons to thalamic targets.

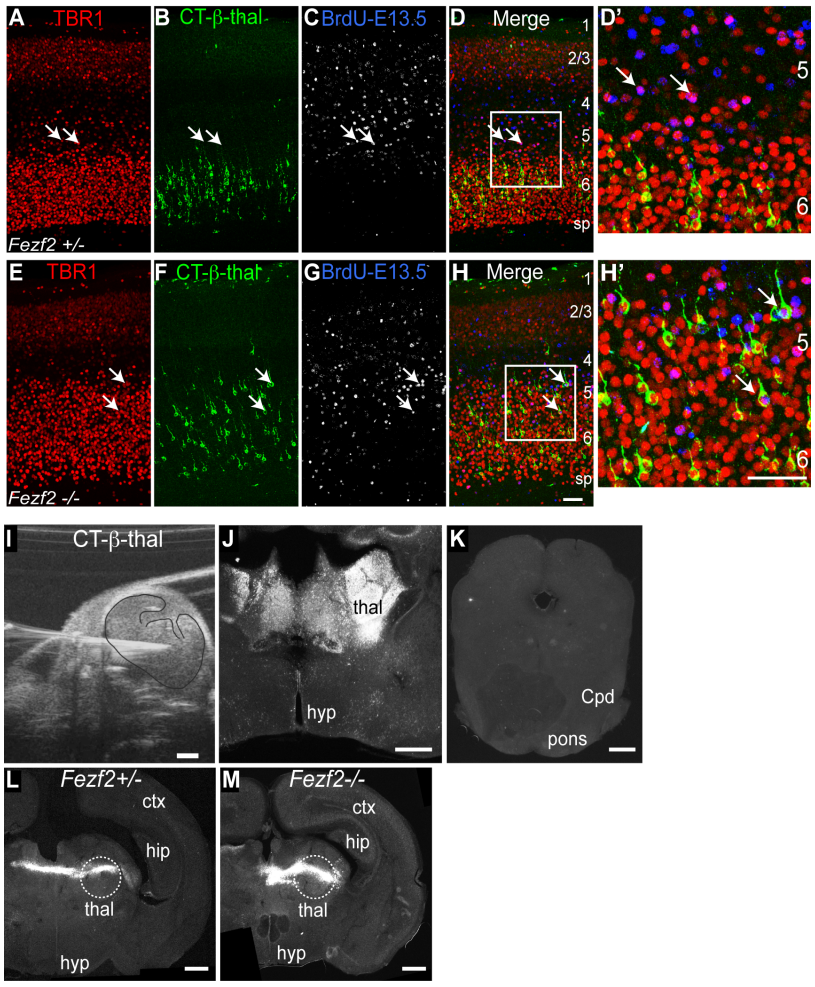

Neuronal birthdating, CTβ-thalamic retrograde tracing and immunohistochemical analyses were used to compare the axonal targets of E13.5-born neurons in *Fezf2*$^{+/-}$ (**A-D'**) and *Fezf2*$^{-/-}$ (**E-H'**) mice. Neurons born on E13.5 were identified by BrdU-saturated nuclei (arrows in **C** and **G**). In *Fezf2*$^{+/-}$ mice, CTβ-thalamic tracing primarily labled TBR1^{+} cells in layer 6 (**B**, Merge **D, D'**). Arrows point to E13.5-born neurons that expressed TBR1, but were not traced by CTβ-thal (**D, D'**). In *Fezf2*$^{-/-}$ mice, ectopic TBR1^{+} cells in layer 5 (**E**), were born at E13.5 and projected axons to the thalamus (**H, H'**). **I-K** An ultrasound image (**I**) showing guided injecton into the thalamus, brain outlined. **J** show injection site in thalamus, **K** shows lack of CTβ in midbrain and hinbrain areas. **L, M** Comparison of injection sites into thalamus in *Fezf2*$^{+/-}$ (**L**) and *Fezf2*$^{-/-}$ (**M**) brains. Ctx, cortex; hip, hippocampus; hyp, hypothalamus; sp, subplate; thal, thalamus; scale bars 50μm in A-H', 500μm for I-M.

CHAPTER 4

Conclusions and future directions

4.1 Recapitulation of research presented

For the past several decades, the field of neurobiology has focused on identifying the molecular mechanisms responsible for orchestrating various cellular processes required for proper cortical development. Although many genes have been established as markers for distinct cortical projection neuron subtypes, few genes have been identified as direct determinants of neuronal identity. Similarly, well-known genetic markers are used to identify individual subclasses of neural stem and progenitor cells, however, genes that are critical for generation of specific subclasses are largely unknown. Here, I presented evidence for two transcription factors, *NfiB* and *Fezf2,* as key regulators of neocortical development. Interestingly, these genes share similar expression patterns within the cortical proliferative zone and in subcerebral projection neurons, yet have unique roles. *Fezf2* regulates subcerebral neuron identity via repression of corticothalamic fate determinant, *Tbr1*. *NfiB* is required for generation of outer radial glia and basal progenitors and for development of corticofugal axonal projections.

4.2 Gaining insight on daughter cell fates generated by radial glial differentiation

Radial glia and outer radial glia asymmetrically divide to produce basal progenitors. However, radial glia are also responsible for the generation of outer

radial glia by asymmetric division (Reillo et al, 2011; Shitamukai et al., 2011; Shitamukai and Matsuzaki, 2012). Given that generation of each neural stem/progenitor subpopulation is critical for neurogenesis and proper cortical development, it is of interest to identify the mechanisms responsible for generating one type of neural stem/progenitor over another by asymmetric cell division. Previously, it was shown that the outcome between symmetric versus asymmetric division was predicted by the cleavage plane orientation of the mother cell with respect to the ventricular surface. For example, in radial glia, a vertical cleavage plane was correlated with symmetric cell division such that the new radial glial daughter cell will inherit half of the apical domain from its mother and grow its own basal process. Conversely, a horizontal cleavage plane was thought to result in asymmetric division. However, the specific fate of daughter cells arising from asymmetric division remained undetermined (Wang, et al., 2011b).

More recently, time-lapse imaging studies performed by LaMonica et al., have advanced our knowledge on the complexity of stem/progenitors cell divisions by revealing that daughter cell fates rely on the timing of horizontal versus vertical cleavage planes. For example, they showed that during early development, a vertical cleavage plane in radial glia resulted in the generation of two radial glial daughter cells, or symmetric division. Yet, during peak neurogenesis, a vertical cleavage plane resulted in asymmetric division, generating one radial glia and one basal progenitor. A horizontal cleavage plane during this developmental stage also resulted in asymmetric cell division, but instead of a basal progenitor, the division generated an

outer radial glial cell. Interestingly, this study also revealed that outer radial glia predominantly divide horizontally. However, unlike that in radial glia, a horizontal cleavage plane in outer radial glia resulted in either two outer radial cells, resembling symmetrical division, or one outer radial glial cell and one basal progenitor (LaMonica et al., 2013). With new understanding of neural stem/progenitor cell division properties, a more precise investigation of how *NfiB* functions in vertical versus horizontal radial glial cell divisions is possible.

NFIB is expressed in radial glia throughout the span of corticogenesis, but expression is weak or absent in basal progenitor and outer radial glial populations (Figure 2.1-2.3) leading us to hypothesize that NFIB regulates the balance between radial glia self-renewing and differentiative cell divisions, thereby directly influencing daughter cell outcomes. In our comparison of $NfiB^{-/-}$ versus $NfiB^{+/+}$ mice, we observed a striking loss of both basal progenitors and outer radial glia during peak neurogenesis indicating a non-cell autonomous effect since neither population express NFIB. However, given that $NfiB^{-/-}$ brains still had a small number of basal progenitors but radial glia appeared unaffected, I predict that *NfiB* specifically functions to promote horizontal cell divisions in radial glia. To address whether this is true, time-lapse imaging and measurements of cleavage plane angles in $NfiB^{-/-}$ and $NfiB^{+/+}$ *in vitro* slice cultures should be performed (as described in Wang et al., 2011b; LaMonica et al., 2013). To complement results from cleavage plane analyses, lineage-tracing by GFP-labeling in wildtype mice would identify the origins of basal progenitors and outer radial glia, since the new developments in trends of vertical and

hortizal divisions (LaMonica et al., 2013) were found in human cortical slices. In addition, implementing a gain-of-function approach by performing *in utero* electroporation of an NfiB-GFP construct into embryos shortly after the start of neurogenesis and later examining for rescue of basal progenitors and outer radial glia would be an important experiment. Together, these approaches would provide additional evidence for whether *NfiB* plays a role in radial glial horizontal division.

4.3 Identifying functional roles of NFIB based on protein structure and post-translational modifications

To date, there are three known isoforms of NFIB protein that are generated as a result of alternative splicing (Kruse and Sippel, 1994a; Wang et al., 2007), but whether each isoform has a unique function remains unknown. Differences in splice variants cause changes to critical regions within NFIB protein. For example, an increase in length at the N-terminus may induce changes in DNA binding and protein dimerization, this in turn may alter the efficacy and or mode of transcriptional regulation. Additionally, sites for potential posttranslational modifications have been identified in each isoform (Kruse and Sippel, 1994b), and this too may have strong implication in protein function. Given that NFIB is critical for a broad range of functions during cortical development and that many known proteins function as distinct isoforms, it is possible that NFIB functions in an isoform-dependent manner. To investigate this possibility, expression analysis for each isoform within the cortex must be performed, as such, the generation of isoform-specific antibodies will be required. Dependent upon results from spatial expression pattern analysis, it would

be interesting to test whether *in utero* electroporation of individual isoform contsructs into *NfiB-/-* brains rescued some of the phenotypes observed. Additionally, transgenic mouse lines could be created in order to investigate how the loss of specific NFIB isoforms effected cortical development.

By performing genome-wide analysis via RNA-sequencing in $NfiB^{-/-}$ and $NfiB^{+/+}$ mice, we identified many downstream effectors of NFIB. We reported that NfiB regulates many genes involved in cell proliferation, neuronal differentiation and axon development (Table 2.3-2.4). However, NFIB is expressed in radial glia and corticofugal projection neurons during similar stages of cortical development (Figure 2.2-2.3) and thus RNA-seq results only reflected differentially expressed genes within the entire cortex, not within individual cell-types. For instance, genes involved in axon development are likely regulated by NFIB within corticofugal projection neurons, not within radial glia. On the other hand, genes associated with cell proliferation and cell cycle progression are probable downstream effectors of NFIB within radial glial cells, not in postmitotic neurons. Given the various functions of NFIB, it is likely that NFIB functions in a cell-type specific manner. One way to address this is by FACS-sorting cortical cells of $NfiB^{+/+}$ and $NfiB^{-/-}$ brains by levels of NFIB (or βGAL) expression. We showed that NFIB is expressed at higher levels in corticofugal neurons compared to its expression in radial glia, thus sorting would result in three separate populations of cells: cells with highest levels of NFIB expression, cells with moderate levels and cells with little or no expression, corresponding to corticofugal projection neurons, radial glia and cells that

presumably do not express NFIB, respectively. After sorting, a genome-wide analysis can once again be performed. Results would identify downstream effectors within specific cell-types. Additionally, it is possible that individual NFIB isoforms have unique functions with respect to cell-type. Thus, upon development of isoform-specific antibodies, it would be interesting to characterize expression patterns of individual NFIB isoforms throughout development.

To gain additional understanding on how NFIB may function so broadly, the potential effects of posttranslational modifications must be further investigated. Upon preliminary characterization of the NFIB, studies revealed multiple sites for phosphorylation and acetylation in two of the three isoforms (Ballif et al, 2004; Mason et al., 2009). It has long been established that phosphorylation can greatly impact protein function, furthermore, there is much evidence supporting the importance for phosphorylation during mammalian brain development. For instance, mutations in tyrosine phosphorylation sites of Dab1, a Reelin adaptor protein, result in defects in cortical lamination and neuronal migration (Howell et al., 2000; Ballif et al., 2004). Furthermore, phosphorylation cascades are critical to many genes important for regulation of the cell cycle (Fisher et al., 2012). Because individual isoforms contain unique phosphorylation sites it is likely that phosphorylation is required for proper execution of NFIB function. By using site-directed mutagenesis, *NfiB* constructs containing replacement of a serine with an alanine at one or more phophorylation site (and an *NfiB* wildtype construct) can generated then transiently transfected into *NfiB*-mutant radial glia *in vitro*. This will then allow a comparison of

cell viability, cell proliferation and neurogenesis, amongst all constructs in order to identify which phosphorylation sites are required for the the function of NFIB in radial glia. Should any phosphorylation sites rescue the function of radial glia *in vitro*, a follow-up *in vivo* rescue experiment could be performed by electroporation of the construct into $NfiB^{+/+}$ and $NfiB^{-/-}$ embryos *in utero*.

Taken together, these proposed experiments would provide additional insight toward the multiple functions of NfiB. Clearly, much work is still needed in order to fully understand the specific roles for NFIB in individual populations of radial glia and corticofugal projection neurons.

4.4 From neocortical development to disease therapies

Development of the mammalian cerebral cortex incorporates a complex progression of gene interactions and cellular processes, such that misregulation of these genes often results in errors in one or more processes including neurogenesis, cortical organization and axonogenesis (Guerrini et al., 2003; Hall and Lalli, 2010; tiberi et al., 2012). Subsequently, these defects lead to neurological disorders such as autism and Amyotrophic Lateral Sclerosis (ALS) (Eisen and Weber, 2001; Nicolson and Szatmari, 2003). Recently, misregulation of NFIB has been implicated in autism spectrum disorder, (Choi et al., 2012), and certain brain cancers (Brun et al., 2009; Ho et al., 2013). Taken together, with its roles in neurogenesis and neural stem/progenitor proliferation, *NfiB* proves an important candidate gene for the development of treatments for neurodevelopmental and neurodegenerative diseases,

and brain cancers. If we can identify the transcriptional mechanisms by which NFIB regulates neurogenesis and/or axonogenesis of corticofugal projections neurons, then it will be possible to generate such neurons *in vitro*, followed by transplantation into diseased patients, with the end goal of restoring cortical function and/or improving quality of life. Of great importance, should we fully understand the network of molecular mechanisms that function during neocortical development, we will gain imperative insight toward molecular targets that may be useful for therapeutics of neurological diseases.

REFERENCES

Alcamo EA, Chirivella L, Dautzenberg M, Dobreva G, Farinas I, Grosschedl R, McConnell SK. 2008. Satb2 regulates callosal projection neuron identity in the developing cerebral cortex. Neuron 57(3):364-377.

Allendoerfer KL, Shatz CJ. 1994. The subplate, a transient neocortical structure: its role in the development of connections between thalamus and cortex. Annu Rev Neurosci 17:185-218.

Angevine JB, Jr., Sidman RL. 1961. Autoradiographic study of cell migration during histogenesis of cerebral cortex in the mouse. Nature 192:766-768.

Arlotta P, Molyneaux BJ, Chen J, Inoue J, Kominami R, Macklis JD. 2005. Neuronal subtype-specific genes that control corticospinal motor neuron development in vivo. Neuron 45(2):207-221.

Arnold SJ, Huang GJ, Cheung AF, Era T, Nishikawa S, Bikoff EK, Molnar Z, Robertson EJ, Groszer M. 2008. The T-box transcription factor Eomes/Tbr2 regulates neurogenesis in the cortical subventricular zone. Genes Dev 22(18):2479-2484.

Bandyopadhyay S, Gronostajski RM. 1994. Identification of a conserved oxidation-sensitive cysteine residue in the NFI family of DNA-binding proteins. J Biol Chem 269(47):29949-29955.

Bani-Yaghoub M, Tremblay RG, Lei JX, Zhang D, Zurakowski B, Sandhu JK, Smith B, Ribecco-Lutkiewicz M, Kennedy J, Walker PR, Sikorska M. 2006. Role of Sox2 in the development of the mouse neocortex. Dev Biol 295(1):52-66.

Basak O, Taylor V. 2007. Identification of self-replicating multipotent progenitors in the embryonic nervous system by high Notch activity and Hes5 expression. Eur J Neurosci 25(4):1006-1022.

Bentivoglio M, Mazzarello P. 1999. The history of radial glia. Brain Res Bull 49(5):305-315.

Britanova O, Alifragis P, Junek S, Jones K, Gruss P, Tarabykin V. 2006. A novel mode of tangential migration of cortical projection neurons. Dev Biol 298(1):299-311.

Britanova O, de Juan Romero C, Cheung A, Kwan KY, Schwark M, Gyorgy A, Vogel T, Akopov S, Mitkovski M, Agoston D, Sestan N, Molnar Z, Tarabykin V. 2008. Satb2 is a postmitotic determinant for upper-layer neuron specification in the neocortex. Neuron 57(3):378-392.

Cajal SRy. 1899. Comparative Study of the Sensory Areas of the Human Cortex: Nabu Press.

Campbell K, Gotz M. 2002. Radial glia: multi-purpose cells for vertebrate brain development. Trends Neurosci 25(5):235-238.

Caviness VS, Jr. 1982. Neocortical histogenesis in normal and reeler mice: a developmental study based upon [3H]thymidine autoradiography. Brain Res 256(3):293-302.

Caviness VS, Jr., Takahashi T. 1995. Proliferative events in the cerebral ventricular zone. Brain Dev 17(3):159-163.

Chaudhry AZ, Lyons GE, Gronostajski RM. 1997. Expression patterns of the four nuclear factor I genes during mouse embryogenesis indicate a potential role in development. Dev Dyn 208(3):313-325.

Chen B, Schaevitz LR, McConnell SK. 2005a. Fezl regulates the differentiation and axon targeting of layer 5 subcortical projection neurons in cerebral cortex. Proceedings of the National Academy of Sciences of the United States of America 102(47):17184-17189.

Chen B, Wang SS, Hattox AM, Rayburn H, Nelson SB, McConnell SK. 2008. The Fezf2, Ctip2 genetic pathway regulates the fate choice of subcortical projection neurons in the developing cerebral cortex. Proceedings of the National Academy of Sciences 105(32):11382-11387.

Chen J-G, Rasin M-R, Kwan KY, Sestan N. 2005. Zfp312 is required for subcortical axonal projections and dendritic morphology of deep-layer pyramidal neurons of the cerebral cortex. Proceedings of the National Academy of Sciences of the United States of America 102(49):17792-17797.

Copp AJ, Greene ND, Murdoch JN. 2003. The genetic basis of mammalian neurulation. Nat Rev Genet 4(10):784-793.

Dahmane N, Sanchez P, Gitton Y, Palma V, Sun T, Beyna M, Weiner H, Ruiz i Altaba A. 2001. The Sonic Hedgehog-Gli pathway regulates dorsal brain growth and tumorigenesis. Development 128(24):5201-5212.

Desai AR, McConnell SK. 2000. Progressive restriction in fate potential by neural progenitors during cerebral cortical development. Development 127(13):2863-2872.

Echelard Y, Epstein DJ, St-Jacques B, Shen L, Mohler J, McMahon JA, McMahon AP. 1993. Sonic hedgehog, a member of a family of putative signaling

molecules, is implicated in the regulation of CNS polarity. Cell 75(7):1417-1430.

Eisen A, Weber M. 2001. The motor cortex and amyotrophic lateral sclerosis. Muscle Nerve 24(4):564-573.

Farkas LM, Huttner WB. 2008. The cell biology of neural stem and progenitor cells and its significance for their proliferation versus differentiation during mammalian brain development. Curr Opin Cell Biol 20(6):707-715.

Fietz SA, Kelava I, Vogt J, Wilsch-Brauninger M, Stenzel D, Fish JL, Corbeil D, Riehn A, Distler W, Nitsch R, Huttner WB. 2010. OSVZ progenitors of human and ferret neocortex are epithelial-like and expand by integrin signaling. Nat Neurosci 13(6):690-699.

Finlay BL, Darlington RB. 1995. Linked regularities in the development and evolution of mammalian brains. Science 268(5217):1578-1584.

Fisher D, Krasinska L, Coudreuse D, Novak B. 2012. Phosphorylation network dynamics in the control of cell cycle transitions. J Cell Sci 125(Pt 20):4703-4711.

Fletcher CF, Jenkins NA, Copeland NG, Chaudhry AZ, Gronostajski RM. 1999. Exon structure of the nuclear factor I DNA-binding domain from C. elegans to mammals. Mamm Genome 10(4):390-396.

Fode C, Ma Q, Casarosa S, Ang SL, Anderson DJ, Guillemot F. 2000. A role for neural determination genes in specifying the dorsoventral identity of telencephalic neurons. Genes Dev 14(1):67-80.

Franco SJ, Muller U. 2013. Shaping our minds: stem and progenitor cell diversity in the mammalian neocortex. Neuron 77(1):19-34.

Frantz GD, McConnell SK. 1996. Restriction of late cerebral cortical progenitors to an upper-layer fate. Neuron 17(1):55-61.

Gal JS, Morozov YM, Ayoub AE, Chatterjee M, Rakic P, Haydar TF. 2006. Molecular and morphological heterogeneity of neural precursors in the mouse neocortical proliferative zones. J Neurosci 26(3):1045-1056.

Gilbert SF. 2010. Developmental Biology. Sunderland, MA: Sinauer Associates.

Gómez-López S, Wiskow O, Favaro R, Nicolis SK, Price DJ, Pollard SM, Smith A. 2011. Sox2 and Pax6 maintain the proliferative and developmental potential of gliogenic neural stem cells In vitro. Glia 59(11):1588-1599.

Gotz M, Barde YA. 2005. Radial glial cells defined and major intermediates between embryonic stem cells and CNS neurons. Neuron 46(3):369-372.

Gotz M, Huttner WB. 2005. The cell biology of neurogenesis. Nat Rev Mol Cell Biol 6(10):777-788.

Gotz M, Stoykova A, Gruss P. 1998. Pax6 controls radial glia differentiation in the cerebral cortex. Neuron 21(5):1031-1044.

Grandbarbe L, Bouissac J, Rand M, Hrabe de Angelis M, Artavanis-Tsakonas S, Mohier E. 2003. Delta-Notch signaling controls the generation of neurons/glia from neural stem cells in a stepwise process. Development 130(7):1391-1402.

Gronostajski RM. 1986. Analysis of nuclear factor I binding to DNA using degenerate oligonucleotides. Nucleic Acids Res 14(22):9117-9132.

Gronostajski RM. 2000. Roles of the NFI/CTF gene family in transcription and development. Gene 249(1-2):31-45.

Gronostajski RM, Adhya S, Nagata K, Guggenheimer RA, Hurwitz J. 1985. Site-specific DNA binding of nuclear factor I: analyses of cellular binding sites. Mol Cell Biol 5(5):964-971.

Grunder A, Qian F, Ebel TT, Mincheva A, Lichter P, Kruse U, Sippel AE. 2003. Genomic organization, splice products and mouse chromosomal localization of genes for transcription factor Nuclear Factor One. Gene 304:171-181.

Guerrini R, Sicca F, Parmeggiani L. 2003. Epilepsy and malformations of the cerebral cortex. Epileptic Disord 5 Suppl 2:S9-26.

Hall A, Lalli G. 2010. Rho and Ras GTPases in axon growth, guidance, and branching. Cold Spring Harb Perspect Biol 2(2):a001818.

Hamilton A. 1901. The differentiated cells in the central nervous system of the white rat. J Comp Neurol(11):297-320.

Hanashima C, Li SC, Shen L, Lai E, Fishell G. 2004. Foxg1 suppresses early cortical cell fate. Science 303(5654):56-59.

Hansen DV, Lui JH, Parker PR, Kriegstein AR. 2010. Neurogenic radial glia in the outer subventricular zone of human neocortex. Nature 464(7288):554-561.

Haubensak W, Attardo A, Denk W, Huttner WB. 2004. Neurons arise in the basal neuroepithelium of the early mammalian telencephalon: a major site of neurogenesis. Proc Natl Acad Sci U S A 101(9):3196-3201.

Heins N, Malatesta P, Cecconi F, Nakafuku M, Tucker KL, Hack MA, Chapouton P, Barde YA, Gotz M. 2002. Glial cells generate neurons: the role of the transcription factor Pax6. Nat Neurosci 5(4):308-315.

Heng YH, Barry G, Richards LJ, Piper M. 2012. Nuclear factor I genes regulate neuronal migration. Neurosignals 20(3):159-167.

Hevner RF, Haydar TF. 2012. The (not necessarily) convoluted role of basal radial glia in cortical neurogenesis. Cereb Cortex 22(2):465-468.

Hevner RF, Hodge RD, Daza RAM, Englund C. 2006. Transcription factors in glutamatergic neurogenesis: Conserved programs in neocortex, cerebellum, and adult hippocampus. Neuroscience Research 55(3):223-233.

Hevner RF, Shi L, Justice N, Hsueh Y, Sheng M, Smiga S, Bulfone A, Goffinet AM, Campagnoni AT, Rubenstein JL. 2001a. Tbr1 regulates differentiation of the preplate and layer 6. Neuron 29(2):353-366.

Hevner RF, Shi L, Justice N, Hsueh Y-P, Sheng M, Smiga S, Bulfone A, Goffinet AM, Campagnoni AT, Rubenstein JLR. 2001b. Tbr1 Regulates Differentiation of the Preplate and Layer 6. Neuron 29(2):353-366.

Hutton SR, Pevny LH. 2006. SOX2 expression levels distinguish between neural progenitor populations of the developing dorsal telencephalon. Dev Biol 352(1):40-47.

Karfunkel P. 1974. The mechanisms of neural tube formation. Int Rev Cytol 38(0):245-271.

Kowalczyk T, Pontious A, Englund C, Daza RA, Bedogni F, Hodge R, Attardo A, Bell C, Huttner WB, Hevner RF. 2009. Intermediate neuronal progenitors (basal progenitors) produce pyramidal-projection neurons for all layers of cerebral cortex. Cereb Cortex 19(10):2439-2450.

Kriegstein AR, Gotz M. 2003. Radial glia diversity: a matter of cell fate. Glia 43(1):37-43.

Kruse U, Qian F, Sippel AE. 1991. Identification of a fourth nuclear factor I gene in chicken by cDNA cloning: NFI-X. Nucleic Acids Res 19(23):6641.

Kruse U, Sippel AE. 1994a. The genes for transcription factor nuclear factor I give rise to corresponding splice variants between vertebrate species. J Mol Biol 238(5):860-865.

Kruse U, Sippel AE. 1994b. Transcription factor nuclear factor I proteins form stable homo- and heterodimers. FEBS Lett 348(1):46-50.

Kudoh T, Wilson SW, Dawid IB. 2002. Distinct roles for Fgf, Wnt and retinoic acid in posteriorizing the neural ectoderm. Development 129(18):4335-4346.

Kumbasar A, Plachez C, Gronostajski RM, Richards LJ, Litwack ED. 2009. Absence of the transcription factor Nfib delays the formation of the basilar pontine and other mossy fiber nuclei. J Comp Neurol 513(1):98-112.

LaMonica BE, Lui JH, Hansen DV, Kriegstein AR. Mitotic spindle orientation predicts outer radial glial cell generation in human neocortex. 2013. Nat Commun 4:1665.

Leone DP, Srinivasan K, Chen B, Alcamo E, McConnell SK. 2008. The determination of projection neuron identity in the developing cerebral cortex. Curr Opin Neurobiol 18(1):28-35.

Lui JH, Hansen DV, Kriegstein AR. 2011. Development and evolution of the human neocortex. Cell 146(1):18-36.

Malatesta P, Appolloni I, Calzolari F. 2008. Radial glia and neural stem cells. Cell Tissue Res 331(1):165-178.

Martynoga B, Drechsel D, Guillemot F. 2012. Molecular control of neurogenesis: a view from the mammalian cerebral cortex. Cold Spring Harb Perspect Biol 4(10).

Mason S, Piper M, Gronostajski R, Richards L. 2009. Nuclear Factor One Transcription Factors in CNS Development. Molecular Neurobiology 39(1):10-23.

McConnell SK. 1991. The generation of neuronal diversity in the central nervous system. Annu Rev Neurosci 14:269-300.

McConnell SK. 1995. Constructing the cerebral cortex: neurogenesis and fate determination. Neuron 15(4):761-768.

McConnell SK, Kaznowski CE. 1991. Cell cycle dependence of laminar determination in developing neocortex. Science 254(5029):282-285.

McKay R. 1997. Stem cells in the central nervous system. Science 276(5309):66-71.

McKenna WL, Betancourt J, Larkin KA, Abrams B, Guo C, Rubenstein JL, Chen B. 2011. Tbr1 and Fezf2 regulate alternate corticofugal neuronal identities during neocortical development. J Neurosci 31(2):549-564.

Meyer G, Soria JM, Martinez-Galan JR, Martin-Clemente B, Fairen A. 1998. Different origins and developmental histories of transient neurons in the marginal zone of the fetal and neonatal rat cortex. J Comp Neurol 397(4):493-518.

Miyata T, Kawaguchi A, Saito K, Kawano M, Muto T, Ogawa M. 2004. Asymmetric production of surface-dividing and non-surface-dividing cortical progenitor cells. Development 131(13):3133-3145.

Molyneaux BJ, Arlotta P, Hirata T, Hibi M, Macklis JD. 2005. Fezl is required for the birth and specification of corticospinal motor neurons. Neuron 47(6):817-831.

Molyneaux BJ, Arlotta P, Menezes JR, Macklis JD. 2007. Neuronal subtype specification in the cerebral cortex. Nat Rev Neurosci 8(6):427-437.

Monuki ES, Porter FD, Walsh CA. 2001. Patterning of the dorsal telencephalon and cerebral cortex by a roof plate-Lhx2 pathway. Neuron 32(4):591-604.

Muzio L, Di Benedetto B, Stoykova A, Boncinelli E, Gruss P, Mallamaci A. 2002. Conversion of cerebral cortex into basal ganglia in Emx2(-/-) Pax6(Sey/Sey) double-mutant mice. Nat Neurosci 5(8):737-745.

Nagata K, Guggenheimer RA, Enomoto T, Lichy JH, Hurwitz J. 1982. Adenovirus DNA replication in vitro: identification of a host factor that stimulates synthesis of the preterminal protein-dCMP complex. Proc Natl Acad Sci U S A 79(21):6438-6442.

Nauta WJ, Bucher VM. 1954. Efferent connections of the striate cortex in the albino rat. J Comp Neurol 100(2):257-285.

Nicolson R, Szatmari P. 2003. Genetic and neurodevelopmental influences in autistic disorder. Can J Psychiatry 48(8):526-537.

Nieto M, Monuki ES, Tang H, Imitola J, Haubst N, Khoury SJ, Cunningham J, Gotz M, Walsh CA. 2004. Expression of Cux-1 and Cux-2 in the subventricular zone and upper layers II-IV of the cerebral cortex. J Comp Neurol 479(2):168-180.

Noctor SC, Martinez-Cerdeno V, Ivic L, Kriegstein AR. 2004. Cortical neurons arise in symmetric and asymmetric division zones and migrate through specific phases. Nat Neurosci 7(2):136-144.

Noctor SC, Martinez-Cerdeno V, Kriegstein AR. 2007a. Contribution of intermediate progenitor cells to cortical histogenesis. Arch Neurol 64(5):639-642.

Noctor SC, Martinez-Cerdeno V, Kriegstein AR. 2007b. Neural stem and progenitor cells in cortical development. Novartis Found Symp 288:59-73; discussion 73-58, 96-58.

O'Leary DD, Koester SE. 1993. Development of projection neuron types, axon pathways, and patterned connections of the mammalian cortex. Neuron 10(6):991-1006.

Peters A, Jones EG. 1984. Cellular Components of the Cerebral Cortex. Plenum, NY.

Piper M, Moldrich R, Lindwall C, Little E, Barry G, Mason S, Sunn N, Kurniawan N, Gronostajski R, Richards L. 2009. Multiple non-cell-autonomous defects underlie neocortical callosal dysgenesis in Nfib-deficient mice. Neural Development 4(1):43.

Plachez C, Lindwall C, Sunn N, Piper M, Moldrich RX, Campbell CE, Osinski JM, Gronostajski RM, Richards LJ. 2008. Nuclear factor I gene expression in the developing forebrain. The Journal of Comparative Neurology 508(3):385-401.

Pontious A, Kowalczyk T, Englund C, Hevner RF. 2008. Role of intermediate progenitor cells in cerebral cortex development. Dev Neurosci 30(1-3):24-32.

Rakic P. 1972. Mode of cell migration to the superficial layers of fetal monkey neocortex. J Comp Neurol 145(1):61-83.

Rakic P. 1974. Neurons in rhesus monkey visual cortex: systematic relation between time of origin and eventual disposition. Science 183(4123):425-427.

Ramon y Cajal S. 1995. Histology of the Nervous System of Man and Vertevrates. New York, NY: Oxford University Press.

Reillo I, de Juan Romero C, Garcia-Cabezas MA, Borrell V. 2011. A role for intermediate radial glia in the tangential expansion of the mammalian cerebral cortex. Cereb Cortex 21(7):1674-1694.

Rupp RA, Kruse U, Multhaup G, Gobel U, Beyreuther K, Sippel AE. 1990. Chicken NFI/TGGCA proteins are encoded by at least three independent genes: NFI-A, NFI-B and NFI-C with homologues in mammalian genomes. Nucleic Acids Res 18(9):2607-2616.

Sauer FC. 1935. Mitosis in the neural tube. J Comp Neurol(62):377-405.

Sessa A, Mao CA, Hadjantonakis AK, Klein WH, Broccoli V. 2008. Tbr2 directs conversion of radial glia into basal precursors and guides neuronal

amplification by indirect neurogenesis in the developing neocortex. Neuron 60(1):56-69.

Shitamukai A, Konno D, Matsuzaki F. 2011. Oblique radial glial divisions in the developing mouse neocortex induce self-renewing progenitors outside the germinal zone that resemble primate outer subventricular zone progenitors. J Neurosci 31(10):3683-3695.

Shitamukai A, Matsuzaki F. 2012. Control of asymmetric cell division of mammalian neural progenitors. Dev Growth Differ 54(3):277-286.

Smart IH. 1973. Proliferative characteristics of the ependymal layer during the early development of the mouse neocortex: a pilot study based on recording the number, location and plane of cleavage of mitotic figures. J Anat 116(Pt 1):67-91.

Steele-Perkins G, Plachez C, Butz KG, Yang G, Bachurski CJ, Kinsman SL, Litwack ED, Richards LJ, Gronostajski RM. 2005. The Transcription Factor Gene Nfib Is Essential for both Lung Maturation and Brain Development. Molecular and Cellular Biology 25(2):685-698.

Stern CD. 2005. Neural induction: old problem, new findings, yet more questions. Development 132(9):2007-2021.

Sugino K, Hempel CM, Miller MN, Hattox AM, Shapiro P, Wu C, Huang ZJ, Nelson SB. 2006. Molecular taxonomy of major neuronal classes in the adult mouse forebrain. Nat Neurosci 9(1):99-107.

Tarabykin V, Stoykova A, Usman N, Gruss P. 2001. Cortical upper layer neurons derive from the subventricular zone as indicated by Svet1 gene expression. Development 128(11):1983-1993.

Taverna E, Huttner WB. 2010. Neural progenitor nuclei IN motion. Neuron 67(6):906-914.

Tiberi L, Vanderhaeghen P, van den Ameele J. 2012. Cortical neurogenesis and morphogens: diversity of cues, sources and functions. Curr Opin Cell Biol 24(2):269-276.

Valverde F. 1962. Reticular formation of the albino rat's brain stem cytoarchitecture and corticofugal connections. J Comp Neurol 119:25-53.

Wang W, Mullikin-Kilpatrick D, Crandall JE, Gronostajski RM, Litwack ED, Kilpatrick DL. 2007. Nuclear Factor I Coordinates Multiple Phases of

Cerebellar Granule Cell Development via Regulation of Cell Adhesion Molecules. Journal of Neuroscience 27(23):6115-6127.

Wang X, Lui JH, Kriegstein AR. 2011b. Orienting fate: spatial regulation of neurogenic divisions. Neuron 72(2):191-193.

Wang X, Tsai JW, LaMonica B, Kriegstein AR. 2011a. A new subtype of progenitor cell in the mouse embryonic neocortex. Nat Neurosci 14(5):555-561.

Wonders CP, Anderson SA. 2006. The origin and specification of cortical interneurons. Nat Rev Neurosci 7(9):687-696.